NCHRP
REPORT 620

NATIONAL COOPERATIVE HIGHWAY RESEARCH PROGRAM

Development of Design Specifications and Commentary for Horizontally Curved Concrete Box-Girder Bridges

TRANSPORTATION RESEARCH BOARD
OF THE NATIONAL ACADEMIES

TRANSPORTATION RESEARCH BOARD 2008 EXECUTIVE COMMITTEE*

OFFICERS

CHAIR: **Debra L. Miller,** *Secretary, Kansas DOT, Topeka*
VICE CHAIR: **Adib K. Kanafani,** *Cahill Professor of Civil Engineering, University of California, Berkeley*
EXECUTIVE DIRECTOR: **Robert E. Skinner, Jr.,** *Transportation Research Board*

MEMBERS

J. Barry Barker, *Executive Director, Transit Authority of River City, Louisville, KY*
Allen D. Biehler, *Secretary, Pennsylvania DOT, Harrisburg*
John D. Bowe, *President, Americas Region, APL Limited, Oakland, CA*
Larry L. Brown, Sr., *Executive Director, Mississippi DOT, Jackson*
Deborah H. Butler, *Executive Vice President, Planning, and CIO, Norfolk Southern Corporation, Norfolk, VA*
William A.V. Clark, *Professor, Department of Geography, University of California, Los Angeles*
David S. Ekern, *Commissioner, Virginia DOT, Richmond*
Nicholas J. Garber, *Henry L. Kinnier Professor, Department of Civil Engineering, University of Virginia, Charlottesville*
Jeffrey W. Hamiel, *Executive Director, Metropolitan Airports Commission, Minneapolis, MN*
Edward A. (Ned) Helme, *President, Center for Clean Air Policy, Washington, DC*
Will Kempton, *Director, California DOT, Sacramento*
Susan Martinovich, *Director, Nevada DOT, Carson City*
Michael D. Meyer, *Professor, School of Civil and Environmental Engineering, Georgia Institute of Technology, Atlanta*
Michael R. Morris, *Director of Transportation, North Central Texas Council of Governments, Arlington*
Neil J. Pedersen, *Administrator, Maryland State Highway Administration, Baltimore*
Pete K. Rahn, *Director, Missouri DOT, Jefferson City*
Sandra Rosenbloom, *Professor of Planning, University of Arizona, Tucson*
Tracy L. Rosser, *Vice President, Corporate Traffic, Wal-Mart Stores, Inc., Bentonville, AR*
Rosa Clausell Rountree, *Executive Director, Georgia State Road and Tollway Authority, Atlanta*
Henry G. (Gerry) Schwartz, Jr., *Chairman (retired), Jacobs/Sverdrup Civil, Inc., St. Louis, MO*
C. Michael Walton, *Ernest H. Cockrell Centennial Chair in Engineering, University of Texas, Austin*
Linda S. Watson, *CEO, LYNX–Central Florida Regional Transportation Authority, Orlando*
Steve Williams, *Chairman and CEO, Maverick Transportation, Inc., Little Rock, AR*

EX OFFICIO MEMBERS

Thad Allen (Adm., U.S. Coast Guard), *Commandant, U.S. Coast Guard, Washington, DC*
Joseph H. Boardman, *Federal Railroad Administrator, U.S.DOT*
Rebecca M. Brewster, *President and COO, American Transportation Research Institute, Smyrna, GA*
Paul R. Brubaker, *Research and Innovative Technology Administrator, U.S.DOT*
George Bugliarello, *Chancellor, Polytechnic University of New York, Brooklyn, and Foreign Secretary, National Academy of Engineering, Washington, DC*
Sean T. Connaughton, *Maritime Administrator, U.S.DOT*
LeRoy Gishi, *Chief, Division of Transportation, Bureau of Indian Affairs, U.S. Department of the Interior, Washington, DC*
Edward R. Hamberger, *President and CEO, Association of American Railroads, Washington, DC*
John H. Hill, *Federal Motor Carrier Safety Administrator, U.S.DOT*
John C. Horsley, *Executive Director, American Association of State Highway and Transportation Officials, Washington, DC*
Carl T. Johnson, *Pipeline and Hazardous Materials Safety Administrator, U.S.DOT*
J. Edward Johnson, *Director, Applied Science Directorate, National Aeronautics and Space Administration, John C. Stennis Space Center, MS*
Thomas J. Madison, Jr., *Administrator, Federal Highway Administration, U.S.DOT*
William W. Millar, *President, American Public Transportation Association, Washington, DC*
Nicole R. Nason, *National Highway Traffic Safety Administrator, U.S.DOT*
James S. Simpson, *Federal Transit Administrator, U.S.DOT*
Robert A. Sturgell, *Acting Administrator, Federal Aviation Administration, U.S.DOT*
Robert L. Van Antwerp (Lt. Gen., U.S. Army), *Chief of Engineers and Commanding General, U.S. Army Corps of Engineers, Washington, DC*

*Membership as of September 2008.

NATIONAL COOPERATIVE HIGHWAY RESEARCH PROGRAM

NCHRP REPORT 620

Development of Design Specifications and Commentary for Horizontally Curved Concrete Box-Girder Bridges

NUTT, REDFIELD AND VALENTINE
Orangevale, CA

IN ASSOCIATION WITH

DAVID EVANS & ASSOCIATES, INC.
San Diego, CA

AND

ZOCON CONSULTING ENGINEERS, INC.
Folsom, CA

Subject Areas
Bridges, Other Structures, and Hydraulics and Hydrology

Research sponsored by the American Association of State Highway and Transportation Officials
in cooperation with the Federal Highway Administration

TRANSPORTATION RESEARCH BOARD

WASHINGTON, D.C.
2008
www.TRB.org

NATIONAL COOPERATIVE HIGHWAY RESEARCH PROGRAM

Systematic, well-designed research provides the most effective approach to the solution of many problems facing highway administrators and engineers. Often, highway problems are of local interest and can best be studied by highway departments individually or in cooperation with their state universities and others. However, the accelerating growth of highway transportation develops increasingly complex problems of wide interest to highway authorities. These problems are best studied through a coordinated program of cooperative research.

In recognition of these needs, the highway administrators of the American Association of State Highway and Transportation Officials initiated in 1962 an objective national highway research program employing modern scientific techniques. This program is supported on a continuing basis by funds from participating member states of the Association and it receives the full cooperation and support of the Federal Highway Administration, United States Department of Transportation.

The Transportation Research Board of the National Academies was requested by the Association to administer the research program because of the Board's recognized objectivity and understanding of modern research practices. The Board is uniquely suited for this purpose as it maintains an extensive committee structure from which authorities on any highway transportation subject may be drawn; it possesses avenues of communications and cooperation with federal, state and local governmental agencies, universities, and industry; its relationship to the National Research Council is an insurance of objectivity; it maintains a full-time research correlation staff of specialists in highway transportation matters to bring the findings of research directly to those who are in a position to use them.

The program is developed on the basis of research needs identified by chief administrators of the highway and transportation departments and by committees of AASHTO. Each year, specific areas of research needs to be included in the program are proposed to the National Research Council and the Board by the American Association of State Highway and Transportation Officials. Research projects to fulfill these needs are defined by the Board, and qualified research agencies are selected from those that have submitted proposals. Administration and surveillance of research contracts are the responsibilities of the National Research Council and the Transportation Research Board.

The needs for highway research are many, and the National Cooperative Highway Research Program can make significant contributions to the solution of highway transportation problems of mutual concern to many responsible groups. The program, however, is intended to complement rather than to substitute for or duplicate other highway research programs.

NCHRP REPORT 620

Project 12-71
ISSN 0077-5614
ISBN: 978-0-309-11750-0
Library of Congress Control Number 2008936983

COPYRIGHT PERMISSION

NOTICE

The project that is the subject of this report was a part of the National Cooperative Highway Research Program conducted by the Transportation Research Board with the approval of the Governing Board of the National Research Council. Such approval reflects the Governing Board's judgment that the program concerned is of national importance and appropriate with respect to both the purposes and resources of the National Research Council.

The members of the technical committee selected to monitor this project and to review this report were chosen for recognized scholarly competence and with due consideration for the balance of disciplines appropriate to the project. The opinions and conclusions expressed or implied are those of the research agency that performed the research, and, while they have been accepted as appropriate by the technical committee, they are not necessarily those of the Transportation Research Board, the National Research Council, the American Association of State Highway and Transportation Officials, or the Federal Highway Administration, U.S. Department of Transportation.

Each report is reviewed and accepted for publication by the technical committee according to procedures established and monitored by the Transportation Research Board Executive Committee and the Governing Board of the National Research Council.

The Transportation Research Board of the National Academies, the National Research Council, the Federal Highway Administration, the American Association of State Highway and Transportation Officials, and the individual states participating in the National Cooperative Highway Research Program do not endorse products or manufacturers. Trade or manufacturers' names appear herein solely because they are considered essential to the object of this report.

Published reports of the

NATIONAL COOPERATIVE HIGHWAY RESEARCH PROGRAM

are available from:

Transportation Research Board
Business Office
500 Fifth Street, NW
Washington, DC 20001

and can be ordered through the Internet at:

http://www.national-academies.org/trb/bookstore

Printed in the United States of America

THE NATIONAL ACADEMIES

Advisers to the Nation on Science, Engineering, and Medicine

The **National Academy of Sciences** is a private, nonprofit, self-perpetuating society of distinguished scholars engaged in scientific and engineering research, dedicated to the furtherance of science and technology and to their use for the general welfare. On the authority of the charter granted to it by the Congress in 1863, the Academy has a mandate that requires it to advise the federal government on scientific and technical matters. Dr. Ralph J. Cicerone is president of the National Academy of Sciences.

The **National Academy of Engineering** was established in 1964, under the charter of the National Academy of Sciences, as a parallel organization of outstanding engineers. It is autonomous in its administration and in the selection of its members, sharing with the National Academy of Sciences the responsibility for advising the federal government. The National Academy of Engineering also sponsors engineering programs aimed at meeting national needs, encourages education and research, and recognizes the superior achievements of engineers. Dr. Charles M. Vest is president of the National Academy of Engineering.

The **Institute of Medicine** was established in 1970 by the National Academy of Sciences to secure the services of eminent members of appropriate professions in the examination of policy matters pertaining to the health of the public. The Institute acts under the responsibility given to the National Academy of Sciences by its congressional charter to be an adviser to the federal government and, on its own initiative, to identify issues of medical care, research, and education. Dr. Harvey V. Fineberg is president of the Institute of Medicine.

The **National Research Council** was organized by the National Academy of Sciences in 1916 to associate the broad community of science and technology with the Academy's purposes of furthering knowledge and advising the federal government. Functioning in accordance with general policies determined by the Academy, the Council has become the principal operating agency of both the National Academy of Sciences and the National Academy of Engineering in providing services to the government, the public, and the scientific and engineering communities. The Council is administered jointly by both the Academies and the Institute of Medicine. Dr. Ralph J. Cicerone and Dr. Charles M. Vest are chair and vice chair, respectively, of the National Research Council.

The **Transportation Research Board** is one of six major divisions of the National Research Council. The mission of the Transportation Research Board is to provide leadership in transportation innovation and progress through research and information exchange, conducted within a setting that is objective, interdisciplinary, and multimodal. The Board's varied activities annually engage about 7,000 engineers, scientists, and other transportation researchers and practitioners from the public and private sectors and academia, all of whom contribute their expertise in the public interest. The program is supported by state transportation departments, federal agencies including the component administrations of the U.S. Department of Transportation, and other organizations and individuals interested in the development of transportation. **www.TRB.org**

www.national-academies.org

COOPERATIVE RESEARCH PROGRAMS

CRP STAFF FOR NCHRP REPORT 620

Christopher W. Jenks, *Director, Cooperative Research Programs*
Crawford F. Jencks, *Deputy Director, Cooperative Research Programs*
David B. Beal, *Senior Program Officer*
Eileen P. Delaney, *Director of Publications*
Hilary Freer, *Senior Editor*

NCHRP PROJECT 12-71 PANEL
Field of Design—Area of Bridges

Michael R. Pope, *California DOT, Sacramento, CA* (Chair)
Bruce V. Johnson, *Oregon DOT, Salem, OR*
Abdeldjelil Belarbi, *Missouri University of Science and Technology, Rolla, MO*
David C. O'Hagan, *Florida DOT, Tallahassee, FL*
Jerry L. Potter, *Livingston, TX*
Geoffrey Swett, *Washington State DOT, Olympia, WA*
Dean W. Van Landuyt, *Texas DOT, Austin, TX*
Nur Yazdani, *University of Texas–Arlington, Arlington, TX*
Gary Jakovich, *FHWA Liaison*
Stephen F. Maher, *TRB Liaison*

FOREWORD

By David B. Beal
Staff Officer
Transportation Research Board

This report provides specifications, commentary, and examples for the design of horizontally curved concrete box-girder highway bridges. The report details the development of the design procedures. Recommended LRFD specifications and design examples illustrating the application of the design methods and specifications are included in appendixes (available on the TRB website at http://trb.org/news/blurb_detail.asp?id=9596). The material in this report will be of immediate interest to bridge designers.

Many concrete box-girder bridges are constructed on horizontally curved alignments. In some instances, problems such as bearing uplift, cracked diaphragms and piers, and lateral tendon breakout have occurred. The AASHTO Bridge Specifications do not adequately address these and other issues, either in the provisions, or commentary.

AASHTO has recently incorporated provisions for the design of horizontally curved steel bridges into the LRFD Bridge Design Specifications. These specifications include specific guidance on when horizontal curvature effects must be considered. Bridge owners and designers need specifications and commentary, as well as examples that provide design guidance for horizontally curved concrete box-girder bridges.

The objective of NCHRP Project 12-71 was to develop specifications, commentary, and examples for the design of horizontally curved concrete box-girder bridges. The research was performed by Nutt, Redfield & Valentine, Orangevale, California; in association with David Evans & Associates, Inc., San Diego, California; and Zocon Consulting Engineers, Inc., Folsom, California. The report and appendices fully document the effort to develop the design procedures. (The appendixes are available on the TRB website at http://trb.org/news/blurb_detail.asp?id=9596)

CONTENTS

CHAPTER 1

Introduction

At one time, bridges on curved alignments were rare; however, modern highway bridges and traffic separation structures are commonly built on a horizontal curve. This change has come about because of higher traffic volumes and speeds, the geometric constraints of the urban environment, and improved structural forms that lend themselves to curved construction.

The concrete box-girder, particularly post-tensioned prestressed concrete that can span large distances, is one such structural form. The cross section of these structures is inherently strong in torsion. This is important because curvature induces high torsion forces. Also, because concrete can be easily molded into the required shape, it is ideal for curved construction. For these reasons, prestressed concrete box-girders have become the structure type of choice in many jurisdictions. A common application of curved structures is in freeway interchanges where connector ramps or "fly-overs" carry traffic from one freeway to another at relatively high speed. Cross sections of curved box-girders may consist of single-cell, multi-cell or spread box beams as shown in Figure 1-1. Because only a very few spread box beam bridges use curved beams, only the first two types were considered in this study.

It has become common practice to analyze and design these structures as if they were straight. Live load distribution is often addressed using the whole-width design approach. Local problems, such as the lateral forces induced by curved prestressing ducts, are often handled using specific design rules and details that have been developed over the years. For the most part, this design approach has been used successfully, but some recent cases of poor bridge performance have made it clear that this approach has its limitations.

Because it is likely that (1) the use of curved structures is going to increase and (2) the geometries of some of these structures will continue to push the limits with respect to the degree of curvature, span lengths and depths, the amount of required prestressing force, and so forth, better guidelines are required for their design. Such guidelines are the purpose of this project.

A significant body of research and development exists relative to the design and analysis of curved prestressed concrete box-girder bridges. Some of this information has found its way into design specifications, but much of it has not. There is a need to collect and analyze this information in order to evaluate its merit for nationwide design rules. Although much of this work has been conducted domestically, a significant body of work has been conducted by other countries and this work also needs to be considered.

Although most issues relative to design of curved concrete box-girders have been studied to some degree, gaps in our understanding need to be filled. With modern computer programs and analytical models calibrated to existing physical

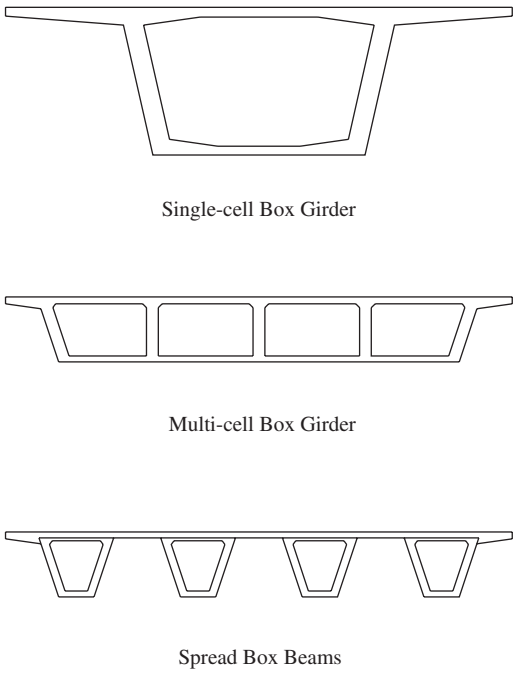

Figure 1-1. Types of cross sections.

and experimental results, most of this can be done through analytical studies. Additional physical testing of existing structures or laboratory experimentation, although important in and of themselves, are beyond the scope of this project and are not necessary to accomplish this project's intended goals.

This report presents the results of a review of the literature and the state of practice with respect to curved concrete box-girder bridges. In addition, detailed results from both global and local response analysis studies are presented. Final recommendations are presented in the final chapter and are implemented in the form of recommended changes to the *AASHTO LRFD Bridge Design Specifications and Commentary* and in analysis guidelines for these types of bridges. Example problems are also presented that illustrate the application of these recommendations.

CHAPTER 2

State-of-Practice Review

Domestic Practice

To obtain a better understanding of current U.S. practice, telephone interviews were conducted with representatives from key state DOTs. The states surveyed included California, Colorado, Florida, Hawaii, Idaho, Oregon, Nevada, New York, Tennessee, Texas, Washington and Wisconsin. Other states were contacted but chose not to participate.

Based on these interviews, current U.S. practice can be summarized as follows:

1. With the exception of California and Washington, most states interviewed have a fairly small inventory of curved concrete box-girder bridges (i.e., <1% each of reinforced and prestressed) although many see the number increasing in the future.
2. Cast-in-place construction is most popular in the West. Other states are tending toward segmental construction (cantilever and span-by-span using both precast and cast-in-place concrete) to avoid conflict with traffic. Colorado has used precast, curved, spliced "U" girders with a cast-in-place deck. The use of precast box-beams in most other states is limited to straight girders. Curvature, when present, is provided by a curved deck slab (i.e., variable overhangs). Northern and eastern states, where weather conditions cause more rapid deck deterioration, tend to avoid prestressed boxes because of the need to provide for future deck replacement.
3. Most curved box-girders are relatively narrow continuous ramp structures. A few are single span, and a significant number of all structures (approx. 20% to 30%) have skewed abutments. A small percentage of structures have skewed multi-column bents. Span lengths are usually less than 160 feet; however, approximately 20% exceed this limit.
4. The trend for the future appears to be dictated by the requirements of a built-up urban environment. More curved alignments, longer spans, more skewed supports, and more segmental construction are expected. Curved precast girder systems may also increase, particularly in Colorado where this type of construction has been successful.
5. Many states have experienced some problems with the performance of curved box-girder bridges, but not many as a percentage of the total. Cracking along the tendon and tendon breakout problems are absent or minimal where sufficient space is provided between the ducts. Torsion and flexural shear cracking seem to be rare and not necessarily limited to curved bridges. A few bearing failures have occurred, but have been avoided in states that avoid bearings altogether or use conservative bearing designs. In some cases, bearing uplift at the abutments has been observed to occur over time and is thought to result from the time-dependant behavior of concrete. Unexpected vertical or horizontal displacements of the superstructure are rare, but California has had some problems on skewed multi-column bents where movement about the c.g. of the column group has caused the transverse shear keys to engage. Lateral displacement of columns has also been observed.
6. Some states have special design rules. A few of these are discussed below.

Many states either use AASHTO LRFD (2004) or are adopting it.

Most states have no special rules for when a three-dimensional (3-D) analysis, such as a grillage or finite element analysis, should be performed and leave it to the discretion of the designer. Many states use an 800-foot radius as the trigger where designers should consider 3-D analysis. Most states have access to computer programs that can perform such an analysis. Almost all states use AASHTO wheel load distribution. California commonly uses the whole-width design approach.

No state had specific guidelines for varying the prestress force in the individual webs of curved box-girder bridges, although at least two states recognize that stresses can vary

transversely across the section and encourage designers to take the initiative to specify varying prestress force. The horizontal curvature of the tendons produces additional tension on the girder toward the inside of the curve, thus mitigating the severity of stress distribution across the section and the need to vary prestress force.

California recently experienced a tendon breakout failure on the 405/55 interchange (Seible, Dameron, and Hansen, 2003). Before that failure, they had published guidelines for designers related to the design of curved post-tensioned bridges (Caltrans, 1996). These guidelines dealt with the need for special detailing in curved webs, including criteria for when these details are not needed. This memo indicated that, because of the 405/55 structure's relatively large radius, tendon ties were not required in this structure. The problem resulted because of a separate Caltrans standard plan, not specifically related to curved bridges, that allowed up to six tendons 4½ inches or less in diameter to be stacked on top of one another without any space in between. Because the 405/55 was a long-span structure, several tendons needed to be stacked, resulting in radial forces being applied over a relatively wide area of essentially unreinforced cover concrete. This is thought to be the primary cause of the failure. Caltrans indicated that they currently have no special policy for prevention of tendon breakout failures except that designers are to provide tendon ties under certain circumstances. Breakout failures have not occurred when these ties are present.

Some other states indicated that they used the Caltrans tendon tie details to prevent tendon breakout failures.

Several states had requirements for providing space between tendons. Oregon requires that no more than three 4-inch-diameter or less ducts be stacked without a space of 1½ inches between a subsequent stack of ducts. The number of stacked ducts is reduced to two for duct diameters exceeding 4 inches. The current AASHTO LRFD specifications have duct spacing requirements that are similar to Oregon's. Texas also indicated that they have similar duct spacing requirements.

Colorado requires a duct spacing of 44% of the duct diameter or 1½ inches minimum. This applies to all ducts (i.e., no stacks). This is more conservative than AASHTO and most other states, but Colorado reports no breakout failures resulting from web curvature.

It appears that duct ties and duct spacing requirements have been successful in preventing tendon breakout failures. However, excessive duct spacing requirements can present problems at midspan and over the bents in continuous concrete box-girder superstructures because of the reduction in prestressing eccentricity and the corresponding increase in prestress forces that results. Because the action of the deck and soffit slabs tends to prevent breakout failures at points of maximum tendon eccentricity in box-girder structures, it is possible that spacing requirements could be relaxed at these locations. Duct spacing requirements do not affect tendon eccentricities where the ducts lie near the mid height of the webs. These are the locations of most breakout failures. These are also areas where actual duct curvatures may be amplified due to the horizontal deviation of tendons to accommodate end anchorage systems. Therefore, it should be possible to refine guidelines on duct spacing so as to both facilitate prestressing economies and prevent breakout failures.

Most states interviewed did not have specific guidelines for the design of bearings in curved box-girder bridges. Some states expressed a preference for certain types of bearings and others try to avoid the use of bearings in curved box-girder bridges.

Design for torsion in most states follows the AASHTO requirements. Colorado expressed a need for better guidelines for combining shear and flexural stresses. Colorado also uses precast "U" girders, which are temporarily braced for torsion during the placement of the cast-in-place deck. At least one state said they ignored torsion design, but this might be because they have only designed large radius bridges.

One point of interest is the combination of global shear and regional transverse bending stresses in the webs of curved box-girder bridges. Caltrans, which uses mostly cast-in-place bridges constructed on falsework, does not combine these stresses. The reasoning is that when the bridge is stressed, and regional transverse bending stresses are first realized, the bridge is on falsework and experiences no flexural or torsion shear stress. By the time falsework has been released, the prestress force is reduced because of relaxation and is not as critical for regional transverse bending. Other states have no specific guidelines and leave it to the designer to determine how these stresses should be combined.

Several states have standard details for concrete box-girder bridges. Most of these deal with prestress duct patterns and web reinforcing. Some of these were discussed above.

The requirements for the number and spacing of interior diaphragms vary among the states. The current AASHTO *Standard Specifications for Highway Bridges* (AASHTO, 1996) has specific requirements for the number and spacing of interior diaphragms in concrete box-girder bridges and several states use these or similar requirements. Diaphragms are not required in curved bridges with a radius of 800 feet or greater. For a radius between 400 and 800 feet the maximum diaphragm spacing shall not exceed 80 feet, and when the radius falls below 400 feet the maximum diaphragm spacing is 40 feet.

The *AASHTO LRFD Bridge Design Specifications* state that diaphragms are required in curved concrete box-girder bridges with a radius of 800 feet or less, but the code implies that their number and spacing are to be determined by the designer and depends on the radius and the dimensions of the

cross section. Specific guidelines on how to determine the number and spacing of interior diaphragms are not provided.

Colorado has standards for curved U girders with a cast-in-place deck that they have used with good success. These bridges often consist of several precast segments spliced together to form a span. Colorado projects that they will use this form more often in the future. It has the advantage of potentially eliminating falsework over traffic

A similar U section, although straight, was developed by NRV for use by a contractor on a bridge originally designed as a cast-in-place multi-cell box. The original design required building the superstructure on falsework set above final grade, lowering it to its final grade position, and then casting a monolithic bent cap to connect the bridge to the column. This approach overcame falsework clearance problems but presented some challenges for the contractor. In the contractor redesign, precast prestressed U sections set at final grade spanned the required falsework opening. Cast-in-place bottom soffit and stem pours were made on either end on the U girders. The cast-in-place pours were monolithic with the columns. A cast-in-place deck was then poured and continuity prestressing used to tie the entire structure together. This approach has some advantages and, as in Colorado, could be used on curved structures.

The Oyster Point Off-ramp in California also had a span consisting of curved precast girders made continuous with a cast-in-place multi-cell box section. This span crossed railroad tracks where falsework was not allowed. As a cost-savings measure, the contractor chose to use curved precast beams rather than straight beams with a curved cast-in-place deck. Girder erection required pick points to be located so that the girders would not "roll" and a temporary tie down system at the ends of the girders during the deck pour.

Despite these examples, curved box-beams appear to be relatively rare.

Foreign Practice

Concrete box-girder bridges are used around the world. Many of these are on horizontally curved alignments. A partial survey of recently constructed curved concrete box-girder bridges outside the United States was conducted by reviewing material published in engineering magazines and trade journals and from personal experience. Many of these bridges were built using segmental construction techniques. Although the survey was not exhaustive, its results are indicative of the bridges being built today.

Canada has been very active in developing design specifications that address the behavior of concrete box-girder bridges. The *Ontario Highway Bridge Design Code* (OHBDC) (1983) was an early attempt to codify design and analysis requirements for these types of bridges. Many of the provisions developed in this early code have influenced the development of the current Canadian Standards Association (CSA) design specifications (2000) and the updated version of the OHBDC (1998). Although curved box-girders are not specifically addressed in these codes, many of the analysis techniques identified for box-girders, such as the orthotropic plate analogy and the grillage analogy methods may be applicable to curved structures.

In Europe, most countries and most designers base their designs on the first principles of structural analysis and design. Although design codes are used, they are generally brief and bridge designers rely on traditional text books such as those by Menn (1990), Schlaich and Scheef (1982), or Strasky (2001); specific course work published by their professors at their university (Leonhardt, Menn, Strasky, etc.); or personal experience.

In Switzerland, the structural code is split into separate booklets. One each for loadings, concrete and prestressed concrete, steel, wood, and so forth. The two most applicable to NCHRP Project 12-71 (Loadings, and Concrete and Prestressed Concrete) are relatively brief documents compared with the current AASHTO LRFD. In general the Concrete and Prestressed Concrete booklet does not or only deals briefly with special structural configurations such as horizontal curvature. Instead, students at the two Universities, in Zurich and Lausanne, study structural design in a practical manner, preparing them for the professional situation in their own country. The textbook discussed above (Menn, 1990) is very similar to what students will encounter when at the university. Menn, who was a professor for many years, provides some general guidance on the design of horizontally curved beams and skewed bridges.

Swiss bridges on a curved alignment with a large radius are often designed without considering the curvature, except for the bearing design. Many design firms use methods they have developed over the years involving graphs and influence surfaces.

U.S. engineers with experience designing bridges in France have been contacted. It is our current understanding that the French favor precast segmental construction. Typically, these structures use external tendons with deviator blocks. As in most European countries, their design specifications are less prescriptive than those in the United States and designers rely on their own experience as well as other published material to analyze and design these bridges.

Germany has been a leader in the design of concrete box-girder bridges, and engineers like Fritz Leonhardt have been considered pioneers for this type of construction. Germans tend to favor cast-in-place construction. They have their own DIN code, but, as is typical of most European practice, they rely on the engineer to apply first principles in selecting analysis techniques and design details.

Based on the published literature (Branco and Martins, 1984; Danesi and Edwards, 1982 & 1983; Evans and Al-Rifaie, 1975; Goodall, 1971; Grant, 1993; Lim, Kilford, and Moffatt, 1971; Maisal and Roll, 1974; Perry, Waldron, and Pinkney, 1985; Pinkney, Perry, and Waldron, 1985; Rahai, 1996; Rasmussn and Baker, 1998; Trikha and Edwards, 1972) the British have been quite active in researching the behavior of curved concrete box-girder bridges. The British use their own code (BS5400) for bridge design.

The new "Eurocode" is intended to supersede the codes of the major European countries. The Eurocode has been developed over a number of years and is in use. However, this code has appendices that direct the designer to special provisions by individual countries (e.g., the DIN code for Germany and BS5400 for England) and, for the most part, practice still follows the traditional codes of the countries involved.

In Asia, the British BS5400 (India, Malaysia and Hong Kong) and AASHTO (Thailand, Taiwan, Korea and Philippines) codes are widely used. Japan, which has its own code, frequently builds curved concrete box-girder bridges.

The structural code in Brazil is quite brief and all encompassing. It is much more concise than the current U.S. design codes. Curved beams are not covered directly, although there is a section on torsion, but only with general instructions found in most textbooks. Bridges that have alignments with slight curvature are generally designed as straight bridges without consideration for the curve, except that bridge bearings are designed for eccentric loads taking into account the curve of the superstructures.

As of today, Brazil, Argentina, Chile, and Mexico, and some Latin American countries use computers and similar programs to those of the United States.

The AASHTO design specifications (not necessarily LRFD) are widely used by many other countries around the world.

Field Problems

Several failures of stem concrete due to the radial forces developed by curved prestress tendons have occurred over the years. These include the Las Lomas Bridge in 1978, the Kapiolani Interchange in 1981, and the 405/55 HOV Connector OC in 2002. Repair costs for some of these structures were significant (the Kapiolani Interchange was $4,000,000).

Prestress breakout failures have been linked to a combination of the regional action of the web acting as a beam between the top and bottom deck and the local slab action of the concrete cover over the prestressing tendons. Global actions, although theoretically a factor, have been found not to be important in these failures.

Many such failures have occurred even in straight bridges where local curvatures of prestressing ducts occur near the prestress anchorages. These stresses can either add to or subtract from the stresses developed from horizontal alignment of the bridge, depending on the direction of the tendon flare.

Several members of the project team were involved in investigating the 405/55 HOV Connector Overcrossing (OC) failure. Although the curvature of this structure was less than many, several other geometric characteristics of this structure led to the failure. First, because prestress radial forces per duct were under the limit beyond which Caltrans Memo 11-31 required tie reinforcement, none was placed. Also, because the structure had fairly long spans, the structure depth was relatively large as were the prestressing forces in each web. The resulting large number of ducts required (five per stem) for the increased prestress force were placed one on top of the other without any space between. The combination of proportionately larger radial prestress forces applied to a deeper web exacerbated regional concrete stresses. When these stresses were combined with the local stresses generated in the concrete cover over the stacked ducts, concrete cracking and spalling occurred. This particular design pushed the limits for Caltrans design requirements to prevent a breakout failure, and it is generally agreed that had the Caltrans lateral tie detail been used, the failure could have been prevented.

Abutment bearing failure progressing with time was experienced on the I-5 NB to Hwy 217 NB ramp in Oregon. The single cell box-girder is supported on two large bearings at the south abutment. Over time, the entire load at these bearings has shifted to only one of the bearings while the other has experienced uplift. These problems are thought to result from the time-dependent behavior of concrete. This theory is corroborated somewhat by the results observed in the time-dependent analyses of similar structures, although it is thought that currently commercially available software will tend to overpredict the problem because torsion creep is not considered.

Another recent bearing failure occurred on the bridge at Wildcat Road in Shasta County, California. This single-span curved prestressed concrete box-girder bridge was under construction. When the falsework was being removed, the bearings at the abutments began to fail. The outside elastomeric bearing was overloaded and was destroyed and the bearing at the inside of the curve began to lift off. This problem was corrected at the abutments by retrofitting the bridge with prestress bar tie-downs and eliminating the bearings. This essentially converted the seat abutments to end diaphragm abutments. Fortunately, the relatively short bridge length and the fact that most of the prestress shortening had already taken place made this possible.

Stirrups in the outside web were also inadequate to resist the combined effects of torsion and flexural shear in this structure. The web was retrofitted with external prestressing tendons that will correct the problem. This repair was deemed to be preferable to adding extra mild reinforcement within a web overlay.

Figure 2-1. Uplift at edge of bearing.

Figure 2-2. Construction of widened column.

A recent problem with two box-girder bridges in Coahuila, Mexico, that is apparently due to the curvature of the structures has developed. These bridges, which are relatively new, are cast-in-place, post-tensioned, continuous concrete box-girder bridges supported on single bearings at each non-integral single column. These relatively narrow multi-span ramp structures are experiencing ongoing deflections and lateral movement. It is not clear what is causing this behavior, but it is fairly certain that curvature is a factor. The bearings have experienced uplift from rotation of the superstructure as shown in Figure 2-1. The movement was severe enough to remove the superelevation placed in the bridge at the time of construction. Significant cracking of the superstructure was also observed. The bridge owner is attempting to correct the problem by increasing the size of the piers in the transverse direction as shown in Figure 2-2 and jacking and shimming the superstructure back to its original as-built position. The wider piers will allow bearings to be placed eccentric to the centerline of the superstructure and hopefully stabilize the situation. A lightweight overlay is also being considered to completely restore the superelevation.

CHAPTER 3

Published Literature Review

A large body of published literature is related to curved concrete box-girder bridges. Some of the documents most important to this project are discussed below.

Codes and Design Standards

Currently, there is no U.S. code specifically developed for the design of curved concrete box-girder bridges. *AASHTO LRFD Bridge Design Specifications* provide comprehensive specifications with commentary for the design of highway bridges. Our review of Codes and Design Standards is summarized below.

AASHTO, 2004, *AASHTO LRFD Bridge Design Specifications*, 3rd Edition with Interims, AASHTO, Washington, D.C.

A number of sections apply to the design issues associated with curved concrete box-girders. Selected specifications articles are as follows:

- Article 4.6.1.2.2, "Single-Girder Torsionally Stiff Superstructures," allows for the analysis of horizontally curved, torsionally stiff single-girder superstructures for global force effects as a curved spine beam.
- Article 4.6.1.2.3, "Multicell Concrete Box-Girders," allows for the design of horizontally curved cast-in-place multicell box-girders as single-spine beams with straight segments, for central angles up to 34° within one span, unless concerns about force effects dictate otherwise.
- Article 4.6.3.4, "Cellular and Box Bridges," allows for the refined analysis of cellular bridges by any of the methods specified in Article 4.4, "Acceptable Methods of Structural Analysis," except the yield line method, which accounts for the two dimensions seen in plan view and for the modeling of boundary conditions. Models intending to quantify torsional warping and/or transverse frame action should be fully three-dimensional.
- Article 4.7.4.3, "Multispan Bridges," specifies the minimum requirements for the seismic analysis of multispan bridges. Analysis requirements are based on the classification of a bridge as "regular" or "irregular." The classification of a curved bridge includes the maximum subtended angle and whether the spans are continuous or are multiple simple-spans.
- Article 5.4.6, "Ducts," specifies the requirements for duct material and curvature.
- Article 5.8, "Shear and Torsion," specifies comprehensive design procedures for flexural shear and torsion. The modified compression field theory is specified for flexural regions. Strut-and-tie models are specified for regions near discontinuities. Alternative design procedures are permitted for segmental bridges.
- Article 5.9.1.6, "Tendons with Angle Points or Curves," cross references Articles 5.4.6 and 5.10.4 for duct curvature and stress concentration considerations, respectively.
- Article 5.9.5.2.2.2, "Friction," specifies the friction loss due to curvature and includes specific requirements for determining the total 3-D angle change as typically found in curved girders with draped tendons.
- Article 5.10.3.3.3, "Curved Post-Tensioning Ducts," specifies the clear distance between curved ducts as required for tendon confinement as specified in Article 5.10.4.3 but not less than that required for straight ducts.
- Article 5.10.4.3, "Effects of Curved Tendons," specifies that, where tendons are placed in curved webs, additional cover and/or confinement reinforcement shall be provided.
- Article 5.10.4.3.1, "In-Plane Force Effects," defines the in-plane deviation force effects due to the change in direction of the tendon as $F_{u\text{-}in} = P_u/R$ where P_u is the factored tendon force and R is the radius of curvature of the tendon. Specific requirements for local lateral shear on the unreinforced concrete cover are given and neglect any increase in lateral shear capacity for widely spaced tendons. Where the factored in-plane deviation force exceeds the lateral shear resistance

of the concrete cover, tieback reinforcement is required. Where stacked ducts are used in curved girders, the moment resistance of the concrete cover, acting in flexure, shall be investigated, but no specific methodology or stress requirements are provided. For curved girders, the global flexural effects of out-of-plane forces shall be investigated.

- Article 5.13.2.2, "Diaphragms," requires the use of diaphragms at abutments, piers, and hinge joints. Intermediate diaphragms may be used in beams in curved systems or where necessary to provide torsional resistance. Intermediate diaphragms shall be used in curved box-girders with an inside radius of less than 800 feet. Diaphragms may be omitted where tests or structural analysis show them to be unnecessary.
- Article 14.4.1, "General," specifies the movement requirements for joints and bearings. It includes the requirement to consider the effects of curvature, skew, rotations, and support restraint. The commentary includes additional discussion pertinent to curved bridges.

With respect to torsion design, a detailed review of the specifications was performed. The following briefly describes the design methods, outlines the basic steps of designing a box section for the combined actions of flexural shear, torsion, and moment, and includes a discussion (*in italics*) where further guidance is required in interpreting or applying the LRFD specification.

Design Methods

Two basic design methods, specified in Articles 5.8.3 and 5.8.6, depend on construction method and structure type. A sectional model using the modified compression field theory with a variable angle truss model is the basis of Article 5.8.3 and applies in most cases. Article 5.8.6 contains the flexural shear and torsion provisions specific to segmental post-tensioned concrete box-girder bridges. A conservative expression for the concrete contribution and a 45° truss model are assumed.

General Comment – There is a minor conflict between Articles 5.8.3 and 5.8.6. Article 5.8.3 states that Article 5.8.6 may be used for segmental post-tensioned concrete box-girder bridges while Article 5.8.6 states that Article 5.8.6 shall be used for segmental post-tensioned concrete box-girder bridges in lieu of Article 5.8.3. It needs to be clarified whether Article 5.8.6 is a permissible or mandatory procedure for segmental bridges. Additionally, Commentary Article C5.8.6.1 states, "For types of construction other than segmental box-girders, the provisions of Article 5.8.3 may be applied in lieu of the provisions of Article 5.8.6." It appears that the word may should be replaced by shall, unless the intent is to permit Article 5.8.6 as an alternative design method for bridge types other than segmental.

Design Steps (General Sectional Model)

The following outlines the basic steps of designing the exterior web of a box section for the combined actions of flexural shear, torsion, and moment. It is based on the provisions of Article 5.8.3 and, therefore, does not cover the steps for a segmental post-tensioned concrete box-girder bridge.

Step 1 – Determine the Controlling Load Cases

Determine the controlling load cases for the applicable strength limit states. Consider the concurrent actions on the section. As a minimum, consider the following two cases:

1. Maximum flexural shear and concurrent actions
2. Maximum torsion and concurrent actions

Perform Steps 3 through 7 separately for each the above cases and any additional cases that may potentially govern the design.

Step 2 – Determine the Cross-Section Parameters

A_{cp} – total area enclosed by outside perimeter of concrete cross section (Article 5.8.2.1)
p_c – the length of the outside perimeter of concrete cross section (Article 5.8.2.1)

$A_{cp}^2 / Pc \le 2A_o b_v$ (Equation 5.8.2.1-5)

(Comment – LRFD Article 5.8.2.1 does not address the case when the thickness of the flange of a non-segmental box section is less than the effective web width. This is addressed in Article 12.2.10 of the Segmental Guide Specification (Reference 2) and LRFD Article 5.8.6.3 for segmental bridges.)

A_o – area enclosed by the shear flow path (in.^{2}) (Article 5.8.2.1)
d_s – the length of the torsional shear flow path on the exterior web (in.) (Commentary 5.8.2.1)
p_h – perimeter of the centerline of the closed transverse torsion reinforcement (in.) (Article 5.8.2.1)
b_v – effective web width (in.) (Article 5.8.2.9)
d_v – effective shear depth (in.) (Article 5.8.2.9)

Step 3 – Check the Web Width

Verify that the effective web width is adequate to prevent web crushing:

$V_u \le \phi V_n$
$Vn \le 0.25 f_c' b_v d_v + V_p$ (Equation 5.8.3.3-2)

(Comment – It may be prudent to reduce V_n by the torsional shear when web crushing governs the capacity. Provisions for considering the combined flexural shear and torsional shear are required by Article 12.3.1 of the Segmental Guide Specification and LRFD Equation 5.8.6.5-3 for segmental bridges.)

Increase web width if Equation 5.8.3.3-2 is not satisfied.

Step 4 – Calculate Shear Stress

Check if torsion must be considered:

$T_u > 0.25\phi T_{cr}$ (Equation 5.8.2.1-3)

$$T_{cr} = 0.125\sqrt{f_c'}\frac{A_{cp}^2}{p_c}\sqrt{1+\frac{f_{pc}}{0.125\sqrt{f_c'}}}$$ (Equation 5.8.2.1-4)

For $T_u > 0.25\phi T_{cr}$, calculate the equivalent factored shear force, V_u, acting on the web where the flexural shear and the torsional shear are additive as follows:

$V_u = V_{u\,(flexure)} + T_u d_s/(2A_o)$ (Equation 5.8.2.1-7)

(Comment – V_u is determined for a single girder and T_u is acting on the total cross section.)

General Comment – The fifth paragraph of Commentary C5.8.2.1 regarding the equivalent factored shear force would benefit from additional clarification. There is a mention of a stress limit for the principal tension at the neutral axis of the section but the specific code section was not referenced. Article 5.8.5 provides limits on the principal tensile stress in the webs of segmental concrete bridges at the Service III limit state and during construction. As the principal stresses are checked using service load, V_u is not applicable. It appears that the intent of the equivalent factored shear force is to consider the increased shear force and resulting shear stress due to torsion in calculating ε_x, θ, β, and V_c. It appears that equivalent factored shear force should not be considered in determining the required shear capacity, ϕV_n, or the required tensile capacity specified in Article 5.8.3.5.

Using the equivalent factored shear force, V_u, acting on the exterior web where the flexural shear and the torsional shear are additive, calculate the shear stress as follows:

$v_u = (V_u - \phi V_p)/(\phi b_v d_v)$ (Equation 5.8.2.9-1)

(Comment – Note that v_u includes the effects of flexural shear and torsional shear.)

Step 5 – Calculate v_u/f_c' and ε_x and Find θ and β

Calculate v_u/f_c' using v_u calculated in Step 4. This accounts for the increased shear stress due to torsion and will be used to determine θ and β from Table 5.8.3.4.2-1.

Calculate $\varepsilon_x = \dfrac{\left(\dfrac{|M_u|}{d_v} + 0.5N_u + 0.5|V_u - V_p|\cot\theta - A_{ps}f_{po}\right)}{2\cdot(E_sA_s + E_pA_{ps})}$ (Equation 5.8.3.4.2-1) using the equivalent factored shear force, V_u, determined in Step 4.

(Comment – This simply adds the tensions due to flexural shear and to torsion for the exterior web where the flexural shear and torsional shear are additive and appears to be conservative. Collins and Mitchell (1980) pages 399–400, use an equivalent longitudinal tension for combined flexural shear and torsion equal to the square root of the sum of the squares of the individually calculated tensions for flexural shear and for torsion.)

If whole-width design is used, forces acting on the total section are applied. In this case, the shear force is conservatively taken as the equivalent factored shear force, V_u, determined in Step 4 multiplied by the total number of webs.

(Comment – Whole-width design is not specifically addressed and would benefit from clarification in this area.)

This accounts for the increased longitudinal tensile force due to torsion and will be used to determine θ and β from Table 5.8.3.4.2-1.

Using the calculated values of v_u/f_c' and ε_x, find θ and β from Table 5.8.3.4.2-1.

Step 6 – Determine Required Spacing of Stirrups

The amount of transverse reinforcement required for shear is found from

$V_u \le \phi V_n$

(Comment – Clarify that the factored flexural shear, not the equivalent factored shear force, is used for V_u, as the transverse reinforcement for torsion is determined separately.)

$V_n = V_c + V_s + V_p$ (Equation 5.8.3.3-1)

Where

$V_c = 0.0316\beta\sqrt{f_c'}\, b_v d_v$ (Equation 5.8.3.3-3)

$V_s = (A_v f_y d_v \cot\theta)/s$ (Equation C5.8.3.3-1)

$A_v/s = V_s/(f_y d_v \cot\theta)$

The amount of transverse reinforcement required for torsion is found from

$T_u \le \phi T_n$

Where

$T_n = (2A_oA_tf_y\cot\theta)/s$ (Equation C5.8.3.6-2)
$A_t/s = T_n/(2A_of_y\cot\theta)$

For the exterior web of a box section, the combined area of both stirrup legs in the web, $A_{stirrups}$, contributes to A_v and A_t, therefore the maximum spacing of the stirrups, S_{max}, is given by:

$S_{max} = A_{stirrups}/[(A_v/s)_{flexural\ shear} + (A_v/s)_{torsion}]$

Step 7 – Check the Longitudinal Reinforcement

The required tensile capacity of the longitudinal reinforcement on the flexural tension side of the member is found from Equation 5.8.3.5-1.

(Comment – Clarify that the flexural shear, not the equivalent factored shear force, is used for V_u, as the additional longitudinal reinforcement for torsion is determined separately.)

The longitudinal reinforcement required for torsion, in addition to that required for flexure, is found from

$A_l = T_n\, p_h/(2A_of_y)$ (Equation 5.8.3.6.3-2)

Comments:

Article 5.8.3.6.3 would benefit from a clarification that A_l is also in addition to the required tensile capacity from Equation 5.8.3.5-1 when Equation 5.8.3.5-1 exceeds the longitudinal reinforcement required for flexure.

The distribution of A_l within the cross section needs to be clarified. Article 5.3, "Notation," and Article 5.8.6.4, "Torsional Reinforcement," define it as the area of longitudinal torsion reinforcement in the exterior web of the box-girder, which appears to be incorrect. LRFD Equations 5.8.3.6.3-2 and 5.8.6.4-3 are essentially identical to the equation in Article 12.3.8 of the Segmental Guide Specification, which specifies that A_l shall be distributed around the perimeter of the closed stirrups.

Prestressing steel should also be permitted to satisfy Equation 5.8.3.6.3-2 similar to Article 12.3.8 of the Segmental Guide Specification and LRFD Commentary Article C5.8.6.4 for segmental bridges. The area of longitudinal torsion reinforcement in the flexural compression zone should be permitted to be reduced similar to Segmental Guide Specification Article 12.3.9 and LRFD Equation 5.8.6.4-4 for segmental bridges.

Design Steps (Segmental Box-Girder)

The following outlines the basic steps of designing the exterior web of a box section for the combined actions of flexural shear, torsion, and moment. It is based on the provisions of Article 5.8.6 and, therefore, applicable to a segmental post-tensioned concrete box-girder bridge.

Step 1 – Determine the Controlling Load Cases

The design for flexural shear and torsion in segmental bridges shall be performed at the strength limit state per Article 5.8.6.2. The shear component of the primary effective longitudinal prestress force, V_p, shall be added as a load effect with a load factor of 1.0. The component of inclined flexural compression or tension, in the direction of the applied shear, in variable depth members shall be considered when determining the design factored shear force.

In accordance with Article 5.8.5, principal stresses at the neutral axis of segmental bridges shall not exceed the tensile stress limits of Table 5.9.4.2.2-1 at the Service III limit state and Table 5.14.2.3.3-1 during construction

Determine the controlling load cases for each of the three applicable limit states separately (Strength, Service III, and during construction). Consider the concurrent actions on the section. As a minimum, consider the following two cases for each of the limit states:

1. Maximum flexural shear and concurrent actions
2. Maximum torsion and concurrent actions

Perform Steps 3 through 6 separately for each of the above Strength cases and any additional Strength cases that may govern the design.

In Step 4, check the principal stresses separately for each of the above Service III and construction cases and any additional Service III and construction cases that may govern the design.

Step 2 – Determine the Cross-Section Parameters

A_o – area enclosed by the shear flow path (in.^{2}) (Article 5.8.6.3)

b_e – effective width of shear flow path, but not exceeding the minimum thickness of the webs or flanges comprising the closed box section.(in.) b_e shall be adjusted to account for the presence of ducts as specified in Article 5.8.6.1. (Article 5.8.6.3)

b_e may be taken as A_{cp}/p_c (Article 5.8.6.3)

A_{cp} – area enclosed by outside perimeter of concrete cross section (in.^{2}) (Article 5.8.6.3)

p_c – the outside perimeter of concrete cross section (in.) (Article 5.8.6.3)

p_h – perimeter of the centerline of the closed transverse torsion reinforcement (in.) (Article 5.8.6.4)

b_v – effective web width (in.) (Article 5.8.6.5)
d_e – effective depth from extreme compression fiber to the centroid of the tensile force in the tensile reinforcement (in.) (Article 5.8.6.4)
d_v – effective shear depth (in.) (Article 5.8.6.5)

Step 3 – Check if Torsion Must be Considered

Check if torsion must be considered:

$T_u > \frac{1}{3}\phi T_{cr}$ (Equation 5.8.6.3-1)

$T_{cr} = 0.0632K\sqrt{f_c'}\ 2A_o b_e$ (Equation 5.8.6.3-2)

$K = \sqrt{1 + \frac{f_{pc}}{0.0632\sqrt{f_c'}}} \le 2.0$ (Equation 5.8.6.3-3)

f_{pc} = Unfactored compressive stress in concrete after prestress losses have occurred either at the centroid of the cross section resisting transient loads or at the junction of the web and flange when the centroid lies in the flange. (Article 5.8.6.3)

Step 4 – Check the Web Width

Verify the effective web width is adequate to prevent web crushing:

$V_u \le \phi V_n$

$V_n \le 0.379 f_c'^{0.5} b_v d_v$ (Equation 5.8.6.5-2)

$V_u/(b_v d_v) + T_u/(2A_o b_e) \le 0.474 f_c'^{0.5}$ (Equation 5.8.6.5-3)

(Comment – It appears that V_u and T_u should be replaced by V_n and T_n, respectively, in this equation to be consistent with Article 12.3.1b of the Segmental Guide Specification.)

Increase web width if either Equation 5.8.6.5-2 or Equation 5.8.6.5-3 is not satisfied.

Check the allowable principal tensile stress for Service Limit State III and during construction in accordance with Article 5.8.5. Consider the compressive stress due to vertical tendons in the webs. Increase the web width or the vertical prestressing force in the web if the allowable principal stresses are exceeded.

Step 5 – Determine Required Spacing of Stirrups

The amount of transverse reinforcement required for shear is found from

$V_u \le \phi V_n$

$V_n = V_c + V_s$ (Equation 5.8.6.5-1)

Where

$V_c = 0.0632K\sqrt{f_c'}\ b_v d_v$ (Equation 5.8.6.5-4)
$V_s = A_v f_y d_v/s$ (Equation 5.8.6.5-5)
$A_v/s = V_s/(f_y d_v)$

The amount of transverse reinforcement required for torsion is found from

$T_u \le \phi T_n$

Where

$T_n = 2A_o A_v f_y/s$ (Equation C5.8.6.4-2)
$A_v/s = T_n/(2A_o f_y)$

For the exterior web of a box section, the combined area of both stirrup legs in the web, $A_{stirrups}$, contributes to the transverse hoop reinforcement for flexural shear and torsion, therefore, the maximum spacing of the stirrups, S_{max}, is given by

$S_{max} = A_{stirrups}/[(A_v/s)_{flexural\ shear} + (A_v/s)_{torsion}]$

When vertical tendons are provided in the web, the design yield strength for flexural shear and torsion design shall be taken in accordance with Article 5.8.2.8.

Step 6 – Check the Longitudinal Reinforcement

The minimum additional longitudinal reinforcement required for torsion (in addition to that required for other concurrent actions), shall satisfy

$A_l = T_u p_h/(2\phi A_o f_y)$ (Equation 5.8.6.4-3)

Comment: The distribution of A_l within the cross section needs to be clarified. Article 5.3, "Notation," and Article 5.8.6.4, "Torsional Reinforcement," define it as the area of longitudinal torsion reinforcement in the exterior web of the box-girder, which appears to be incorrect. Article 5.8.6.4 contains a conflicting statement that A_l shall be distributed around the perimeter of the closed stirrups in accordance with Article 5.8.6.6 which appears to be correct. LRFD Equation 5.8.6.4-3 is essentially identical to the equation in Article 12.3.8 of the Segmental Guide Specification which specifies that A_l shall be distributed around the perimeter of the closed stirrups.

In determining the required amount of longitudinal reinforcement, the beneficial effect of longitudinal prestressing is taken into account by considering it equivalent to an area of reinforcing steel with a yield force equal to the prestressing force. (Commentary Article C5.8.6.4)

Subject to the minimum reinforcement requirements of Article 5.8.6.6, the area of additional torsion reinforcement in

the flexural compression zone may be reduced by an amount equal to

$M_u/(0.9d_e f_y)$ (Equation 5.8.6.4-4)

AASHTO (2003a) *Guide Specifications for Horizontally Curved Steel Girder Highway Bridges*, American Association of State Highway and Transportation Officials, Washington, D.C.

This is a recently published AASHTO Guide Specification for curved steel bridges, including box-girders. It has been suggested that the design specification contained therein be used as a model for NCHRP Project 12-71. This specification discusses design philosophy and limit states and includes provisions for loads; structural analysis; design of flanges, webs, shear connectors, bearings, splices and connections; deflections; and constructability. It also includes a construction specification and design examples for both an I girder and box-girder bridge.

AASHTO (1999) *Guide Specifications for Design and Construction of Segmental Concrete Bridges*, 2nd Edition with Interims, American Association of State Highway and Transportation Officials, Washington, D.C.

This second edition of the guide specifications for segmental concrete bridges was prepared for use in conjunction with the *Standard Specifications for Highway Bridges (non-LRFD)*, and subsequent interim revisions to these specifications. This publication, which was developed by a broad-based committee organized by the American Segmental Bridge Institute, embodies several concepts, which are significant departures from previous design and construction provisions. It is based on recent research in the United States and abroad. The committee included representatives of state DOTs, the FHWA, academicians, consulting engineers, contractors, and suppliers. Some of the details of this specification were discussed above.

Design Philosophy

A number of books and papers have been written about the design of concrete box-girder bridges. Many of these discuss the effect of horizontal curvature on the behavior of these bridges. A few of these publications are discussed below.

Menn, C. (1990) *Prestressed Concrete Bridges*, ISBN 3-7643-2414-7, Birkhauser Verlag, Basel

This book provides engineers with a comprehensive overview of the fundamental principles governing the design and construction of concrete bridges. The content is based on the author's direct experience gained from the design and construction of bridges in Switzerland. Although much of the content is based on Swiss standards and practices, the material stresses fundamental principles. This book covers straight, skewed, and curved bridges consisting of both open sections and closed box sections. The book addresses issues applicable to horizontally curved box-girder bridges.

Article 4.6.4, "Detailing," discusses the deviation forces generated by curved post-tensioning tendons. The deviation force per unit length is determined as the tendon force divided by the radius of curvature of the tendon. An example of the regional transverse bending moment in the web of a horizontally curved member is presented.

Article 5.1.4, "Structural Models for Bridge Superstructures," provides guidance on developing analytical models that can be applied to curved box-girder bridges. For example, techniques for developing grillage models of multi-cell box-girders are presented.

Article 5.3.2(b), "Web Design for Shear and Transverse Bending," presents a rational method for the design of webs subject to combined shear and regional transverse bending, a condition that occurs in horizontally curved post-tensioned box-girder bridges. The method is based on Swiss practice and neglects the concrete contribution to the shear capacity. Shear-regional transverse bending interaction diagrams are presented.

Article 5.3.4, "Diaphragms," discusses the function, necessity, and design of internal diaphragms. Diaphragms are recommended at abutments and piers. The use of intermediate diaphragms is usually not necessary in straight and lightly curved box-girder bridges.

Article 6.1.3(b) "Influence of Girder Curvature," discusses the qualitative difference in superstructure displacements due to temperature and shrinkage versus longitudinal prestressing in horizontally curved bridges.

Article 7.6, "Curved Girder Bridges," is devoted entirely to horizontally curved bridges. The article includes subsections on Conceptual Design, Analysis, Transformation of Torque into Torsional Sectional Forces, Prestressing, and Prestressing Concept and Tendon Layout.

The discussion of the conceptual design of curved box-girders points out the role of torsion in design and how, at ultimate loads, torsion and bending moment can be redistributed. The effect of torsion on bearing forces may require the bearings to be placed away from the webs. Expansion bearings must be able to accommodate both temperature and prestress shortening displacements, which will be in different directions.

The book presents a simplified method for analyzing curved bridges iteratively. The method does not satisfy compatibility equations exactly, but greatly simplifies the computational effort. An example is given. Simple vector diagrams are presented to illustrate how torsional section forces are developed by a variation in the direction of longitudinal bending moments due to the curvature of the superstructure and resisted by shear flow around the perimeter of the box section.

Prestressing can produce longitudinal and transverse bending and shear forces as well as torque in curved box-girder bridges. Torsion, which can increase flexural stresses, must be considered in determining the required prestressing force. Prestressing can also be used to enhance torsional and transverse bending resistance, although this is often avoided for economic reasons.

Sennah, K. M., and Kennedy, J. B. (2001) "State-of-the-Art in Curved Box-Girder Bridges," *Journal of Bridge Engineering*, ASCE, Vol. 6, No. 3, pp. 159–167.

The objective of this paper was to provide highlights of the most important references related to the development of current guide specifications for the design of straight and curved box-girder bridges. As such, it provided an excellent bibliography from which to identify other papers that were reviewed in detail. Subjects discussed in this review included (1) different box-girder bridge configurations, (2) construction issues, (3) deck design, (4) load distribution, (5) deflection and camber, (6) cross-bracing requirements, (7) end diaphragms, (8) thermal effects, (9) vibration characteristics, (10) impact factors, (11) seismic response, (12) ultimate load-carrying capacity, (13) buckling of individual components forming the box cross section, (14) fatigue, and (15) curvature limitations provided by the codes for treating a curved bridge as a straight one. The literature survey presented herein encompasses (1) the construction phase, (2) load distribution, (3) dynamic response, and (4) ultimate load response of box-girder bridges.

ASCE Committee on Construction Equipment and Techniques (1989) "Concrete Bridge Design and Construction in the United Kingdom," *Journal of Construction Engineering and Management*, Vol. 115, No. 4, pp. 618–635.

The design and construction of concrete bridges in the United Kingdom has changed rapidly during recent decades. Better analytical methods, increased mechanization, and better planning in the construction of these bridges have brought this about. However these steps have also resulted in new problems for the engineer, contractor, and supervisor. This paper shows the different approaches on several factors. The paper is divided into three parts as follows:

1. The design of bridges in classes for span and type with reference to the pertinent factor for that design;
2. The contractor's approach to construction that illustrates the need for flexibility in the construction method in order to meet contract deadlines; and
3. The views of the supervising engineer and his means of achieving a balance between the designer's intentions and the contractor's proposals.

Schlaich, J., and Scheef, H. (1982) *Concrete Box-Girder Bridges*, ISBN 3 85748 031 9, International Association for Bridge and Structural Engineering, Zurich, Switzerland

This publication is the outcome of a comprehensive survey of concrete box-girder bridges. The publication is divided into three main parts, "Design," "Structural Analysis," and "Dimensioning and Detailing." A comprehensive reference list is included. The publication addresses straight, skew, and curved bridges.

The "Design" section covers several aspects of curved bridges. Recommendations are given for when the longitudinal bending moments can be determined as for a straight bridge and then combined with the torsional effects without considering the coupling of the two effects on each other. Alternative substructure configurations are discussed for curved bridges.

The "Structural Analysis" section discusses the mutual influence of the longitudinal bending moments and torsional moments for horizontally curved bridges. A simple table of equations based on classical curved beam theory is presented for several different loading conditions of a curved single-span bridge with fixed supports.

The "Dimensioning and Detailing" section covers several aspects of curved bridges. Dimensioning and reinforcement of the web for flexural shear, torsion, and regional transverse bending is addressed, including a rational method of designing the web reinforcement for combined shear and regional transverse bending. The influence of horizontal curvature on the movements at bearings is also discussed.

Response of Curved Concrete Box-Girder Bridges

Global Analysis

Most published research seems to be directed toward the global response of box-girder bridges. Several analytical techniques have been studied. Many of these are relatively complex, but many others are suitable for production design practice. Our current belief is that a properly applied grillage analogy method provides good results and may be most suitable for analyzing bridges with significant curvature. The following paragraphs discuss some of the papers and reports that were reviewed.

Al-Rifaie, W. N., and Evans, H. R. (1979) *An Approximate Method for the Analysis of Box-girder Bridges that are Curved in Plan*, Proc., Int. Association of Bridges and Structural Engineering, Int. Association for Bridge and Structural Engineering (IABSE), pp. 1–21.

An approximate method for analyzing curved box-girder bridges using the nodal section method is described. This

method, originally developed for straight box-girders, has been adapted for curved box-girders and is useful for preliminary design of these structures. The method developed applies to simple-span, single-cell box-girders.

In this procedure, the transverse nodal section is idealized as a plane frame. Nodes on the frame are assumed to be fixed against translation but free to rotate. Each frame is analyzed and the reactions at the nodes are determined. The reactions are then applied to longitudinal plates that represent the components of the box-girder. The plates can only resist in-plane forces. The final step is to apply a "sway correction" procedure that will make the displacements of the nodes in each of the transverse nodal sections compatible with the deflections of the nodes along the edges of the longitudinal plates. This approach results in substantial computational savings over the finite element method and is well suited to preliminary design studies.

The method was checked against finite element results for model bridges representing both concrete and steel box-girders. Several different span-to-radius ratios and loading conditions were considered. In general, good correlation was found for critical stresses, although some discrepancy was found for non-critical stresses. The method as developed does not accurately account for shear lag in the deck.

Studies have extended this method to multi-cell box-girders and have developed methods to account for shear lag in straight box-girders. These refinements are also being considered for curved box-girders.

Bazant, Z., and El Nimeiri, M. E. (1974) "Stiffness Method for Curved Box-girders at Initial Stress," ***Journal of the Structural Division*****, Vol. 100, No. 10, pp. 2071–2090.**

A sophisticated numerical method of analysis of the global behavior of long curved or straight single-cell girders with or without initial stress is presented. It is based on thin-wall beam elements that include the modes of longitudinal warping and of transverse distortion of the cross section. Deformations due to shear forces and transverse bi-moment are included, and it is found that the well-known spurious shear stiffness in very slender beams is eliminated because the interpolation polynomials for transverse displacements and for longitudinal displacements (due to rotations and warping) are linear and quadratic, respectively, and an interior mode is used. The element is treated as a mapped image of one parent unit element and the stiffness matrix is integrated in three dimensions, which is numerical in general, but could be carried out explicitly in special cases. Numerical examples of deformation of horizontally curved bridge girders, and of lateral buckling of box arches, as well as straight girders, validate the formulation and indicate good agreement with solutions by other methods. This method is most applicable to steel box-girders and is of little use to our project.

Buragohain D. N., and Agrawal, B. L. (1973) "Analysis of Curved Box-Girder Bridges," ***Journal of the Structural Division*****, Vol. 99, No. 5, pp. 799–819.**

A discrete strip energy method is presented for the analysis of curved box-girder bridges of arbitrary cross section and various forms of curved folded plate structures simply supported at the two ends and composed of elements that may, in general, be segments of conical frustra. The method described applies to orthotropic material properties, arbitrary cross sections, constant curvature, and pinned supports at both ends. The method is based on harmonic analysis in the circumferential direction. The total potential energy of the structure is discretized into energy due to extension and bending and energy due to shear and twisting. The two types of circumferential strip elements are obtained by using a modified finite difference discretization in the transverse direction. The use of minimum energy principles yields two types of element matrices assembled to form the overall stiffness matrix of the structure following stiffness matrix procedures. Results of two examples obtained by the method are compared with available solutions. The applicability of this paper to NCHRP 12-71 is limited because it only applies to simply supported bridges, and the tool (software) to implement this method is not readily available.

Choudhury, D., and Scordelis, A. C. (1988) "Structural Analysis and Response of Curved Prestressed Concrete Box-Girder Bridges," ***Transportation Research Record 1180*****, Transportation Research Board, National Research Council, Washington, D.C., pp. 72–86.**

A numerical finite element analysis method for linear-elastic analysis and nonlinear material analysis of curved prestressed concrete box-girder bridges is demonstrated through two examples. A curved nonprismatic thin-walled box-beam element is used to model the bridges. The cross section of the element is a rectangular single-cell box with side cantilevers. Eight displacement degrees of freedom, including transverse distortion and longitudinal warping of the cross section, are considered at each of the three element nodes. Prestressing, consisting of post-tensioned bonded tendons in the longitudinal direction, is considered. For nonlinear material analysis, the uniaxial stress-strain curves of concrete, reinforcing steel, and prestressing steel are modeled. The shear and the transverse flexural responses of the box-beam cross section are modeled using trilinear constitutive relationships based on cracking, yielding, and ultimate stages. The first example demonstrates the versatility

of the numerical method in determining the linear-elastic distribution of forces in a three-span prestressed box-girder bridge of curved plan geometry and variable cross section. Dead load, live load, and prestressing load cases are analyzed. In the second example, overload behavior and ultimate strength of a three-span curved prestressed concrete box-girder bridge under increasing vehicular load are investigated. The different response characteristics of the bridge induced by different transverse locations of the overload vehicle are presented.

Although the finite element formulation might be detailed and comprehensive and conducive to studying the ultimate behavior of concrete box-girder bridges, its applicability to the planned global elastic analysis studies is limited due to its complex nature.

Chu, K. H. and Pinjarkar, S. G. (1971) "Analysis of Horizontally Curved Box-Girder Bridges," *Journal of the Structural Division*, Vol. 97, No. 10, pp. 2481–2501.

A finite element method for the analysis of simply supported curved girder bridges with horizontal sector plates and vertical cylindrical shell elements is outlined. Stiffness coefficients of sector plates are presented herein whereas stiffness coefficients of shell elements are based on Hoff's solution of Donnell's equations. The authors claim that this analysis is much more accurate than other methods of analysis.

Results of a sample bridge analysis are shown with stresses and deflections reported for a simply supported multi-cell concrete bridge. Some interesting results, particularly those with respect to the effect of radius of curvature, were obtained. Although a comparison is made of the results of a curved twin box-girder bridge obtained by the proposed method and another approximate analytical method (Tung, 1967), no comparisons with other (simpler) analysis methods are given. The FEM analysis tool itself is not readily available and thus is of limited use, but the results of the analysis can serve as a comparison case for measuring the accuracy of other methods, if more detail on the presented example can be obtained.

Bridge Design System (BDS) (1986) *A Computer Program for Analysis and Design of Multi-Cell Box-girder Bridges*, ECC.

The described software program is the most commonly used software for design of multi-cell box-girder bridges. Bridges are modeled as plane frames ignoring all horizontal curve effects. This modeling technique is significant for NCHRP Project 12-71 because the technique is commonly used in practice and its limits of applicability need to be investigated.

Computers and Structures, Inc. (1998) "SAP2000 – Integrated Finite Element Analysis and Design of Structures," CSI, Berkeley, California.

This reference constitutes the concrete structure portion of the SAP2000 Manual, with emphasis on design code check analysis. SAP2000 features integrated modules for design of both steel and reinforced concrete structures. The program provides the user with options to create, modify, analyze, and design structural models. The program is structured to support various design codes for the automated design and check of concrete frame members. The program currently supports several foreign and domestic design codes. Given that the design code check features of the program focus on frame analysis, these design code checks are of limited usefulness for the specialized needs of curved concrete box-girder bridge "local" or sectional ("regional") analysis. But the program is, of course, very useful for global analysis.

Chapter II of this reference outlines various aspects of the concrete design procedures of the SAP2000 program. This chapter describes the common terminology of concrete design as implemented in SAP2000. Each of six subsequent chapters gives a detailed description of a specific code of practice as interpreted by and implemented in SAP2000. Each chapter describes the design loading combination, column and beam design procedures, and other special consideration required by the code.

Aside from the obvious use as a SAP user reference, this document is useful as a summary (and side-by-side comparison) of various design codes for concrete columns and beams. Other than this, it is of limited direct utility to NCHRP Project 12-71. There is no coverage of design or analysis of prestressing in this document.

Fu, C. C., and Tang, Y. (2001) "Torsional Analysis for Prestressed Concrete Multiple Cell Box," ASCE *Journal of Engineering Mechanics*, Vol. 127, No. 1, pp. 45–51.

Using the Softened Truss Model, the authors present the formulation for calculating torsional effects in a multi-cell reinforced and prestressed concrete box-girder bridge. This paper asserts that because concrete box-girder sections are not made of thin webs and flanges, the stress distribution in these components is not constant and varies through the thickness, causing the effective stiffness of the member to be less than that observed at low values of load (torque). The formulation is coded in a computer program and the results from an example problem are presented. This research may be of some value to NCHRP Project 12-71 if the methodology can be simplified and used as the basis of simplified methods for calculating torsional effects. However,

the presented paper, in its current form, is too complex to be used in practical design situations or for parametric studies.

Lopez, A., and Aparico, A. C. (1989) "Nonlinear Behavior of Curved Prestressed Box-Girder Bridges, *IABSE Periodica*, Zurich, Vol. 132, No. 1, pp. 13–28.

This paper describes an analytical study of the ultimate strength of horizontally curved reinforced and prestressed concrete box-girder bridges. The analysis was performed using materially nonlinear plane stress finite elements (i.e., panels) that exhibited membrane action. The material was assumed to have a variable modulus of elasticity that was strain dependent. Panel behavior was based on the evolutive truss analogy with peak stress reduction (Vecchio and Collins, 1986). Reinforcing steel and prestress strand were stressed uniaxially according to an assumed multi-linear stress strain relationship. Section warping was not considered. Classical matrix analysis techniques were used to perform the analysis.

A five-span bridge was selected to study the difference between linear and nonlinear response. Live loads were located at various transverse positions and the behavior was observed as the intensity of these loads was increased. Based on these studies the following conclusions were drawn:

1. The structural response was highly nonlinear at ultimate loads.
2. The form and degree of internal force redistribution at ultimate loads depended on the loading case considered.
3. Internal forces were redistributed due to progressive cracking and structural coupling between bending and torsion.
4. The type of failure depended on the loading case considered.
5. Ultimate internal force response could be evaluated accurately using plastic sectional analysis.
6. Transverse prestressing significantly affected post-cracking response.

The following criteria are proposed for design of curved prestressed box-girder bridges.

1. The response of the bridge under service loads can be accurately predicted using elastic models.
2. Elastic models cannot accurately (and will often nonconservatively) predict the ultimate limit state.
3. When using linear analysis to determine the factor of safety against failure, cracked flexural and torsional section properties should be used to determine demands and plastic sectional analysis should be used to determine capacities.

Meyer, C. (1970) "Analysis and Design of Curved Box-Girder Bridges," *Structural Engineering and Structural Mechanics Report No. UC SESM 70-22*, University of California, Berkeley.

The history of curved bridges and the highway geometric requirements of these structures are discussed. The report outlines the methods developed over the years for analyzing curved bridges. These include straight beam approximation, curved beam theory, refined curved beam theories, plate and grillage analysis methods, finite element analysis, and the finite strip method analysis of curved folded plates. Refined curved beam theories are required to analyze thin-walled box sections that can experience warping of the cross section in the transverse direction. Because concrete box sections have relatively thick walls, warping is generally small and ordinary curved beam theory can be used successfully.

Two methods of analysis are developed in the form of computer programs. The first program, FINPLA2, uses the finite element method. The second program, CURSTR, uses the finite strip method of curved folded plates. The solution methodology requires that loadings be applied in the form of Fourier series. The programs yield essentially the same results.

The CURSTR program was used to study wheel load distribution in 1-, 2-, 3-, and 4-cell concrete box-girder bridges. Several parameter studies were conducted with different curvatures, span lengths, deck widths, depth-to-span ratios, and loading configurations.

With respect to single-cell boxes, the following observations were made:

1. The girder on the inside of the curve is stiffer than the girder on the outside of the curve and will attract more load.
2. Load distribution improves with an increase in curvature. This behavior is independent of span, cell width, and depth-to-span ratio.
3. The girder on the outside of the curve has a larger statical moment because of its longer span.
4. The combination of items 1 and 3 results in nearly equal moments in the two girders.
5. The influence of span length on load distribution is similar to straight girders.
6. The influence of depth-to-span ratio is also similar.

For two-cell boxes:

1. The moments in the middle girder and the girder on the inside of the curve increase with curvature.
2. The moment in the girder on the outside of the curve decreases with curvature up to a certain level and then starts to increase.

3. The influence of span on load distribution is small.
4. Cell width accelerates the curvature effects.

The response of 3- and 4-cell box-girders exhibits similar characteristics to 1- and 2-cell boxes.

With respect to negative moments over a "fixed" support,

1. The girders may be assigned moments proportional to their moments of inertia.
2. Load distribution is generally worse in continuous bridges.

For design, approximate methods are justified and even preferred in most cases. A girder moment distribution factor is developed:

$$\alpha = 1 + \frac{B}{R}\left[2.1 - \frac{L'}{600}\right]$$

Bridges with curvatures radii large than 1000 ft. may be considered straight for analysis purposes.

Nakai, H., and Heins, C. P. (1977) "Analysis Criteria for Curved Bridges," ***Journal of the Structural Division*****, ASCE, Vol. 103, No. 7, pp. 1419–1427.**

The paper reports on a series of stiffness equations and limiting angle equations developed for determining the need for analysis of a bridge as a curved structure. The equations consider the type of supporting element, (i.e., open girder, spread box, or single-cell box), bending and torsional stiffness and central angles, and the induced stresses and deformation. It appears that these equations are specific to steel girders and warping torsion is a part of this methodology. However, the overall approach may be used or modified to apply to concrete bridges and NCHRP Project 12-71, especially for flowcharting the decision path for analysis.

The paper provides equations for moment, stress, and deflection of curved and straight bridges. Design criteria for curved bridges have been formulated using these equations, along with parametric studies. The range for the parameter ψ, which "relates the cross-sectional geometry and the spacing between the outside girders, is determined for multiple I, twin box, and monobox-girders. Data for multicell girders are not available from this paper. The bounds for the torsional stiffness parameter κ are derived and depend on "the central angle," which is the total horizontal angle the girder passes through between supports, the torsional rigidity of the cross section, and EI. The deflection ratio is primarily dependent on γ, which "reflects the bending and torsional stiffness of the girders." The relationships between γ and the central angle were also found for the three bridge types studied.

Conclusions made in the paper are as follows:

1. A series of stiffness parameter equations and limiting angle equations have been presented, which provide information to the designer in determining the need for a curved girder analysis. The expressions are functions of the girder types, bending and torsional stiffness, and central angles.
2. The evaluation of κ gives the following criteria: "when κ is less than 0.4, evaluation of stresses due to pure torsion may be omitted. When κ is greater or equal to 10, evaluation of stresses due to warping may be omitted."

Sennah, K. M., and Kennedy, J. B. (2002) "Literature Review in Analysis of Curved Box-Girder Bridges," ***Journal of Bridge Engineering*****, ASCE, Vol. 7, No. 2, pp. 134–143.**

The curvilinear nature of box-girder bridges, along with their complex deformation patterns and stress fields, have led designers to adopt approximate and conservative methods for their analyses and design. Recent literature on straight and curved box-girder bridges has dealt with analytical formulations to better understand the behavior of these complex structural systems. Few authors have undertaken experimental studies to investigate the accuracy of existing methods. This paper presents highlights of references pertaining to straight and curved box-girder bridges in the form of single-cell, multiple-spine, and multi-cell cross sections. The literature survey presented herein deals with (1) elastic analysis, and (2) experimental studies on the elastic response of box-girder bridges.

The elastic analysis techniques discussed include

1. Orthotropic Plate Theory Method
2. Grillage Analogy Method
3. Folded Plate Method
4. Finite Strip Method
5. Finite Element Method

The orthotropic plate method lumps the stiffness of the deck, webs, soffit, and diaphragms into an equivalent orthotropic plate. The Canadian Highway Bridge Design Code (Canadian Standards Association, 1988) recommends limiting this method to straight bridges with multi-spine cross sections. Parameter studies indicated that acceptable results are given for bridges with three or more spines.

In the grillage analogy method, the multi-cellular structure is idealized as a grillage of beams. The CHBDC does not recommend this method be used for sections with less than three cells or box beams. This method requires special attention to the modeling of shear lag and the torsional stiffness of closed cells. When modeling is properly done, this method yields results that compare well with finite element techniques.

The folded plate method uses plates to represent the deck, webs, and soffit of box-girders. Diaphragms are not modeled. The plates are connected along their longitudinal edges and loads are applied as harmonic load functions. The method is time consuming and only applicable to restrictive support conditions.

The finite strip method has been widely researched. It is essentially a special case of the finite element method but requires considerably less computational effort because a limited number of finite strips connected along their length are used. Its drawback is that it is limited to simply supported bridges with line supports and thus not applicable as a general use analysis tool for production design.

With the advent of powerful personal computers and computer programs, the finite element method has become the method of choice for complex structural problems. Many researchers have applied this technique to the analysis of curved box-girder bridges. A problem that occurs is that a large number of flat plate elements are required to properly model the curved elements of a curved bridge. Several researchers have attempted to overcome this difficulty by developing special elements or using special substructuring techniques. The versatility of this method has allowed researchers to investigate several aspects of bridge behavior, including dynamics, creep, shrinkage, and temperature.

Curved box-girder structures cannot be accurately analyzed using the classical curved beam theory developed by Saint-Venant because it does not account for warping, distortion, and bending deformations of the individual wall elements of the box. Vlasov first developed an adaptation of Saint Venant theory to thin-walled sections. Even this adaptation does not account for all warping and bending stresses. Considerable research effort has been expended over the years to develop computational techniques to overcome shortcomings in the present theory.

Several laboratory experiments involving model box-girder bridges have been conducted over the years. In general, these experiments have shown good agreement with analytical results, particularly those obtained using the finite element method of analysis.

In conclusion, the finite element method, though more difficult to apply, accounts for all relevant behavior in curved box-girder bridges and yields the most reliable analysis results. Many computer programs have been developed specifically for box-girder bridges, but most of these are not commercially available.

Turkstra, C. J., and Fam, A. R. M. (1978) "Behavior Study of Curved Box Bridges," *Journal of the Structural Division*, ASCE, Vol. 104, No. 3, pp. 453–462.

A numerical analysis of several single-cell curved box-girder sections with variable curvature, length, web spacing, number of diaphragms, and loading was performed. The effects of these parameters on longitudinal stresses are considered, based on selected numerical results. Implications for preliminary design are presented for both concrete and composite concrete/steel sections

Reilly, R. J. (1972) "Stiffness Analysis of Grids Including Warping," *Journal of the Structural Division*, ASCE, Vol. 98, No. 7, pp. 1511–1523.

Two methods of including warping effects in the stiffness method of analysis are presented. Method B seems to be superior to Method A for cases where the warping constant is not large. In the limiting case where $I_w = 0$, the warping effects disappear and leave only the familiar GI_x/L. When I_w is small relative to I_x (approximately $pL > 5$ for each element) computational errors grow, because the stiffness matrix tends to become singular as the elements on the main diagonal associated with warping approach zero. This is not a serious practical problem, as good solutions can be obtained using an ordinary grillage analysis, neglecting warping for structures where warping stiffness is small and p is large. Composite bridges seem to fall near the borderline where warping can be neglected. The bridge used in the example above was non-composite so that warping would be significant. Bimoment and warping torsion are obtained for grillage structures. Results of computer programs based on these methods are shown to agree closely with published solutions for straight beams, a curved beam, and a curved highway bridge.

Meyer, C., and Scordelis, A. C. (1971) "Analysis of Curved Folded Plate Structures," *Journal of the Structural Division*, Vol. 97, No. 10, pp. 2459–2480.

A finite strip method of analysis is presented which can be used to analyze curved folded plate structures simply supported at the two ends and composed of elements that may, in general, be segments of conical frustra. The method is based on a harmonic analysis in the circumferential direction, with the loadings expressed by Fourier series, and on a finite element stiffness analysis in the transverse direction. The direct stiffness method is used to assemble the structure stiffness matrix and to determine displacements and element stresses. A description of a general computer program developed for the analysis and the results of several examples are also given.

Okeil, A. M., and El-Tawil, S. (2004) "Warping Stresses in Curved Box-Girder Bridges: Case Studies," *Journal of Bridge Engineering*, Vol. 9, No. 5, ASCE.

This paper discusses case studies performed on 18 actual composite steel-concrete box-girder bridges. These analytical

studies were conducted using the computer program ABAQUS and a special 7-degree-of-freedom beam-column element that can account for warping. These studies, which were designed to investigate warping-related stresses in these bridges, found that in all cases the effect of warping stress was insignificant. The 1997 AASHTO curved girder specifications limits the span-to-radius ratio for designing the bridges as straight. These ratios were found to be conservative by a factor of 2 or more when it comes to the need to consider warping. (Given that concrete box-girders will have thicker webs and soffits, they are even less vulnerable to warping, and it is likely that the effects of warping can be ignored in almost all of these bridges.)

Laboratory Experiments

Most, although not all, laboratory experiments related to curved concrete box-girder bridges have been conducted on small-scale Plexiglas or metal models of these bridges. A large-scale test of a concrete structure was performed at the University of California at Berkeley during the 1970s. In general, these tests have shown that refined analytical techniques predict structural behavior quite well. The following paragraphs discuss published papers and reports on these tests in greater detail.

Aneja, I. K., and Roll, F. (1971) "A Model Analysis of Curved Box-Beam Highway Bridge," *Journal of the Structural Division*, Vol. 97, No. 12, pp. 2861–2878.

Fabrication, preparation, and instrumentation of a Plexiglas model of a horizontally curved box-beam highway bridge are described. The model was extensively instrumented with rosette strain gages at three cross sections. Experimental data for three lane-loading conditions were obtained. An approximate theoretical analysis of the model was obtained by using the finite element method, which showed that finite element models with curved shell elements provide better predictions than those with straight plate elements. A typical comparison between the experimental and theoretical stress distribution across the mid-span gage section for one of the loading conditions is shown graphically. The comparison shows a good agreement between the shapes but not the magnitudes of the stress plots obtained experimentally and theoretically. Experimental data at the three gage sections for each load condition is also given.

Aslam, M., and Godden, W. G. (1975) "Model Studies of Multicell Curved Box-Girder Bridges," *Journal of the Engineering Mechanics Division*, Vol. 101, No. 3, pp. 207–222.

A model study on the static response of curved box-girder bridges is presented, and a close agreement is found between the test and analytical results. The prototype bridge was a four-cell reinforced concrete design that was 33 ft 10 in. (10.31 m) wide and 4 ft 10 in. (1.47 m) deep and had a radius of curvature of 282 ft (86 m). A 1/29 scale aluminum model was studied for spans of 60 in. (1,500 mm), 45 in. (1,140 mm), and 30 in. (760 mm), with or without a midspan radial diaphragm. The quantities measured were (1) Boundary reactions; (2) strains at a radial section close to midspan; and (3) deflections at selected points. The data were reduced by computer, and distribution graphs of tangential plate forces, radial-bending moments, and deflections were plotted by Calcomp plotter. Based on the model data, some general observations are made regarding the behavior of curved box-girder bridges.

Fam, A. R. M. and Turkstra C. J. (1976) "Model Study of Horizontally Curved Box-Girder," *Journal of the Structural Division*, Vol. 102, No. 5, pp. 1097–1108.

This paper describes an experimental study of a single-span horizontally curved Plexiglas box-girder beam with diaphragms and flange overhangs. Static loads were applied at midspan to cause a complex pattern of membrane and bending stresses with the effects of diaphragms clearly evident. Experimental results in typical cases are shown graphically and compared with the results of a special-purpose finite element program developed especially for curved box analysis. This program used the softened truss model theory applied to a prestressed concrete multiple-cell box. In this theory, the concrete torsional problem is solved by combining equilibrium and compatibility conditions and constitutive laws of materials. Until now, the theory has been applied only to the case of pure torsion with a single-cell section. An algorithm is presented to deal with the torsional problem for reinforced concrete and prestressed concrete box-girder bridge superstructures with multiple-cell sections. Results are compared with previous theoretical and experimental work for single-cell cases. Good agreement was obtained between experimental and analytical results.

Heins, C. P., Bonakdarpour, B. P., and Bell, L. C. (1972) "Multicell Curved Girder Model Studies," *Journal of the Structural Division*, Vol. 98, No. 4, pp. 831–843.

The behavior of a single two-span, three-cell Plexiglas model is predicted by the Slope Deflection Fourier Series Technique. This analytical technique had previously been applied to only open cross-sectional, I-type bridge systems. The model was tested under various static concentrated loads. The resulting experimental deflection, rotation, and strain data for some loadings are reported. Effects of single and multicell torsional properties are examined. Results indicate that single-cell properties can be applied in the analysis, and warping effects may be neglected.

Scordelis, A. C., Elfgren, L. G., and Larsen, P. K. (1977) "Ultimate Strength of Curved RC Box-Girder Bridge," *Journal of the Structural Division*, Vol. 103, No. 8, pp. 1525–1542.

Results obtained in a study of a large-scale curved two-span four-cell reinforced concrete box-girder bridge model are presented. The model, which was a 1:2.82 scale replica of a prototype, had overall plan dimensions of 72 ft (21 m) long by 12 ft (3.7 m) wide. The radius of curvature was 100 ft (30.5 m). This represents the sharpest curvature normally used for bridges in the California highway system. Experimental and theoretical results are considered for reactions, steel and concrete strains, deflections, and moments due to conditioning overloads producing stress values as high as 2.5 times the nominal design stress. The loading to failure and the ultimate strength behavior is examined. The excellent live-load overload capacity of the bridge is evaluated and comparisons are made with the similar behavior of an earlier tested straight bridge model. Conclusions appropriate for the design of this type of bridge are given.

Design Issues

Bearings

Although several bearing failures consisting of uplift, overload, or binding have been experienced in curved box-girder bridges, no published research exclusively addressing this issue was found. However, because an accurate 3-D analysis will account for differences in bearing forces and displacements, several references that deal with global analysis and laboratory experimentation deal with this issue (Aslam and Godden, 1975; Scordelis et al., 1977; Choudhury and Scordelis, 1988; Sennah and Kennedy, 2002). This issue is also discussed in some textbooks (Menn, 1990).

Diaphragms

Diaphragms help prevent excessive distortions of the cross section, facilitate wheel load distribution, and distribute transverse load. The following two papers discuss research on determining the number and spacing of interior diaphragms in box-girder bridges.

Oleinik, J. C. and Heins, C. P. (1975) "Diaphragms for Curved Box-Girder Bridges," *Journal of Structural Engineering*, Vol. 101, No. 10, pp. 2161–2178.

A finite difference procedure is used to determine the response of a single-span curved single box-beam bridge with any number of interior diaphragms. The bending and torsional distortions as well as cross-sectional distortions can then be determined throughout the curved box-girder. The forces that are determined include bending moment and flexural shear, pure torsion, warping torsion, and bi-moment. These forces, in addition to distortional functions, yield resulting normal bending, normal warping, and normal distortional stresses. The technique is then used to determine the dead load and live load response of a series of typical curved box beams. A study of the data has resulted in a series of empirical design equations.

Abendroth, R. E., Klaiber, F. W., and Shafer, M. W. (1995) "Diaphragm Effectiveness in Prestressed-Concrete Girder Bridges," *Journal of Structural Engineering*, Vol. 121, No. 9, pp. 1362–1369.

Each year many prestressed-concrete (P/C) girder bridges are damaged by overheight vehicles or vehicles transporting overheight loads. The effects of this type of loading on P/C bridge behavior were investigated for various types and locations of intermediate diaphragms. The research included a comprehensive literature review; a survey of design agencies; the testing of a full-scale, simple-span, P/C girder-bridge model with eight intermediate diaphragm configurations, as well as a model without diaphragms; and the finite element analyses of the bridge model assuming both pinned- and fixed-end conditions. The vertical load distribution was determined to be essentially independent of the type and location of the intermediate diaphragms, while the horizontal load distribution was a function of the intermediate diaphragm type and location. Construction details at the girder supports produced significant rotational-end restraint for both vertical and horizontal loading. Both the vertical and horizontal load distributions were affected by the girder-end restraint. A fabricated intermediate structural steel diaphragm was determined to provide essentially the same type of response to lateral and vertical loads that was provided by the reinforced-concrete intermediate diaphragms currently used by the Iowa DOT.

Flexure and Flexural Shear

Beyond the issue of global analysis, the mechanism for resisting flexural and shear stresses in box-girders is important. The mechanisms of shear resistance and its interaction with flexural stresses in reinforced and prestressed concrete have been well researched (Marti, 1999, and Vecchio and Collins, 1986). Also, the effectiveness of the deck and soffit slabs in resisting flexural compressive forces has been studied. This includes the phenomenon commonly known as shear lag. Several published papers and reports have dealt with these issues. Some of these are discussed below.

Chang, S. T., and Zheng, F. Z. (1987) "Negative Shear Lag in Cantilever Box-Girder with Constant Depth," *Journal of Struct. Eng.*, Vol. 113, No. 1, pp. 20–35.

This paper addresses the classical phenomenon of shear lag in box-girders and draws attention to distinguishing between positive and negative shear lag. The effects of shear lag and negative shear lag in cantilever box-girders are analyzed through a variation approach and finite element techniques. Expressions are derived to determine the region of negative shear lag effect with the interrelation of span/width parameters involved. The theoretical results obtained are compared with a Plexiglas model test. Finally, conclusions are drawn with regard to further study and research.

Positive shear lag is the phenomenon in which, near the support of a cantilever, flange longitudinal stresses near the web are larger than away from the web. But for a cantilever box-girder with constant depth under a uniform load, away from the support, the bending stress in the deck near the webs is smaller than the stress away from the webs. This is a result of negative shear lag. Using the principle of minimum potential energy, following Reissner's procedure with slight modifications, shows that the additional moment created by flange shear deformation plays an important role in both positive and negative shear lag. For a single point load at the free end of the cantilever, only positive shear lag is created. When there is a uniformly distributed load along the full span of the cantilever box-girder however, negative shear lag occurs. The region of the cantilever affected by negative shear lag is from the free end to more than ¾ of the cantilever length from the free end. Negative shear lag affects a larger region than positive shear lag.

With a finite element model analysis, three load cases were considered; a distributed load, a point load, and a combination of a downward point load and an upward distributed force. This analysis showed that negative shear lag occurred only with the first load case of a distributed load. This model was consistent with the results from the minimum potential energy method.

Negative shear lag depends on not only the load case but also the boundary conditions. The ratio of the length of the cantilever to the width of the box-girder affects the amount of moment caused by shear. As the ratio increases, both positive and negative shear lag decrease.

Actual testing using a Plexiglas model confirmed the theoretical results. When a uniform load is applied, not only is positive shear lag more severe compared with a point load, but negative shear lag is also present. A cross-sectional analysis of shear stress in the flange is taken at several locations. Near the fixed end where shear lag is greatest, the bending stress near the web is much larger than the stress away from the webs. At a cross section where negative shear lag is significant, the bending stress away from the webs is greater than the stress near the webs.

This paper is only indirectly applicable to this project because the paper does not deal specifically with curved girders. However, given that shear lag effects are an important consideration in developing analysis and design strategies, the conclusions in this paper, and the theoretical solutions are noteworthy. In short, the relevant conclusions are

1. Positive shear lag may occur under both point and uniform load, but negative shear lag occurs only under uniform load.
2. Negative shear lag also depends on the ratio of L/b, where b is the net width of the box section. The smaller the ratio, the more severe are the effects of positive and negative shear lag.
3. Negative shear lag depends on the boundary condition of displacement as well as on the external force applied to the girder.
4. In cantilever box-girders, although the negative shear lag yield in the region of the bending stress is small, the relative additional stress induced by this effect is often considerably greater. It cannot be neglected. It should never be believed that in all cases only positive shear lag is produced.

Chang, S. T., and Gang, J. Z. (1990) "Analysis of Cantilever Decks of Thin-Walled Box-Girder Bridges," *Journal of Structural Eng.*, Vol. 116, No. 9, pp. 2410–2418.

This paper, which addresses the cantilever decks ("wings") of single-cell box-girder bridges, does not make any distinction about the effects of horizontal curves, but it does present some useful qualitative information about cantilever deck evaluation, in general.

The paper reports on a spline finite strip approach used to analyze the cantilever decks. Effects of distortion of thin-walled box sections are taken into account by treating the cantilever deck as a slab with horizontally distributed spring supports along the cantilever root. Perspex model tests were conducted in the model structural laboratory at Tong Ji University. The results based on the spline finite strip method are compared with those of the model test. Simplified solutions are also given for the distribution of transverse moment along the cantilever root.

A Plexiglas model of a single-cell box-beam was evaluated. As a point load moved transversely across the box-girder, the bending stress and membrane stress at the root of the overhang of the deck were obtained. From this analysis, it was observed that it is reasonable to treat the cantilever decks as

cantilever slabs with horizontally distributed spring support along the cantilever root with the spring constant *K* depending on dimensions and material properties of the deck.

The spline finite strip analysis was shown to be in close agreement with actual model test results. Tests showed that the moment along the cantilever root approaches zero as the longitudinal distance from the point load increases. The maximum moment at the root is when the point load is at the end of the cantilever and approximately zero when the load is not on the cantilever. There is also sagging in the cantilever around the point load. Although sagging moment is only local, many point loads at the same longitudinal location can cause significant sagging moment, so this should not be ignored.

Conclusions made in this paper are as follows:

1. Cantilever decks of thin-walled box-girder bridges can be treated as cantilever slabs with horizontally distributed spring support along the cantilever root, taking into account the influence of local distortion of the box section.
2. Spline finite strip results, based on the simplified idealization of the cantilever decks of thin-walled box-girder bridges, are in close agreement with test results. The sagging moment at the cantilever root can be obtained in conjunction with information tabulated in the article.
3. In cantilever slabs of infinite length and large cantilever length, sagging moment cannot be ignored. The sagging moment may be taken from information also provided in the article.

Other than the general information provided for evaluating cantilever decks of straight box-girder bridges, there is no specific information pertaining to curved box-girders.

Hasebe, K., Usuki, S., and Horie, Y. (1985) "Shear Lag Analysis and Effective Width of Curved Girder Bridges," *J. Eng. Mech.*, Vol. 111, No. 1, pp. 87–92.

This paper develops guidelines and graphs for estimating the effective width of curved girder bridges. The methodology is formulated by substituting the flange stress derived from present theory into the equation of effective width definition for the curved girders. The required information in formulating the effective width rule for design of curved girder bridges is provided. The actual longitudinal stress distributions for the curved girders are evolved from the present theory for shear lag in order to determine the effective width. The thin-walled curved girders used in this investigation are based on box and channel cross sections and are analyzed for a uniform lateral load and for a concentrated load.

Numerical examples are shown for several problems to investigate the effect on effective width of curved girder bridges. The values of the effective width obtained by the present theory are compared with those of the straight girder bridges. According to the results, it is acceptable to say the values of effective width of curved girder bridges are the same (approximately) as the values of the straight girder bridges. This is a very important conclusion for NCHRP Project 12-71.

The inner and outer effective widths are denoted as λ_1 and λ_2, respectively, for a curved girder. λ_0 is half of the effective width for a straight beam and 2b = width of the flange. Effective width ratio is defined as the ratio of an effective width to the actual breadth of the flange. The parametric study involves calculating the effective width ratio for simply supported girders and comparing results of (1) point load at mid span versus uniformly distributed load, (2) present theory versus folded plate theory, (3) inner and outer effective width ratio for curved girders versus effective width ratio for straight girders, and (4) box cross section versus channel cross section. In the test, the curved beam has a radius of curvature R = 4L and b/L = 0.1. In the case of a concentrated loading, the values of the effective width ratio are at minimum at the center of the span length and increase rapidly toward the supports. However, in the case of a uniformly distributed loading, the values are at maximum at the mid span and decrease toward the supports. The values of effective width ratio of the present theory are lower than the folded plate theory curves, and the inside and outside effective width ratio agree with the values of the straight beams, irrespective of cross-sectional shapes or types of load distributions.

The authors analyze the inner and outer effective widths at mid span relative to the curvature R/L. For a box-girder under a distributed load, the effective widths remain fairly constant for b/L = 0.1 when R/L > 2 and only decreases slightly for b/L = 0.2. With a point load and b/L = 0.1, the effective width also remains fairly constant for R/L > 4. When b/L = 0.2 with a point load however, the effective widths deviate significantly for small R/L.

For a curved girder, as b/L increases, the difference between the inner and outer effective widths becomes significant, especially for box-girders. For small values of b/L however, those two values are almost identical.

One needs to be careful when R/L is small, b/h is small, or b/L is large, especially under concentrated loads. Otherwise, it is reasonable to assume the effective width of a curved girder is equal to that of a straight girder for practical applications.

Torsion

Torsion design is currently addressed by the AASHTO LRFD code and, in the case of box-girders, is integrated

with shear design. Recent studies (Rahal and Collins, 2003) indicate that this approach yields good results when the correct value of θ is used. Several other papers on the subject of torsional resistance have been reviewed and it is concluded that the current design methods are acceptable. Only minor clarifications of the current specifications and guidelines for applying them to box-girders are required. Following is a summary of the papers that were reviewed on torsion design.

Collins, M. P., and Mitchell, D. (1980) "Shear and Torsion Design of Prestressed and Non-Prestressed Concrete Beams," *Journal of the Prestressed Concrete Institute*, Vol. 25, No. 5, pp. 32–1000.

This document presents design proposals for flexural shear and torsion of prestressed and non-prestressed concrete beams based on the compression field theory. A rational method is proposed which addresses members subject to flexural shear, torsion, combined flexural shear and flexure, and combined torsion, flexural shear and flexure. Early design procedures using truss models are also presented. The compression field theory, a development of the traditional truss model for flexural shear and torsion, considers in addition to the truss equilibrium conditions, geometric compatibility conditions and material stress-strain relationships. The compression field theory can predict the failure load as well as the complete load-deformation response. Measured and predicted response of numerous members is presented. The proposed design recommendations are provided in code format. Comparisons with the provisions of the ACI 318-77 and CEB codes are provided. Numerous worked examples are provided that demonstrate the proposed method.

Rahal, K. N., and Collins, M. P. (1996) "Simple Model for Predicting Torsional Strength of Reinforced and Prestressed Concrete Sections," *ACI Structural Journal*, Vol. 93, No. 6, pp. 658–666.

A noniterative method for calculating the ultimate torsional strength and the corresponding deformations of reinforced and concentrically prestressed concrete sections is presented. This method, based on the truss model, avoids the need for iterations by making simplifying assumptions about the thickness of the concrete diagonal, the softening of the concrete due to diagonal cracking, and the principal compressive strains at ultimate conditions. A simple check on the spalling of the concrete cover is implemented. The calculated torsional capacities of 86 beams are compared with the experimental results and very good agreement is obtained.

Rahal, K. N., and Collins, M. P. (2003) "Experimental Evaluation of ACI and AASHTO-LRFD Design Provisions for Combined Shear and Torsion," *ACI Structural Journal*, Vol. 100, No. 3, pp. 277–282.

The experimental results from four large nonprestressed specimens loaded in combined flexural shear and torsion are used to evaluate the torsion design procedures of ACI 318-02 and AASHTO-LRFD. Both sets of procedures calculate the required amounts of hoop reinforcement for torsion based on a space truss model with compression diagonals inclined at an angle of θ to the longitudinal axis. It is shown that the ACI provisions give very conservative results if the recommended value of 45 degrees is used for θ. If the lower limit of 30 degrees is used, however, some unconservative results are possible. The AASHTO-LRFD provisions predicted values of θ of approximately 36 degrees for these specimens and gave accurate estimates of the strengths.

Fu, Chung C, and Yang, Dailli (1996) "Designs of Concrete Bridges with Multiple Box Cells due to Torsion Using Softened Truss Model" *ACI Structural Journal*, Vol. 93, No. 6, pp. 696–702.

Using a softened truss model, this paper presents a method for torsional design of multicell concrete bridges. Earlier researchers have successfully shown the development for solving single-cell torsion by combining the equalibrium, compatibility, and the softened constitutive laws of concrete. By solving the simultaneous equations based on the membrane analogy, multicontinuous or separate cells can be solved.

Hsu, T. T. C. (1997) "ACI Shear and Torsion Provisions for Prestressed Hollow Girders," *ACI Structural Journal*, Vol. 94, No. 6, pp. 787–799.

New torsion design provisions have been proposed for the 1995 ACI Building Code. As compared with the 1989 provisions, these generalized 1995 provisions have three advantages: First, they are applicable to closed cross sections of arbitrary shapes. Second, they are applicable to prestressed concrete. Third, they are considerably simplified by deleting the "torsional concrete contribution" and its interaction with flexural shear. These new provisions are suitable for application to concrete guideways and bridges because these large structures are always prestressed and are often chosen to have hollow box sections of various shapes. This paper discusses the background of the new code provisions, suggests modifications to code formulas, and illustrates the application of the code provisions to prestressed hollow girders by way of a guideway example.

Wheel Load Distribution

Wheel load distribution has been the subject of many of the analytical studies cited earlier. Other studies are discussed in the following paragraphs.

Song, S. T., Y. H. Chai, and S. E. Hida (2001) "Live Load Distribution in Multi-Cell Box-Girder Bridges and its Comparison with the AASHTO LRFD Bridge Design Specifications," Final Report to Caltrans for Contract Number 59A0148.

This report presents the results of a series of analyses done on box-girder bridges with normal and skewed supports and straight and curved geometry. The analysis models included 3-D finite element as well as grillage and single line of elements for superstructure. The goal of the project was to evaluate the LRFD live load distribution factors for box-girder bridges. However, the modeling techniques used and verified for this project can be used as guidelines for NCHRP Project 12-71.

Zokaie, T., K. D. Mish, and R. A. Imbsen (1993) "Distribution of Wheel Loads on Highway Bridges," Phase 3, Final Report to NCHRP 12-26 (2).

This report presents a computer program (LDFac) developed for modeling bridge superstructure with straight or skewed supports and obtaining live load distribution factors. Although this computer program did not consider curved geometry specifically, the modeling process and load placement guidelines may be used for analysis of curved bridges as well. One of the key issues discussed in this report is the modeling of distortion of box-girders in a grillage analysis via an equivalent shear deformation parameter.

Zokaie, T., T. A. Osterkamp, and R. A. Imbsen (1991) "Distribution of Wheel Loads on Highway Bridges," Final Report to NCHRP 12-26 (1).

This report presents a series of guidelines for analysis of various bridge types. The guidelines include calculation of equivalent section property parameters to be used in plate and grillage analyses, as well as guidelines for setting the boundary conditions. Although the research did not specifically consider curved bridge geometry, many of the guidelines for modeling and analysis using common analysis tools are applicable to modeling that will be needed in NCHRP Project 12-71 global analysis studies.

Tendon Breakout and Deviation Saddles

Prestress tendon breakout in curved bridges has occurred on bridges over the years. It is evident from observing the reasons for these failures that they can be prevented through close attention to details such as tendon spacing and tie back reinforcement. The following paragraphs summarize the references reviewed on the subject.

Beaupre, R. J., et al. (1988) *Deviation Saddle Behavior and Design for Externally Post-Tensioned Bridges,* Research Report 365-2. Center for Transportation Research, University of Texas at Austin, Austin, Texas.

This report is the second in a series outlining a major study of the behavior of post-tensioned concrete box-girder bridges with post-tensioning tendons external to the concrete section. It presents the results of an experimental program in which ten very accurately sealed reinforced concrete models of typical tendon deviators were tested. Detailed instrumentation led to a very good understanding of the behavior of the various patterns of reinforcement in the deviators. The models included two very different patterns of detailing, several arrangements of tendon inclinations, and both normal and epoxy-coated reinforcement.

The report evaluates the results with respect to both simplified conventional analysis methods and strut-and-tie models. The results provide the basis for deviator design recommendations and several examples are presented to illustrate the practical use of these recommendations.

Caltrans (1996) *Bridge Memo to Designers Manual*, Memo 11-31 Curved Post-Tensioned Bridges, California Department of Transportation, Sacramento, California

Memo 11-31 addresses the design of curved post-tensioned concrete box-girders for lateral prestress forces. The force effects considered are tendon confinement and web regional transverse bending. The lateral prestress force, F, is determined by dividing the jacking force (P_j) per girder by the horizontal radius (R) of the web. A standard detail for tendon confinement (see Figure 3-1) is required for all webs with a $P_j/R > 100$ kN per m or a horizontal radius (R) of 250 m or less. The regional transverse bending moment in the web is taken as $M_u = 0.20Fh_c$ where h_c is the clear distance between the top and bottom slabs. This assumes the web to act as a simple beam spanning the top and bottom slabs with a concentrated load, F, acting at mid-height of the web. The resulting simple beam moment is reduced 20% for continuity. The load factor is taken as 1.0. The design of stirrup reinforcement does not combine regional transverse bending and shear requirements. Graphs are provided to check webs for containment of tendons and adequate stirrup reinforcement to resist regional transverse bending.

A review of the 405/55 failure has led to the identification of several issues related to the Caltrans Memo to Designers 11-31. These are discussed below.

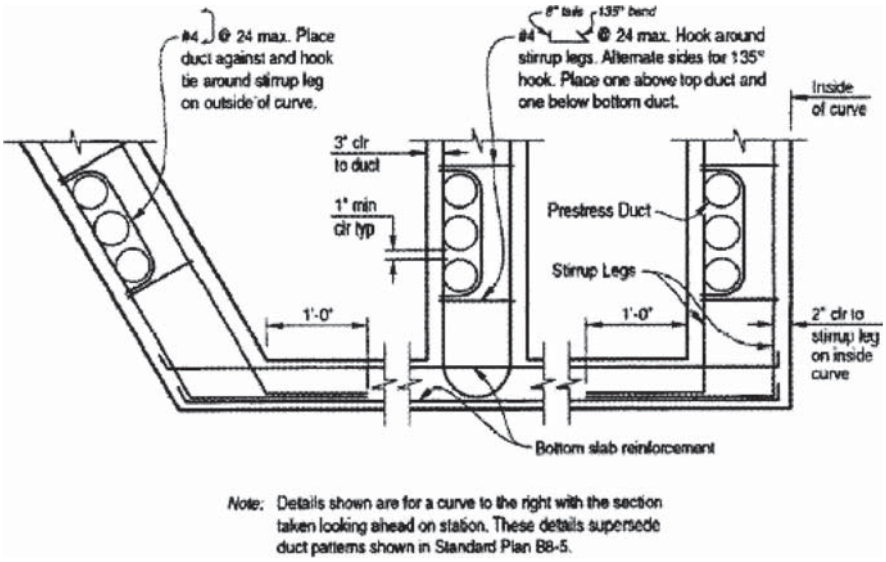

The designer should be aware of the following regarding the use of Caltrans MTD 11-31:

- MTD 11-31 does not state the range of P_{jack} per girder, maximum number of ducts, P_{jack}/R, minimum radius, maximum girder height, etc. for which the memo was developed and intended.
- MTD 11-31 is a step function as to when "Detail A" is required. Detail A is required whenever $P_{jack}/R>7$ kips/ft (100 kN per meter) per girder or the horizontal radius (R) is 800' (250 meters) or less. The P_{jack}/R requirement appears to be based solely on shear in the local slab without any consideration for flexure in the cover concrete. Note that Caltrans Standard Plan B8-5 and Detail A in MTD 11-31 do not limit the number of ducts in a bundle for duct diameters of 4.5" or less. AASHTO limits the number of ducts in a bundle to three.
- The spacing of the duct ties per Detail A is 24". AASHTO LRFD 5.10.4.3 states "The spacing of the confinement reinforcement shall not exceed either 3.0 times the outside diameter of the duct or 24.0 IN." Typical duct diameters are 4.5" or less, thus Detail A will not comply with AASHTO LRFD requirements.
- In MTD 11-31, the web flexural reinforcement is designed with a load factor of only 1.0. Note that the AASHTO LRFD Bridge Design Specifications require a load factor of 1.2, which is more conservative. In MTD 11-31, the web is treated as a beam with the simple beam moment reduced by 20% for continuity between the web and slabs (refer to Figure 7).

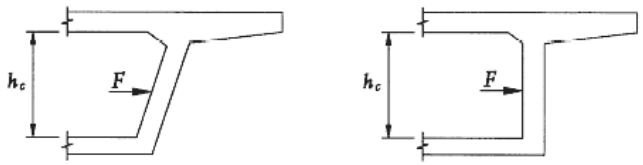

$$M_u = (1.0)(0.8)(1/4)(P_j / R)(h_c) = 0.20(F)h_c$$

FIGURE 7

Figure 3-1. Caltrans detail A.

- The design charts in MTD 11-31 do not appear to consider BDS 8.17.1 "Minimum Reinforcement" which requires that $\phi M_n > 1.2M_{cr}$ unless the reinforcement provided is at least one-third greater than that required by analysis.
- The interaction of global shear and regional bending is recognized in MTD 11-31 but is intentionally not combined. The reinforcement required for each effect is determined individually and the greater of the two is provided.

Figure 3-1. (continued).

Cordtz, K. (2004) *Design of Curved Post-Tensioned Bridges for Lateral Prestress Forces*, David Evans and Associates, Inc., Roseville, California.

This document presents the internal guidelines of David Evans and Associates, Inc., for the design of horizontally curved post-tensioned concrete box-girders for lateral prestress forces. The primary focus is on the regional beam action of the webs and local slab action of the cover concrete over the tendons. The document provides a discussion of the actions on curved post-tensioned girders, identifies those actions not completely addressed in current design codes and guidelines, and recommends design procedures that reflect current best practice.

Local slab action of the concrete cover over the tendons has been identified as the major cause of failure in several curved post-tensioned bridges that did not have duct or web ties. For a web without duct or web ties, the cover concrete is the only element restraining the lateral prestress force. The cover concrete acts as a plain concrete beam to restrain the lateral prestress force. The local slab is subject to lateral shear and bending from the lateral prestress force. Specific requirements for local lateral shear are given in AASHTO LRFD 5.10.4.3.1 "In-Plane Force Effects." No specific design methodology for local flexure is given by AASHTO. The document provides interim recommendations for the tensile stresses in the cover concrete. Where duct ties are required, the document recommends the use of a rational method for design such as a strut and tie model.

The vertical reinforcement in the web is subjected to combined global shear and regional transverse bending due to regional beam action. No specific design methodology for these combined actions is given by AASHTO. The document provides interim recommendations for the design of the stirrups.

A flowchart is presented that outlines the recommended procedures. Numerous worked examples are also provided.

Podolny, W., Jr. (1985), "The Cause of Cracking in Post-Tensioned Concrete Box-girder Bridges and Retrofit Procedures," *Journal of the Prestressed Concrete Institute*, March-April 1985.

This article discusses the types of problems that lead to cracking in post-tensioned concrete box-girder bridges and have been encountered in both Europe and the United States. Cracking is attributed in a broad sense to the following factors: inadequate flexural and shear capacity, non-consideration of thermal stresses, insufficient attention to stresses developed by curvature of tendons, improper or inappropriate construction techniques, lack of quality workmanship to meet the tolerances necessary for problem free structures, and understrength materials. It is noted that in general the cause of cracking can be attributed to the superposition of stresses of multiple effects.

The article discusses the pullout of horizontal curved tendons that occurred on several cast-in-place post-tensioned concrete box-girder bridges. In two of these structures, there was a combination of relatively sharp horizontal curvature, thin concrete cover over the tendons, and the bundling of large-sized tendons close together. Podolny divides the analysis of the failures of these bridges in three separate actions:

1. The global or overall girder action of the bridge together with its supporting piers and abutments.
2. Regional beam action of each web supported at the top and bottom flanges as a beam.
3. Local slab action of the concrete cover over the tendons.

It appears that for both of these bridges, local slab action of the concrete cover over the tendons was the primary cause of the failure, but the regional beam action could have been a contributory cause and could, by itself, have overstressed some of the stirrups. The global action had a very small effect on these failures.

Seible, F., Dameron, R., and Hansen, B. (2003), *Structural Evaluation of the 405-55 HOV Connector and the Curved Girder Cracking/Spalling Problems*. StD&A, San Diego, California.

This document is a detailed (70 pages, including illustrations) project report on results of structural evaluation of the 405-55 HOV Connector's curved girder cracking/spalling problems. The report provides background on the observed cracking and spalling (caused by horizontal breakout of web

tendons in the multicell boxes), summarizes occurrences of similar problems at Las Lomas (California) and Kapiolani (Hawaii), and then documents a step-by-step analysis of the 405/55 bridge. The steps followed include global, regional, and local analysis, as suggested by Podolny. The regional and local analysis use detailed finite element modeling with cracking concrete constitutive models, but various hand calculation methods for evaluating regional and local effects are also described and demonstrated as a check on the detailed analysis. The report also provides an in depth summary of Caltrans's Memo to Designers (MTD) 11-31 and points to some potential shortcomings (under the right set of unusual circumstances) of the Memo. The report then lists eight contributory causes for the damage that occurred, but concludes that the one cause which, if corrected would have prevented the damage, was the omission of duct ties from the design.

Although this report is very structure-specific and contains detailed project information that should not be directly referenced in a set of design specifications, it provides a useful reference for summarizing the various analyses (both hand calculation and finite element) appropriate to this class of problems, especially at the "regional" and "local" level for girder cross-section and web evaluation.

Strasky, J., 2001, *Influence of Prestressing in Curved Members*, Betonve Mosty, Report TK21, Prauge, Czech Republic.

The influence of prestressing in curved members is discussed. To mitigate the effect of radial prestressing forces in the webs of box-girders, it is recommended that prestress tendons be separated vertically where they pass near the middle of the web. This will spread the radial forces and result in lower stresses tending to rip the strand out of the side of the web. Care is also required for tendons in the soffit of segmentally constructed bridges (straight or curved) where tendons are anchored in blisters along the length of the bridge and deviated across the width of the soffit, resulting in transverse tensile stresses that can fail the soffit. Such a failure occurred in a bridge constructed with a gantry in Austria. The vertical curvature of these tendons in a haunched bridge can also present a problem.

Van Landuyt, D., and Breen, J. E. (1997) *Tendon Breakout Failures in Bridges*, Concrete International, American Concrete Institute, Farmington Hills, MI, November 1997.

The article discusses the pullout failure of horizontal curved tendons that occurred on several cast-in-place post-tensioned concrete box-girder bridges. In both of these structures, there was a combination of relatively sharp horizontal curvature, thin concrete cover over the tendons, and the bundling of large-sized tendons close together. It appears that for both of these bridges local slab action of the concrete cover over the tendons was the primary cause of the failure.

The article discusses the theory of transverse stresses in curved box-girder cross sections due to post-tensioning including "distributed radial force arch action." Horizontal curved post-tensioned bridges are subjected to the following three separate actions:

1. The global or overall girder action of the bridge together with its supporting piers and abutments.
2. Regional beam action of each web supported at the top and bottom flanges as a beam.
3. Local slab action of the concrete cover over the tendons.

The article discusses the current design philosophy of the California DOT, the Texas DOT, the AASHTO *Guide Specifications for the Design and Construction of Segmental Concrete Bridges*, and the AASHTO *Load and Resistance Factor Design Bridge Design Specifications* for tendon confinement.

A test program was carried out by the authors on webs without tendon confinement reinforcement. Both closely and widely spaced ducts (duct spacing less than or greater than one duct diameter, respectively) were tested, and different lateral shear failure modes were observed. Recommendations for lateral shear capacity are proposed that are more conservative than the AASHTO LRFD Specifications and yielded a consistently narrow range of factors of safety for the four test specimens (1.99 to 2.34). A recommendation for a design methodology for the flexure of the concrete cover is not proposed because of the lack of understanding of its behavior. The test specimens did not fail in regional transverse bending of the web due to the formation of a second load path after formation of flexural cracks in the web. The load path is envisioned primarily as a vertical one with the lateral prestress load carried through flexural bending of the web until cracking. Once cracking occurred, the stiffness was reduced and the load was carried primarily through longitudinal arching until a local lateral shearing failure occurred. A University of Texas thesis (Van Landuyt, 1991) that discusses this research in greater detail was also reviewed.

Time Dependency

The redistribution of stresses due to creep and shrinkage may be important in curved concrete bridges. This issue is discussed in at least one of the references previously described (Menn, 1990). A paper further exploring this issue is described below.

Zhang, L., Liu, M., and Huang, L. (1993) *Time-Dependent Analysis of Nonprismatic Curved PC Box-Girder Bridges*,

Conference Proceeding Paper, Computing in Civil and Building Engineering, pp. 1703–1710.

This proceeding consists of papers presented at the Fifth International Conference on Computing in Civil and Building Engineering held in Anaheim, California, June 7–9, 1993. The proceedings cover five major areas of concern: (1) computing in construction, (2) geographic information systems, (3) expert systems and artificial intelligence, (4) computing in structures, and (5) computing in transportation. Within these broad topics are subjects such as (1) computer analysis of cable-stayed bridges; (2) artificial intelligence in highway CAD systems; (3) automated systems for construction bidding; (4) effect of automation on construction changes; (5) optimal seismic design of structures; and (6) CAD instruction for civil engineering students. The book also presents several papers discussing different aspects of multimedia information systems and geographic information systems.

Vehicular Impact

Vehicular impact in curved bridges is different than in straight bridges. A paper addressing this subject is discussed below.

Rabizadeh, R. O., and Shore, S. (1975) "Dynamic Analysis of Curved Box-Girder Bridges," *Journal of the Structural Division*, ASCE, Vol. 101, No. 9, pp. 1899–1912.

The finite element technique is used for the forced vibration analysis of horizontally curved box-girder bridges. Annular plates and cylindrical shell elements are used to discretize the slab, bottom flanges, and webs. Rectangular plate elements and pin-jointed bar elements are used for diaphragm discretization. The applied time varying forcing function used in this analysis represents a vehicle that is simulated by two sets of concentrated forces with components in both the radial and transverse direction. The position of these concentrated forces is moved at a constant radial velocity in circumferential paths on the bridge. The effect of centrifugal forces is considered and the effect of damping of the bridge is neglected in the analysis. The mass condensation technique is used to reduce the number of coupled differential equations obtained from the finite element method. The resulting differential equations are solved by the linear acceleration method. Several bridges with practical geometries are analyzed and impact factors are calculated.

Seismic Response

Several papers and reports have addressed the seismic response of curved box-girder bridges. Most of these deal with substructure response and are beyond the scope of this study. However, at least one presentation (no paper available) has implications for superstructure design. This study is described below.

Ibrahim, A. M. M., et al. (2005) *Torsional Analysis and Design of Curved Bridges with Single Columns - LFD vs. LRFD Approach*, Paper presented at the Western Bridge Engineers Conference, Portland, OR.

This unpublished study compared torsional superstructure design of a curved concrete box-girder bridge subjected to seismic loading using the Load Factor Design approach currently used by Caltrans and the AASHTO LRFD method. Torsion is induced in the superstructure not only by curvature, but also by column plastic hinging of the single column bent during an earthquake. Caltrans practice is to design the superstructure in bridges with monolithic columns to remain elastic. In this case, the limitation on seismically induced torsional forces resulting from column yielding causes a redistribution of superstructure forces in the box-girder.

Design Optimization

Several combinations of slab and web width can be selected to resist the applied loads. Although design optimization is generally not the subject of design specifications, at least one paper reviewed addressed this issue.

Ozakea, M., and Tavsi, N. (2003) "Analysis and Shape Optimization of Variable Thickness Box-Girder Bridges in Curved Platform," *Electronic Journal of Structural Engineering International*, Vol. 3, Queensland, Australia.

This paper deals with the development of reliable and efficient computational tools to analyze and find optimum shapes of box-girder bridges in curved planforms in which the strain energy or the weight of the structure is minimized subject to certain constraints. The finite strip method is used to determine the stresses and displacements based on Mindlin-Reissner shell theory. An automated analysis and optimization procedure is adopted which integrates finite strip analysis, parametric cubic spline geometry definition, automatic mesh generation, sensitivity analysis, and mathematical programming methods. It is concluded that the finite strip method offers an accurate and inexpensive tool for the optimization of box-girder bridges having regular prismatic-type geometry with diaphragm ends and in curved planform.

Detailing

The detailing of prestressed concrete in bridges is addressed by several agencies that commonly use this structural form.

A general reference published by VSL International, a large prestresser with international experience, is discussed below.

Rogowsky, D. M. and Marti, P. (1991) *Detailing for Post-Tensioning*, VSL International Ltd., Bern, Switzerland.

Detailing for Post-Tensioning includes discussions and examples demonstrating the forces that are produced by post-tensioning, in particular, those in anchorage zones and regions of tendon curvature. Emphasis is placed on the use of strut-and-tie models to determine the tensile reinforcement requirements. Article 4.4, "Tendon Curvature Effects," deals with special issues associated with curved tendons, including in-plane deviation forces, out-of-plane bundle flattening forces, minimum radius requirements, and minimum tangent length requirements. The radial force generated by a curved tendon is given as P/R where P is the tendon force and R is the radius of curvature of the tendon. Methods for preventing tendon breakout in thin curved webs include adequate lateral shear capacity of the concrete cover (adequate cover) or providing tieback reinforcement.

Summary

A considerable body of research has been conducted on box-girder bridges. Much of this is useful to this project.

With respect to global response analysis, research can be broadly divided between steel and concrete bridges. Concrete bridges have been found to be stiff enough so that torsion warping can generally be ignored. Sophisticated elastic analysis techniques such as finite element methods have been shown to produce excellent results that compare well with physical testing. It is therefore not necessary to do any more sophisticated research on this subject. It is necessary for our project to explore the accuracy of less sophisticated methods such as grillage analysis. If grillage analysis methods can be shown to produce reliable results, than they can be used both in design and as a verification tool for even less sophisticated analysis methods. The goal is to identify the simplest methods that can be used safely.

It also seems that several potential configurations of curved box-girder bridges need further study from the designer's point of view. Although some research work has been performed on skewed bridges, bearings, and interior diaphragms, most of it has not found its way into design specifications. Part of our goal is to develop design procedures to handle these issues.

Conventional reinforced and prestressed concrete design methods can be used for curved concrete box-girder design, provided accurate global demands can be established. Considerable work has been performed over the years in these areas. Torsion design, particularly as it applies to box-girders is well established, and further refinement of these methods is beyond the scope of this project.

The local behavior of prestressed tendons in curved concrete box-girder bridges is an issue to be addressed by this project. Although excellent research has been conducted at the University of Texas (Van Landuyt, 1991) this needs to be studied further using available analytical techniques.

CHAPTER 4

Global Response Analysis Studies

This chapter summarizes the work performed for global response analysis and the results and conclusions obtained from this study. Additional detailed results are presented in Appendix E.

Objective

The global behavior of a curved bridge can be distinctly different from a straight bridge. The curvature results in off-center placement of loads and, subsequently, such loads induce torsion into the superstructure. The torsion, in turn, causes the shear stresses on the outside of the curve to increase. Also, the curved geometry of the bridge will result in development of transverse moments, which can increase the normal stresses on the outside edges of the bridge and can result in higher tension and/or compression stresses. Post-tensioned bridges also have an additional equivalent transverse load, which can result in significant tension on the inside of the curve and compression on the outside edge. The magnitudes of such effects depend on the radius of curvature, span configuration, cross-sectional geometry, and load patterns among other parameters. The structural analysis required to capture such effects, in most cases, is beyond the scope of day-to-day normal bridge design activities.

The objective of the global analysis study in this research was to quantify the effect of increased shear force and normal stresses in the cross section, identify common trends, and find approximate modeling methods to obtain accurate results for design purposes. In particular, shear forces and normal stresses due to dead loads, live loads, and post-tensioning were studied to obtain analysis modeling limitations and develop empirical adjustment factors for simplified analysis. A set of special studies was also performed to review the effect of diaphragms, pier connection (bearing versus monolithic), and skewed abutments on curved bridges.

Model Verification

3-D finite element analysis using plate and shell elements is accepted as the most accurate level of analysis available for box-girder bridges. However, the magnitude of analysis cases desirable for parametric studies in this project was such that a more simplified model was desirable. Given that the parametric studies are based on bridges with radial supports, available guidelines for grillage analysis were used. In order to make sure that the grillage and finite element models produced similar results, a detailed model of a three-span bridge on a tight curve (400-ft radius) was created and results were compared for various load effects. The models are shown in Figures 4-1 and 4-2. The results for superstructure dead load and a concentrated midspan load obtained from the two models (grillage and finite element) for a two-cell box are compared in Table 4-1. These results indicate a very close comparison. As a result, grillage models were used throughout the rest of the study as the basis of comparisons and such results are deemed accurate for all practical purposes. Guidelines for performing an analysis with a grillage analogy are included in Appendix C. These guidelines may be used for design purposes when the bridge configuration requires it.

Parameter Studies

Analysis Cases

To study the effect of various bridge parameters on the response of curved bridges, a parametric study was performed which focused on the variation of span configuration and length, bridge cross-section geometry, and loading.

Four bridge cross-section shapes were considered:

- Single-cell box based on a typical cast-in-place cross section,
- Single-cell box based on a typical precast cross section,
- Two-cell box based on a typical cast-in-place cross section, and
- Five-cell box based on a typical cast-in-place cross section.

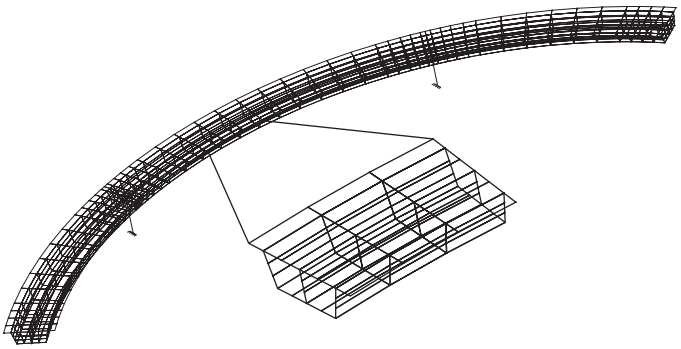

Figure 4-1. Finite element model of the bridge used for model verification.

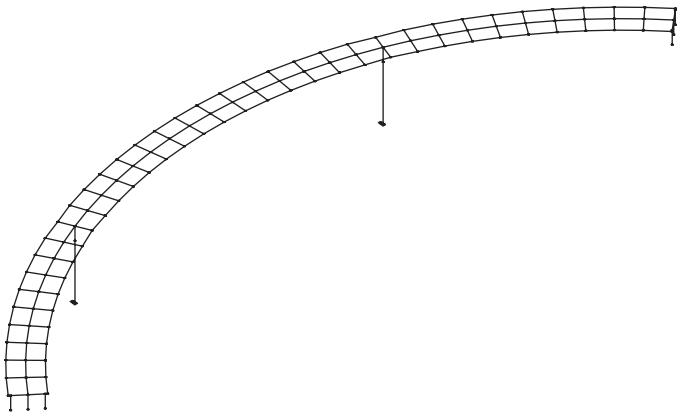

Figure 4-2. Grillage model of the bridge used for model verification.

The typical cross sections are shown in Figures 4-3, 4-5, 4-7, and 4-9. The section geometry remains the same for various bridge span lengths, with the exception of the overall section depth. Also, in order to simplify the analysis cases and automate the model generation, without jeopardizing the global behavior of the bridge, the cross section was idealized as shown in Figures 4-4, 4-6, 4-8, and 4-10. The cross-section properties used for the analytical models are shown in Tables 4-2 through 4-5

For each cross-section type, five typical bridge models were considered:

- Single Span – 200 ft long;
- Single Span – 100 ft long;
- Three Span – 200, 300, and 200 ft long;
- Three Span – 150, 200, and 150 ft long; and
- Three Span – 75, 100, and 75 ft long.

Each of the three-span bridges was analyzed with two types of piers to identify the effect of softer versus stiffer transverse pier stiffness. The stiffer columns were 6 ft by 8 ft which can also be considered similar in behavior to a multi-column pier. The softer columns are 6 ft by 6 ft, 7 ft by 7 ft, and 8 ft by 8 ft for the short, medium, and long bridges respectively. All column heights were assumed to be 50 ft to the point of fixity at the base. It was assumed that the pier and abutment diaphragms were relatively stiff, i.e., they had a moment of inertia of 5000 ft^4.

Each of the above 32 bridges was configured as a straight bridge and as curved bridges with radii of 200, 400, 600, 800, and 1000 feet, resulting in 192 bridge configurations.

Structural Analysis

Each bridge configuration was modeled as a spine model (in which one line of elements was used for superstructure,

Table 4-1. Comparison of results, grillage vs. FEM – two cell box.

Action	Location	DL			LL2C		
		Grillage	FEM	Grillage/FEM	Grillage	FEM	Grillage/FEM
Midspan Span 2 Deflections (inches)	Left	-4.40	-4.31	1.02	-0.23	-0.26	0.91
	Right	-3.87	-3.80	1.02	-0.25	-0.23	1.10
Midspan Span 2 Moments (ft. kips)	Gross	52103	53523	0.97	3791	3829	0.99
	Left Girder	14016	16290	0.86	1197	1190	1.01
	Center Girder	21523	21735	0.99	1566	1504	1.04
	Right Girder	16565	15499	1.07	1028	1135	0.91
Negative Bent 3 Moments (ft. kips)	Gross	-91261	-94623	0.96	-3095	-3235	0.96
	Left Girder	-27469	-27309	1.01	-1007	-845	1.19
	Center Girder	-38265	-39494	0.97	-1342	-1526	0.88
	Right Girder	-25528	-27820	0.92	-746	-864	0.86

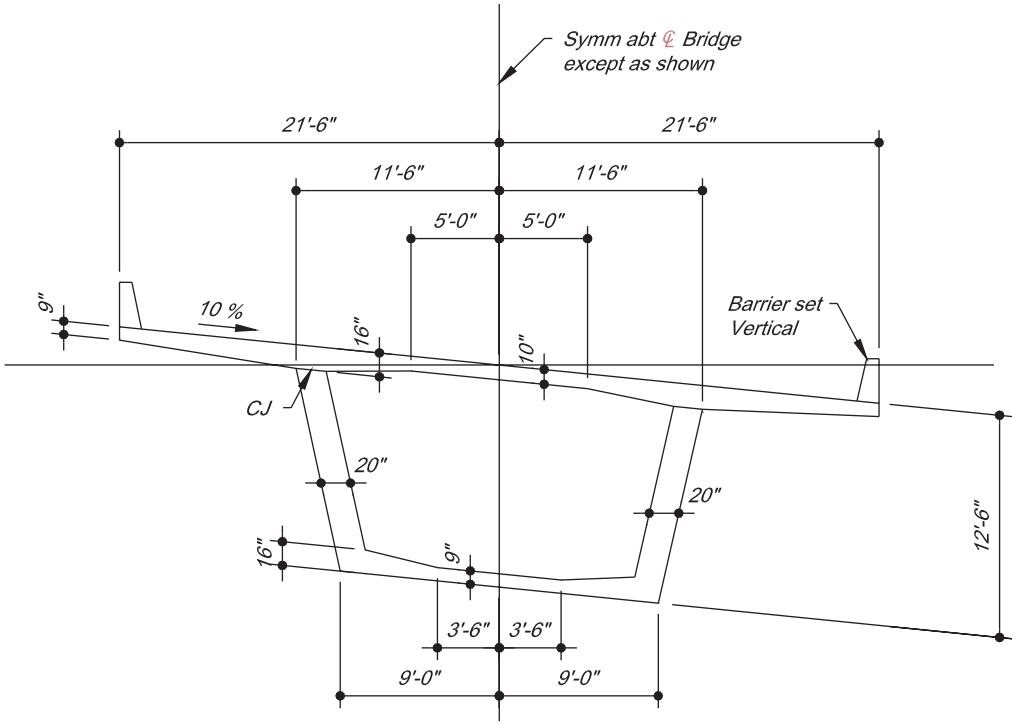

Figure 4-3. Typical single-cell cast-in-place cross section.

located along the centerline of the bridge), and also as a grillage analogy (grid) model (where each web line was modeled as a line of elements along its centerline and transverse elements along radial lines were used to connect them in the transverse direction). Typical spine and grillage modeling techniques are shown in Figures 4-11 and 4-12. Each model uses several elements per span in the longitudinal direction of the bridge. Each span element is limited to a central angle of 3.5 degrees as recommended in Appendix C.

The section properties for the spine model were based on the entire section. An example of these for the two-cell cross section is shown in Table 4-2.

The section properties for the grillage model included a set of properties for the exterior girder, a set of properties for the interior girder, and a set of properties for the transverse element. Furthermore, the transverse element shear area was calculated via a special formula to account for the warping on the cells. An example of these properties for the two-cell section is shown in Table 4-3. The transverse element properties may be different for each element based on its width and therefore is shown here for a unit width. The members on the outside of the curve were longer than the ones on the inside. Likewise, the widths of transverse members along the outside of the curve were larger than those of the members along the inside. The actual member property used in analysis was

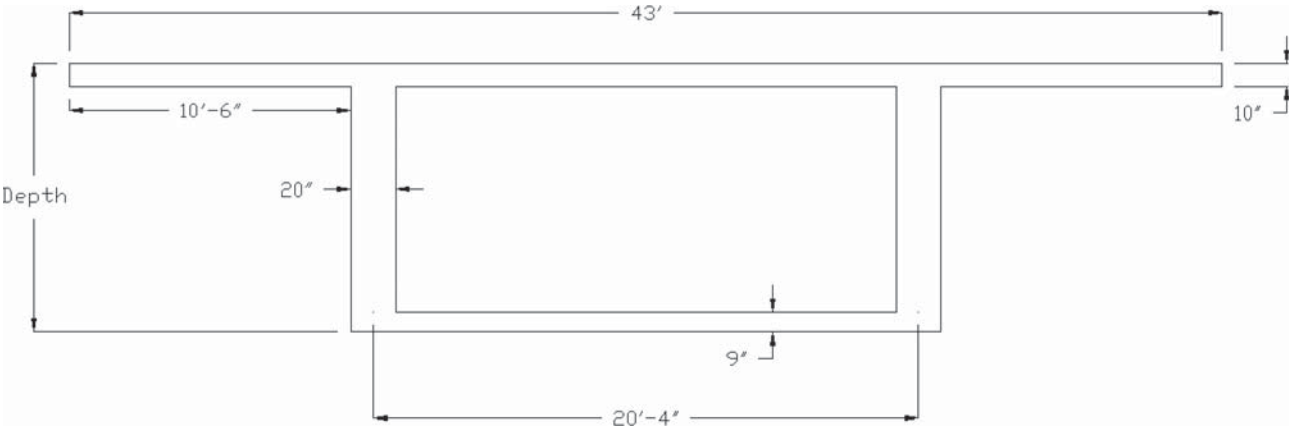

Figure 4-4. Idealized single-cell cast-in-place cross section.

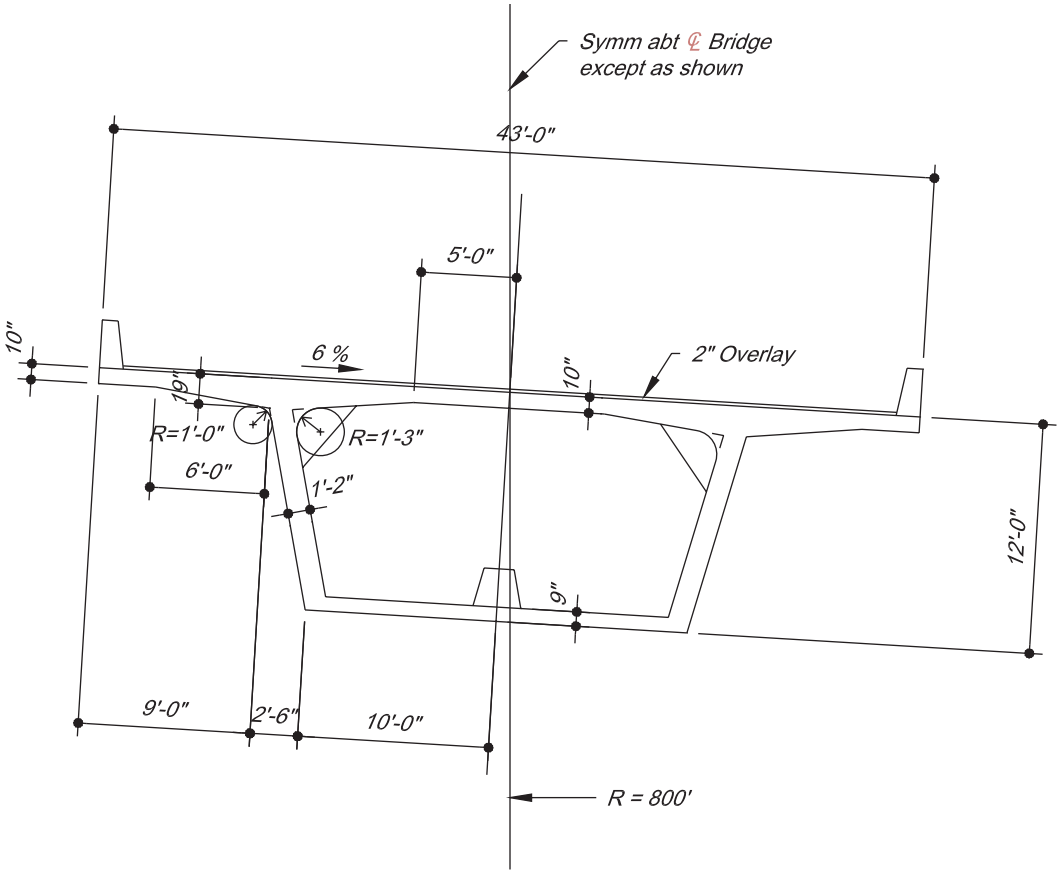

Figure 4-5. Typical single-cell precast cross section.

calculated by multiplying the values shown here by the average width of each element, except that "Izz" is multiplied by L^3.

The bent cap and abutment diaphragms were assumed to be relatively rigid. Cap and column element properties are shown in Table 4-4.

Loads

Each bridge configuration was subjected to dead load (self weight), live load, and post-tensioning loads. A concentrated load of 100 kips was used to simulate the live load.

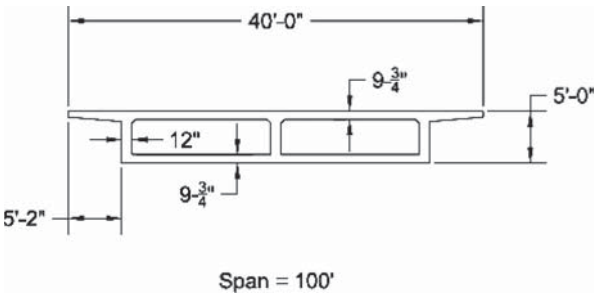

Figure 4-7. Typical two-cell cast-in-place cross section.

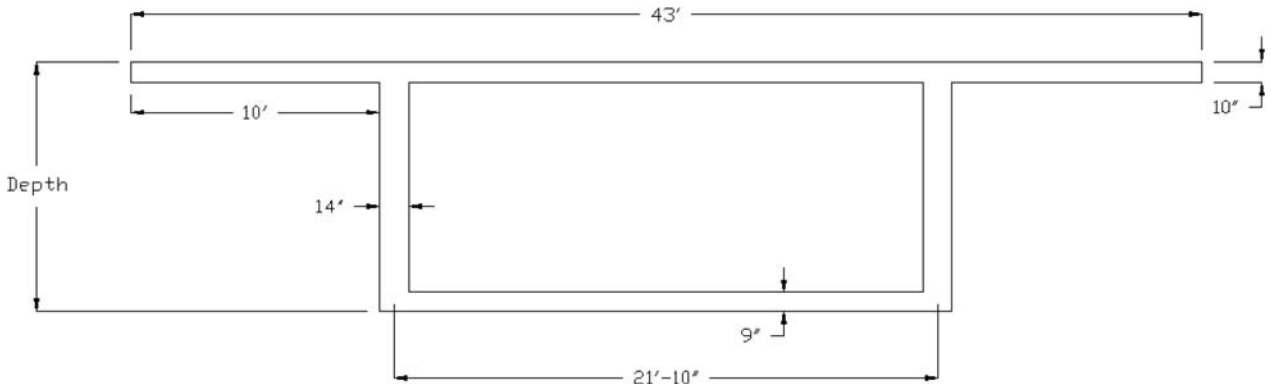

Figure 4-6. Idealized single-cell precast cross section.

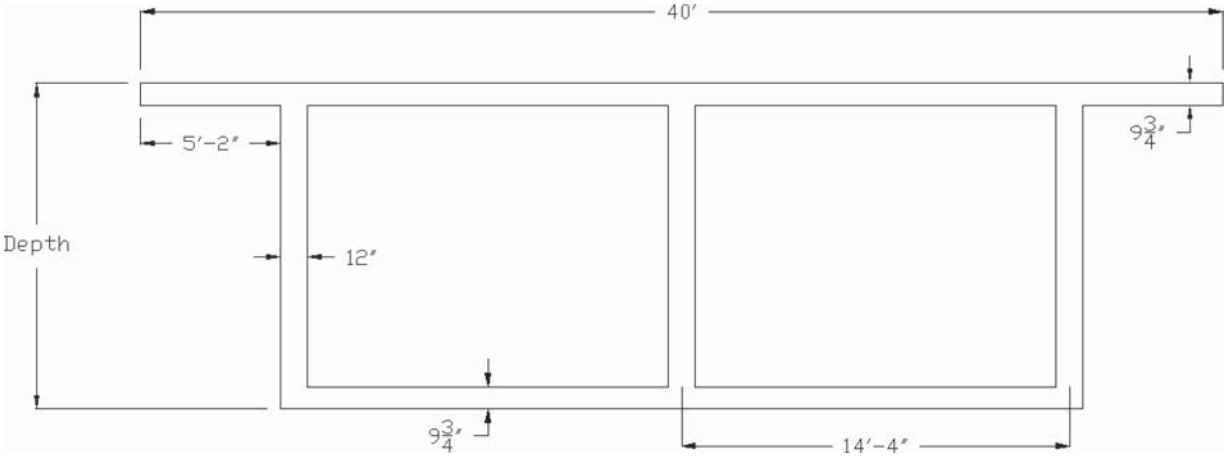

Figure 4-8. Idealized two-cell cast-in-place cross section.

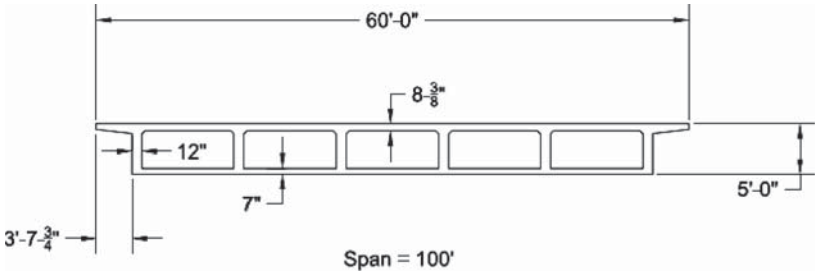

Figure 4-9. Typical five-cell cast-in-place cross section.

This loading captures the effect of concentrated axle loads and may magnify its effect on curved bridges to some extent; therefore, it is justified as a simplification for a conservative upper bound. This load was applied at the middle of the bridge and transversely was located at various positions: (1) on outside web, (2) on inside web, (3) on center of bridge, and (4) on all webs, i.e., equally distributed over the bridge width. Maximum stresses occur when the entire bridge width is loaded, therefore, the results from this case were studied in more detail when developing guidelines for design. Post-tensioning was also applied along all webs of the section. The prestress effects are modeled as equivalent loads at nodes, i.e., the axial forces along the prestress path are applied at each end of each element which in effect is the same as modeling the prestress tendon as a series of straight lines. In case of grillage models, additional load cases were studied by loading only the inside and only the outside webs.

Results Review

The following results were obtained for each load case and compared from spine and grillage models:

- Midspan Deflection at middle of center span;
- Midspan Rotation at middle of center span;
- Midspan Longitudinal Bending Moment at middle of center span;

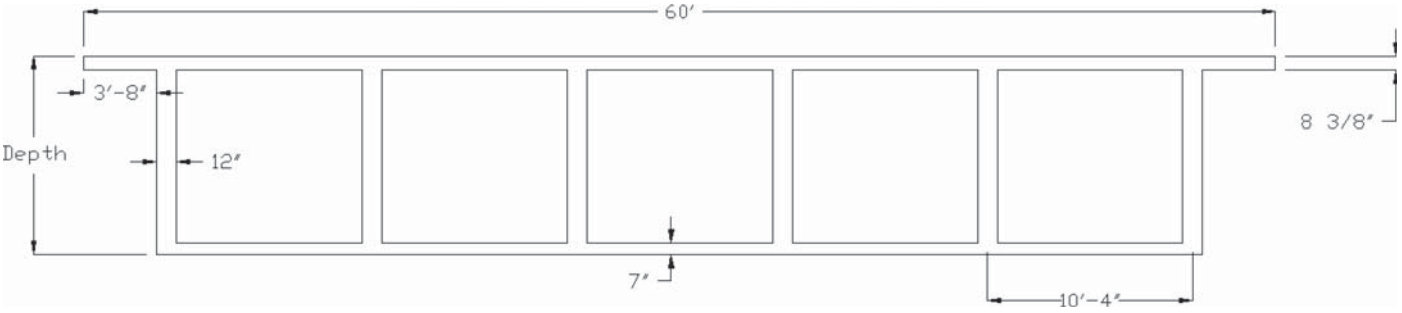

Figure 4-10. Idealized five-cell cast-in-place cross section.

Table 4-2. Section properties for two-cell curved line (spine) bridge model.

	200 ft. Single Span	100 ft. Single Span	200/300/200 ft. Multi-Span	150/200/150 ft. Multi-Span	75/100/75 ft. Multi-Span
CG (ft)	4.53	2.24	5.46	4.06	2.01
Area (ft2)	81.73	66.73	87.73	78.73	65.23
Avy (ft2)	56.60	56.60	56.60	56.60	56.60
Avz (ft2)	30.00	15.00	36.00	27.00	13.50
Iyy (ft4)	1,326.25	256.23	2,028.29	1,037.00	197.80
Izz (ft4)	9,544.20	7,488.61	10,366.44	9,133.08	7283.05
Jxx (ft4)	1,559.82	365.08	2,213.30	1,267.24	286.74
Depth (ft)	10.0	5.0	12.0	9.0	4.5

- Midspan Transverse Bending Moment at middle of center span;
- Midspan End Shear at first abutment in single span and at start of middle span in 3-span case;
- Midspan Normal Stress at bottom outside corner of cross section, at middle of center span; and
- Midspan Normal Stress at bottom inside corner of cross section, at middle of center span.

The graphical review of results included scatter-grams of each response quantity from spine and grillage models. An example of such graphs is shown in Figure 4-13.

The ratio of stresses and shear forces from the spine model to those of the grillage model were also obtained to review the effect of radius of curvature and modeling technique. An example of such graphs is shown in Figures 4-14a and 4-14b.

Summary of Results

Numerous scattergrams were plotted for each of the results listed in the previous section and bridge types shown in Figures 4-4 through 4-10. Figure 4-14 shows the plots with the most divergent results (i.e., with values furthest away from 1.00) between the spine and grillage models. As a result, the outside web shear force and longitudinal stress are the main effects that need attention in design. To better quantify these results and the effects of curvature on various bridge types, ratios of results for various bridge models were combined and plotted as shown in Figures 4-15 through 4-18. Average

Table 4-3. Section properties for two-cell grillage bridge model.

EXTERIOR GIRDER	200 ft. Single Span	100 ft. Single Span	200/300/200 ft. Multi-Span	150/200/150 ft. Multi-Span	75/100/75 ft. Multi-Span
CG (ft)	4.23	2.06	5.13	3.78	1.85
Area (ft2)	25.03	20.03	27.03	24.03	19.53
Avy (ft2)	18.87	18.87	18.87	18.87	18.87
Avz (ft2)	10.00	5.00	12.00	9.00	4.50
Iyy (ft4)	386.50	73.28	594.75	301.19	56.45
Izz (ft4)	216.76	208.19	219.34	215.31	207.11
Jxx (ft4)	519.94	121.69	737.77	422.41	95.58
INTERIOR GIRDER	**200 ft. Single Span**	**100 ft. Single Span**	**200/300/200 ft. Multi-Span**	**150/200/150 ft. Multi-Span**	**75/100/75 ft. Multi-Span**
CG (ft)	5	2.50	6.00	4.50	2.25
Area (ft2)	31.67	26.67	33.67	30.67	26.17
Avy (ft2)	18.87	18.87	18.87	18.87	18.87
Avz (ft2)	10.00	5.00	12.00	9.00	4.50
Iyy (ft4)	541.74	106.59	823.13	425.04	82.44
Izz (ft4)	399.43	399.02	399.60	399.35	398.97
Jxx (ft4)	519.94	121.69	737.77	422.41	95.58
Transverse Element	**200 ft. Single Span**	**100 ft. Single Span**	**200/300/200 ft. Multi-Span**	**150/200/150 ft. Multi-Span**	**75/100/75 ft. Multi-Span**
CG (ft)	5	2.50	6.00	4.50	2.25
Area (ft2)	1.63	1.63	1.63	1.63	1.63
Avy (ft2)	0.01	0.01	0.01	0.01	0.01
Avz (ft2)	1.63	1.63	1.63	1.63	1.63
Iyy (ft4)	34.38	7.21	50.94	27.32	5.61
Izz (ft4)	0.14	0.14	0.14	0.14	0.14
Jxx (ft4)	68.58	14.25	101.69	54.47	11.05

Table 4-4. Section properties for cap and column elements.

	Cap Section	6' x 18' Column	8' x 8' Column	7' x 7' Column	6' x 6' Column
Area (ft^2)	108	108	64	49	36
A_{vy} (f_t^2)	108	108	64	49	36
$A_{vz\,(ft}^{\ 2}$)	108	108	64	49	36
I_{yy} (ft^4)	5000	324	341.33	200.08	108
Izz(ft^4)	5000	2916	341.33	200.08	108
Jxx(ft^4)	5000	1296	1365.33	800.33	432

Table 4-5. Dead load shear results for 200 ft/single span skew.

	Obtuse (Element 1)		Acute (Element 21)	
Straight	Value	**Ratio**	Value	**Ratio**
Radial	-389.35	**1**	-387.84	**1**
Skew-Left	-605	**1.55387184**	-190.65	**0.49156869**
Skew-Both	-392.94	**1.0092205**	-342.23	**0.88239996**
	Obtuse (Element 1)		Acute	
400' Radius	Value	**Ratio**	Value	**Ratio**
Radial	-577.89	**1**	-189.78	**1**
Skew-Left	-782.91	**1.3547734**	-58.279	**0.30708715**
Skew-Both	-614.14	**1.0627282**	-183.66	**0.96775213**

ratios and standard deviations were also calculated for each group of bridges with same cross-section type and loading. These results are the primary source of the recommendations for design at the end of this study. Figures 4-15 and 4-17 show the ratios of Curve to Straight Bridge spine models. These figures reveal the limit of radius of curvature beyond which the curvature effects may be ignored altogether and the bridge may be analyzed as if it were straight. The ratios of "Spine to Grillage Model" shown in Figures 4-16 and 4-18 reveal if a curve spine model can be used in cases of tighter curvatures and the limit of this type of model to obtain accurate results for design purposes. In the case of the spine models, shear forces were obtained by considering the shear flow from torsion in addition to the vertical shear. The stresses were also obtained from the combined effect of axial force and longitudinal and transverse moments.

Figures 4-15 through 4-19 are for the four bridge cross sections (cast-in-place single-cell (CIP1), precast single-cell (PC1), cast-in-place two-cell (CIP2), and cast-in-place five-cell (CIP5)) with different pier configurations and span lengths. Therefore, points designated as **PC1_6x6_sp3m_dl** are for a single cell precast bridge (PC1) with a 6 x 6 pier (6x6), 3-span configuration of medium length spans (sp3m) and dead load response (dl).

Detailed results from the parameter studies are presented in Appendix E.

Conclusions of the Parametric Study

Study of the above results led to the following conclusions:

- Bridges with L/R less than 0.2 may be designed as if they were straight. Figures 4-15 and 4-17 reveal results are within 4% of a curved spine model when this is done.
- Bridges with L/R less than 0.8 may be modeled with a single-girder spine model using a curved (spine) model and lateral effects shall be included in the analysis. Figure 4-18 shows that longitudinal stresses will be

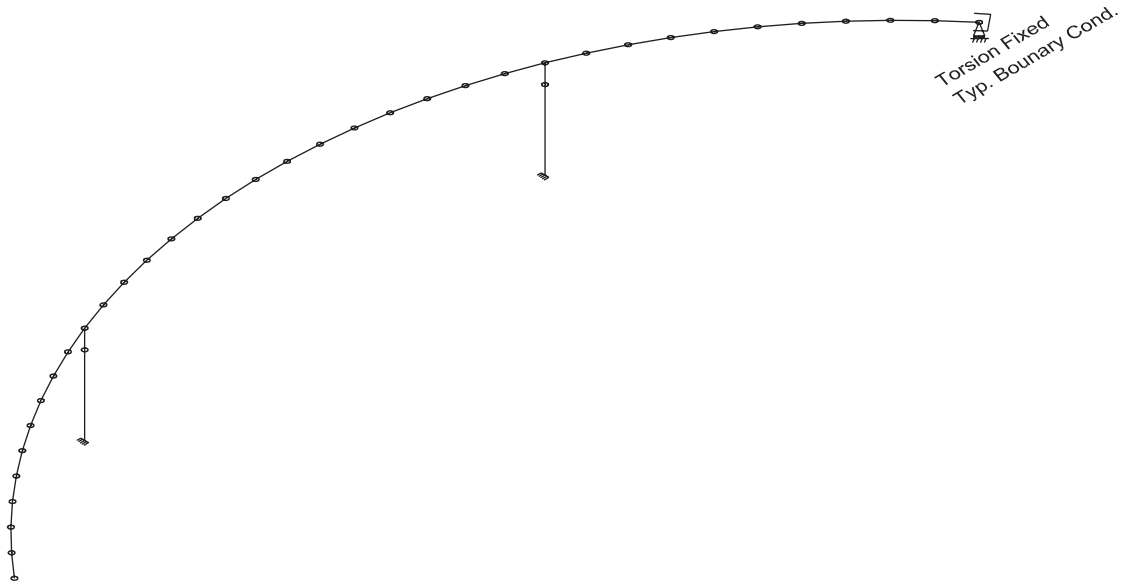

Figure 4-11. Typical curved line (spine beam) bridge model (showing 3-span unit).

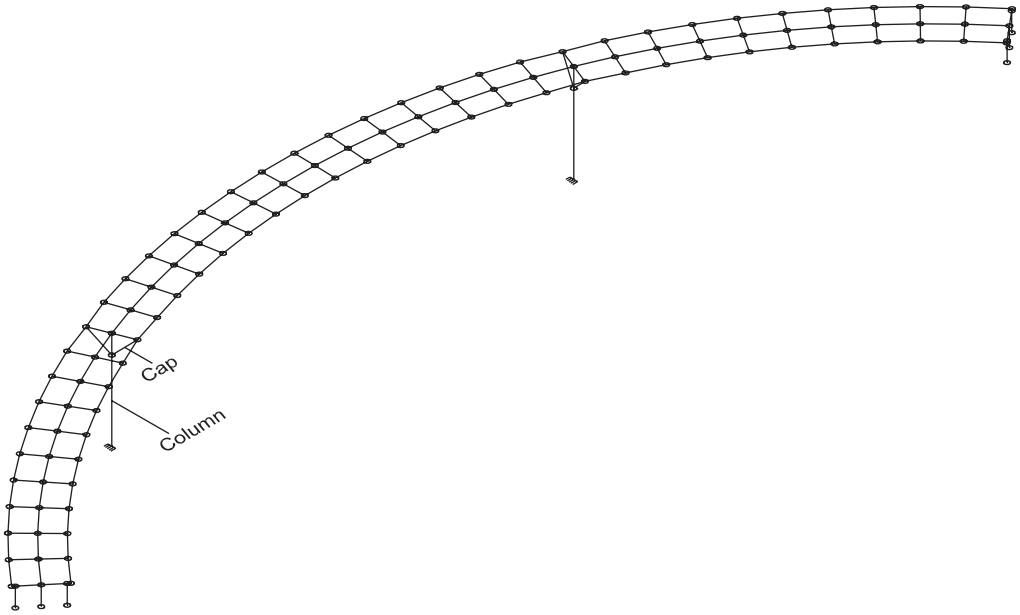

Figure 4-12. Typical curved grillage bridge model (showing 3-span unit with 3 webs).

unconservative by less than 4% up to this limit unless the bridge has a low span length-to-width ratio (i.e., short-span 5-cell sections)

- Bridges with L/R larger than 0.8 shall be analyzed with more detailed analysis models such as grillage or finite element models. Figures 4-16 and 4-18 reveal that spine beam analysis will generally become increasingly unconservative beyond the 0.8 L/R limit.
- Curved bridges with length-to-width ratios of less than 0.2 and an L/R larger than 0.2 also require detailed analysis as revealed by the unconservative results for tightly curved short-span 5-cell bridges in Figures 4-16 and 4-18.

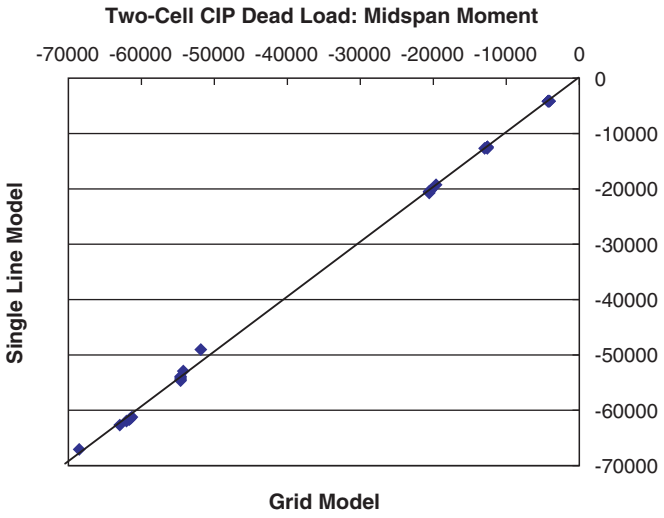

Figure 4-13. Scatter-gram comparison of results from spine and grillage models.

- Bearing forces (i.e., shear at the abutments) obtained from a spine model must consider the effect of torsion. Bearings must be designed considering the curvature effect.

Special Studies

In addition to the above parametric study, special studies were performed to get a better understanding of the effect of diaphragms, bearing conditions, skewed abutments, and long-term creep when combined with curved geometry.

Diaphragm

All 5-cell grillage bridge models used in the parametric study were also modified to have a stiff diaphragm in the center of each span. The results from each model with and without diaphragms were compared for dead load, live load, and post-tensioning. These results were compared using scatter-grams and ratios (line diagrams) similar to the results shown in Figures 4-19 and 4-20. The overall conclusion from these results is that interior diaphragms have minimal effect on the shear and stress responses and therefore may be eliminated altogether.

To verify the conclusions relative to interior diaphragms, the two-cell finite element model used in the model verification studies was modified to include interior diaphragms. These diaphragms were placed at the center of one of the end spans and at one of the third points in the center span. These diaphragms were located on one side of the midpoint of the bridge, which was otherwise symmetrical. Results were compared on both sides of the bridge and found to be nearly

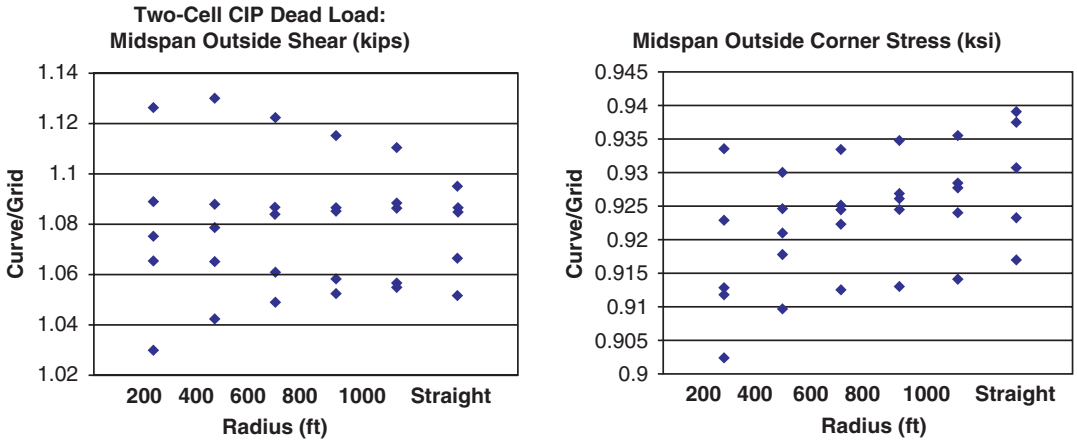

a) Midspan Outside Girder Shear Ratio

b) Longitudinal Stress Ratio

Figure 4-14. Line graphs of shear and stress ratios of results from spine and grillage models.

symmetrical. Therefore, the diaphragms were shown to have very little effect on the global response of the bridge.

Bearings at the Bents

The purpose of this study was to determine if bridges with integral and non-integral bents respond differently to curve effects. All three-span five-cell spine and grillage bridge models used in the parametric study were also modified to have a point bearing support at the piers; i.e., free to move in transverse or longitudinal directions. The results were studied using scatter-grams and ratio (line) diagrams comparing the results from spine to grillage models. It was found that, in general, magnitudes of curve to straight results are in the same order as the integral bridges. Therefore, the final conclusion is that, as long as the support conditions are modeled correctly, the same guidelines for modeling limitations are equally applicable to integral and non-integral conditions.

Skewed Abutments

A two-cell single-span (200 ft long) and a two-cell three-span bridge (200ft-300ft-200ft) were modified to have 30-degree skew support at the left support and another case with 30-degree

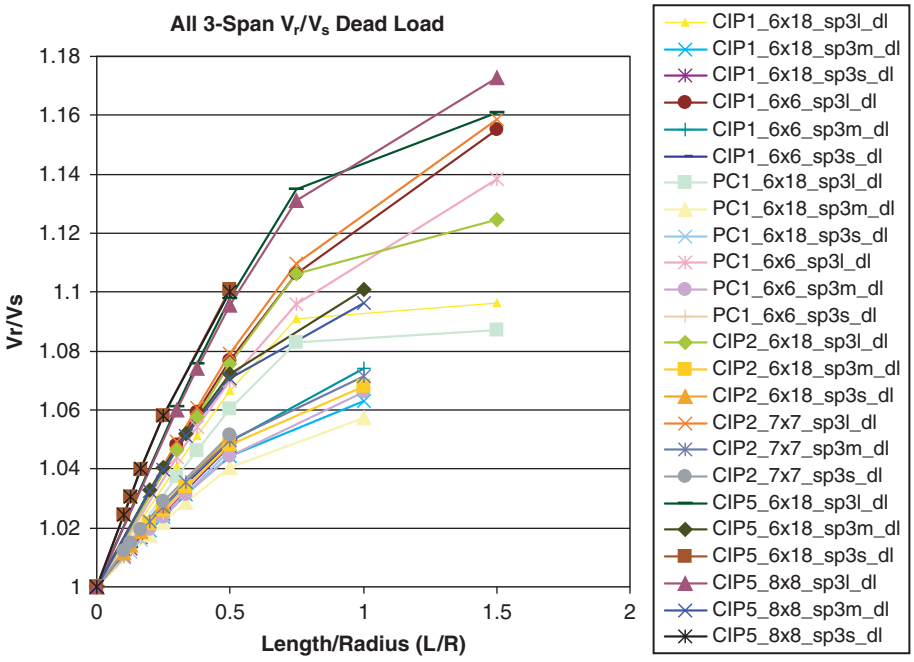

Figure 4-15. Ratio of outside web dead load shear forces in curved (V_r) to straight (V_s) bridges where length equals middle span length.

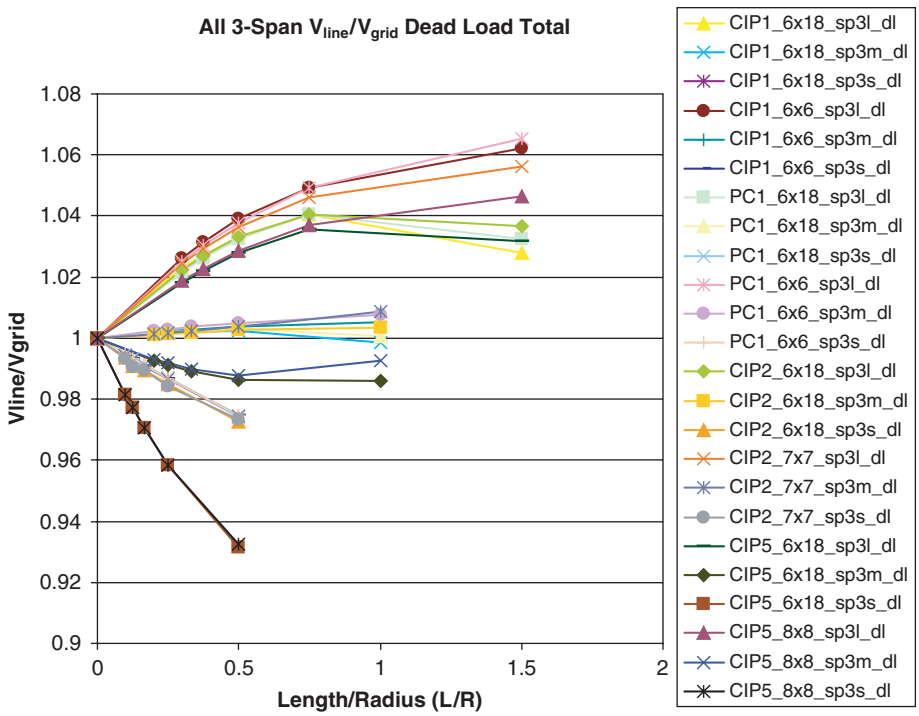

Figure 4-16. Ratio of outside web dead load shear forces from spine to grillage model.

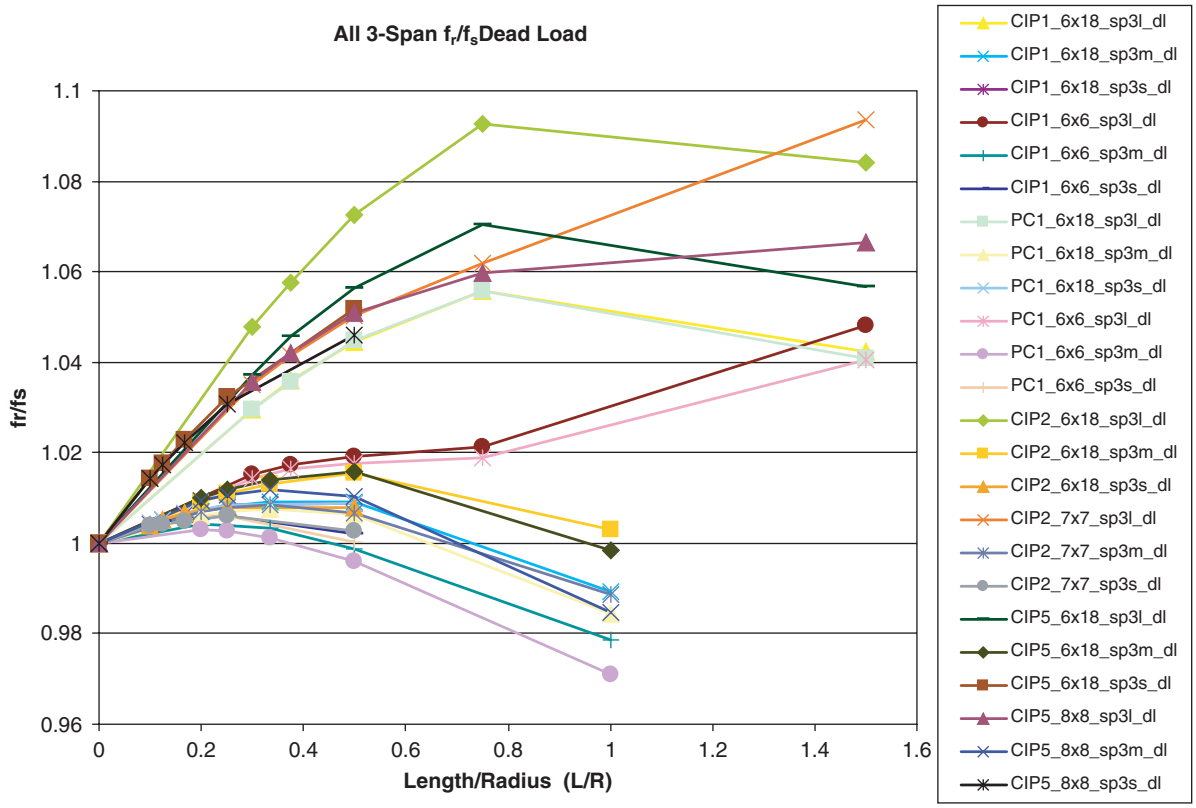

Figure 4-17. Ratio of outside corner dead load longitudinal stress in curved to straight bridge.

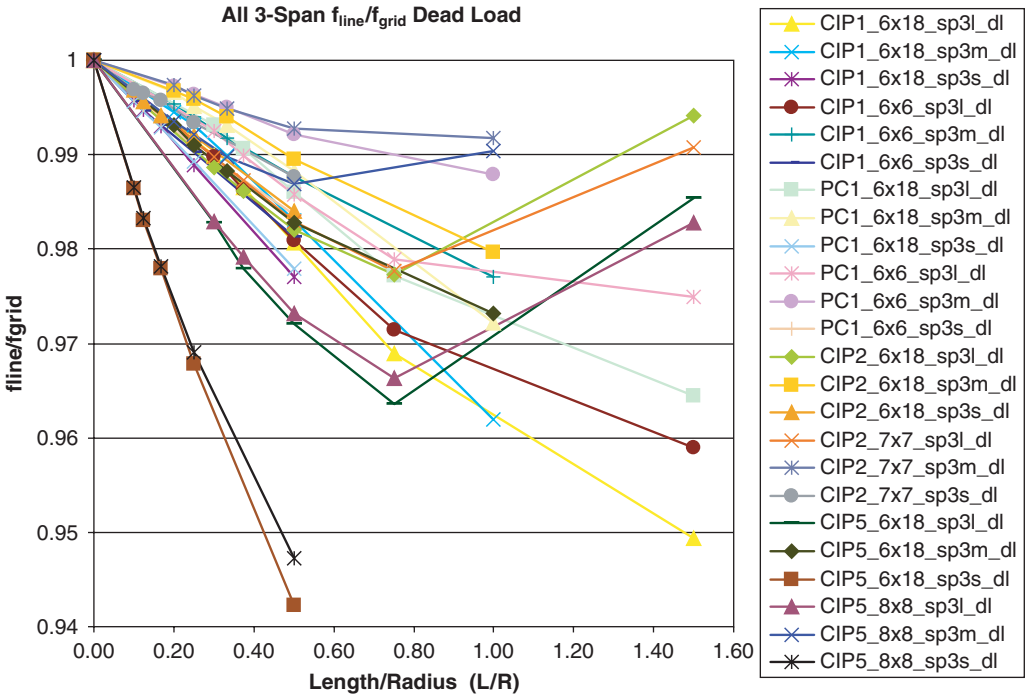

Figure 4-18. Ratio of outside corner dead load longitudinal stress from spine to grillage model.

skew support at both ends, see Figure 4-21. The abutments were supported on rollers. The obtuse and acute abutment shear values were compared in straight and skewed bridges with and without curved alignment. The simple span bridge results were compared for dead load and live load and the three span results were compared for dead load responses. The results are shown in Tables 4-5 through 4-7. The final outcome of these results is that the curved alignment does not aggravate the effect of skewed abutments and therefore, any consideration taken for straight bridges can be equally valid for curved bridges. These corrections will be necessary when the bridge is designed using a spine beam analysis. Skew can be automatically accounted for in a grillage analysis approach as shown in Figure 4-21.

Long-Term Creep

The effect of the time-dependant properties of concrete (principally creep) on the response of curved bridges was investigated using the LARSA 4D computer program, which

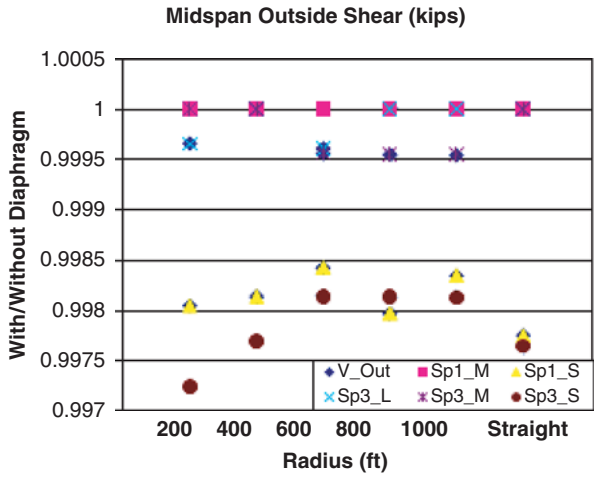

Figure 4-19. Scatter-gram comparison of live load results from grillage models with and without interior diaphragm.

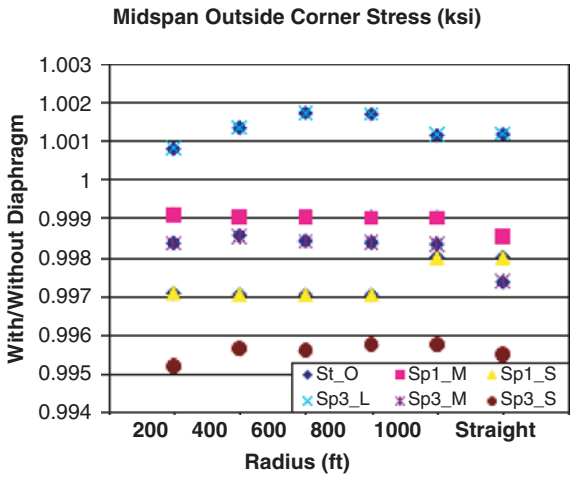

Figure 4-20. Line graph of ratio of results from grillage models with and without interior diaphragm.

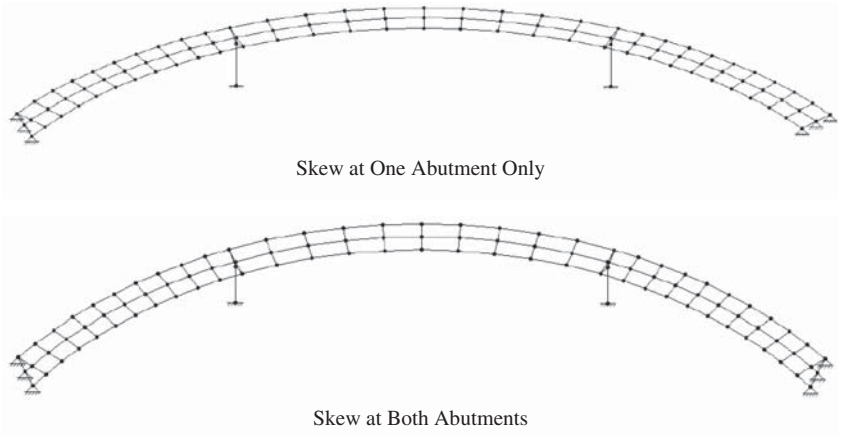

Figure 4-21. Skew configurations studied.

can consider both the 3-D geometry of the bridge plus the time-dependant behavior of concrete. The same structure used in the comprehensive example problem was analyzed over a period of 10 years. The bridge was modeled as a 3-D spine beam. In addition, the model was modified by changing the curve radius in two cases and changing the length of the end span in another case. Therefore, four models were evaluated. In all cases the abutments were fixed against torsion. The end span and radii of these bridges are shown in Table 4-8

The long-term deflection of Models 1 through 3 did not appear to be affected by the radius of the bridge. Therefore, methods used for adjusting cambers for straight bridges would appear to be applicable to curved bridges analyzed as three-dimensional spine beams.

The major concern, however, was abutment bearing reactions. These will change over time. This is manifested by the change in the torsion reaction at the abutment, which in turn will affect the bearing reactions. Table 4-9 summarizes the dead load and prestress results from the four models investigated.

The following conclusions can be drawn from this limited study:

- The torsion reaction and thus the relative bearing forces in continuous curved concrete box-girder bridges vary over time and depend on both the radius of the curve and the relative length of the end span with respect to the center span. The forces in outside bearings will increase and inside bearings will decrease. Given the many possible bridge-framing configurations, it is difficult to make an accurate assessment of time-dependent bearing forces.
- The above study assumed bridges constructed on falsework. Segmentally constructed bridges are expected to behave differently.
- The LARSA 4D program does not consider torsion creep, as is the case with most other commercially available software. Torsion creep is expected to mitigate long-term changes in bearing forces, as would modeling the flexibility of bearing systems subjected to torsion loads from the superstructure.

Given these conclusions, it would appear to be safe to analyze curved concrete box-girder bridges using commercially available software, particularly for segmentally constructed bridges. It is recommended that the vertical flexibility of bearings be considered in these analyses.

Table 4-6. Live load shear results for 200 ft/single span skew.

	Obtuse (Element 1)		Acute	
Straight	Value	**Ratio**	Value	**Ratio**
Radial	-577.89	**1**	-189.78	**1**
Skew-Left	-782.91	**1.3547734**	-58.279	**0.30708715**
Skew-Both	-614.14	**1.0627282**	-183.66	**0.96775213**
	Obtuse (Element 1)		Acute	
400' Radius	Value	**Ratio**	Value	**Ratio**
Radial	-81.618	**1**	-12.007	**1**
Skew-Left	-116.15	**1.42309295**	12.526	**-1.0432248**
Skew-Both	-85.079	**1.04240486**	-9.1316	**0.76052303**

Table 4-7. Dead load shear results for 400 ft radius, 200/300/200 ft multi-span skew.

	Obtuse (Element 1)		Acute	
Straight	Value	**Ratio**	Value	**Ratio**
Radial	-297.35	**1**	-296.59	**1**
Skew-Left	-378.79	**1.27388599**	-197.35	**0.66539668**
Skew-Both	-378.02	**1.27129645**	-197.66	**0.66644189**
	Obtuse (Element 1)		Acute	
400' Radius	Value	**Ratio**	Value	**Ratio**
Radial	-370	**1**	-202.2	**1**
Skew-Left	-452.84	**1.22389189**	-135.81	**0.67166172**
Skew-Both	-453.89	**1.22672973**	-135.81	**0.67166172**

Table 4-8. Models of two-cell bridge used to study the effect of creep.

Model Number	Radii (ft)	End Span Length (ft)
1	400	200
2	800	200
3	1600	200
4	400	140

Table 4-9. Time dependence of abutment torsion moment.

Model Number	Torsion Moment 7 Days (ft-kips)	Torsion Moment 3600 Days (ft-kips)	% Difference
1	-8826	-10034	13.7
2	-7357	-9262	25.9
3	-6395	-8500	32.9
4	-4012	-5842	45.6

In the absence of such an analysis, it is recommended that dead load torsion reactions at the abutment from a 3-D spine beam analysis be increased by approximately 20% for the final condition and bearings or bearing systems be designed to envelope both the initial and final conditions. This is a crude recommendation, but given the mitigating factors not considered in this limited study, it should provide a reasonable hedge against bearing failure. In the case of a grillage analysis, the same adjustment can be made by resolving bearing reactions into a torsional moment, increasing that moment by 20%, and recalculating the new bearing forces.

CHAPTER 5

Regional and Local Response Analysis Studies

Three types of actions, as shown in Figure 5-1, have been considered in the analysis work for this project.

1. Global or overall girder action of the bridge together with its supporting piers and abutments.
2. Regional beam action of each web supported at the top and bottom flanges as a beam.
3. Local action of the concrete cover over the tendons, and/or local lateral shear/breakout failure adjacent to the ducts. This is sometimes referred to as Lateral Tendon Breakout (LTB)

Global or overall girder action of the bridge together with its supporting piers and abutments is covered in Chapter 4. This chapter focuses on "regional" and "local" action.

Regional beam action considers each web as a beam supported at the top and bottom flanges. The regional moments can be determined from a 2-D frame analysis of the cross section. The prestress lateral force is determined individually for each web with due consideration for the allowable variation in prestress force between webs. The compressive reactive forces on the concrete are applied as distributed loads on the webs and as concentrated loads at the centerlines of the slabs. The system is in static equilibrium and the support reactions will be zero.

Local slab action of the concrete cover over the tendons has been identified as a major cause of failure in several curved post-tensioned bridges that did not have duct or web ties. For a web without duct or web ties, the cover concrete is the only element restraining the lateral prestress force. The cover concrete acts as a plain concrete beam to restrain the lateral prestress force, F, as shown in Figure 5-2. The "local slab" is subject to lateral shear and bending from the lateral prestress force. The web is subject to regional transverse bending which results in tensile stresses on the local slab.

Detailed local analysis models were used to evaluate the local stresses resulting from longitudinal tendons generating transverse forces on curved webs. Finite element (FE) models were developed to perform parameter studies, investigate capacities and damage modes, and prescribe a methodology to prevent such damage. Detailed 3-D, nonlinear analyses were performed using ABAQUS Version 6.5 "damaged plasticity" concrete cracking model. Such models provided tendon horizontal force plots versus deformation, and these, in combination with strain contour and crack pattern plots show the evolution of damage with increasing force. Comparison of such plots among different geometries and reinforcing schemes provides quantitative and qualitative parameter sensitivity evaluation.

The FE analyses were used to provide insights into where damage first accumulates and develops, but these parameter sensitivity comparisons are not exhaustive, and there are limitations to what can and cannot be reliably predicted by FE analysis. A limitation of the parameter studies, for example, is that, for cases with reduced cover, the web thickness was held constant, and this tends to increase the moment arm to the web stirrups, which partially offsets the reduction in strength associated with reduced cover.

Limitations on the FE simulations, for example, include the fact that ultimate failures caused by discrete crack propagation are difficult to predict. FE analysis practitioners (e.g., members of ACI/ASCE Committee 447 "Finite Element Analysis of Reinforced Concrete") have a range of opinions on how best to predict the propagation of individual cracks in a structure component with a lot of rebar. Some advocate the use of fracture-mechanics-based algorithms shown to predict propagation of single cracks in plain concrete reasonably well. But for practical FE analysis of concrete with a lot of rebar and a lot of cracks, the industry standard approach is to use smeared crack models, as was used here.

What these models do reasonably well is predict "zones of likely crack formation" and strain distributions in concrete and rebar, which provide insight into causes and triggers for failure. Experience and judgment is required for the interpretation of the results. The work herein is based on

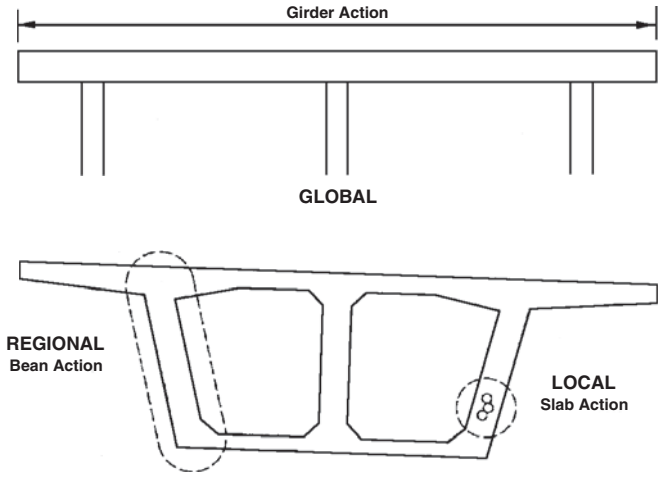

Figure 5-1. Types of actions considered.

(so has the limitations of) the constitutive formulations within the ABAQUS program, a widely distributed, well-respected commercial product for solving problems with a high degree of material nonlinearity.

This program was chosen partly because of the authors' degree of experience using it, but also to demonstrate the use of a widely available tool that other interested engineers or researchers could use to examine their own special design cases. ABAQUS is certainly not the only product available for this type of analysis.

Despite the limitations noted, the authors believe the FE work herein has demonstrated an approach to modeling box-girder cross-sections, especially a method for applying the loads and boundary conditions, and this has satisfied one of the goals for this project.

Ultimately, the design code recommendations in this report were developed by our team's years of collective design and construction observation experience, research of literature and existing codes, extensive hand calculations (similar to what we think designers should use), global analysis, and the local FE analysis.

Local Analysis Validation/Demonstration Case (UT Test Case)

The local analyses were begun with a validation case simulating Specimen "BC" from prior research conducted at the University of Texas (Van Landuyt, 1991). The case studied is a ⅓ scale representation of the configuration of Las Lomas, a well-known bridge that failed in lateral tendon breakout.

Test Model and Test Conduct

The following test model and test conduct description come from the test report and thesis: "The Effect of Duct Arrangement on Breakout of Internal Post-Tensioning Tendons in Horizontally Curved Concrete Box Girder Webs," by D.W. Van Landuyt, 1991.

The box cross-section was a scaled version of Las Lomas with changes made for simplifying construction (Figure 5-3). To avoid having to build cantilever forms, the girder was built and tested in an inverted position. This did not significantly affect results (it was assumed by the researchers that gravity loads are unimportant to breakout). The model top slab therefore represents the bottom slab at Las Lomas, etc. The top slab thickness at Las Lomas varied transversely and the

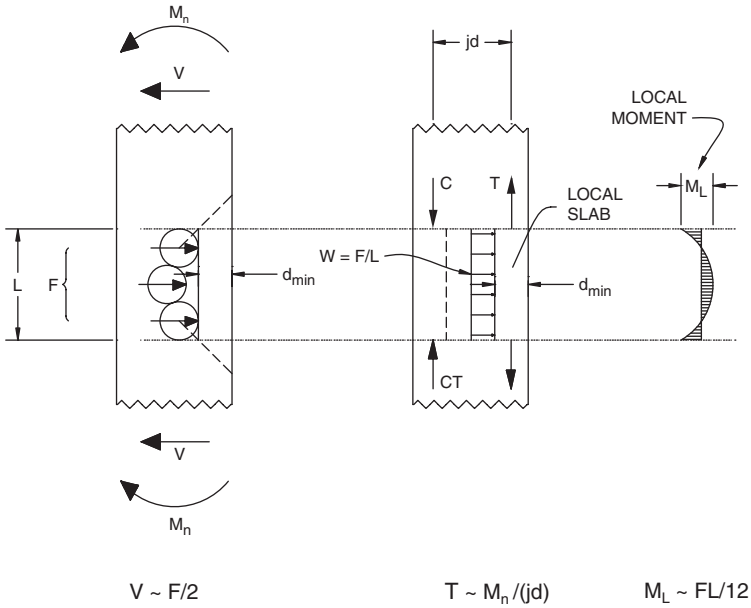

Figure 5-2. Regional and local actions on a web.

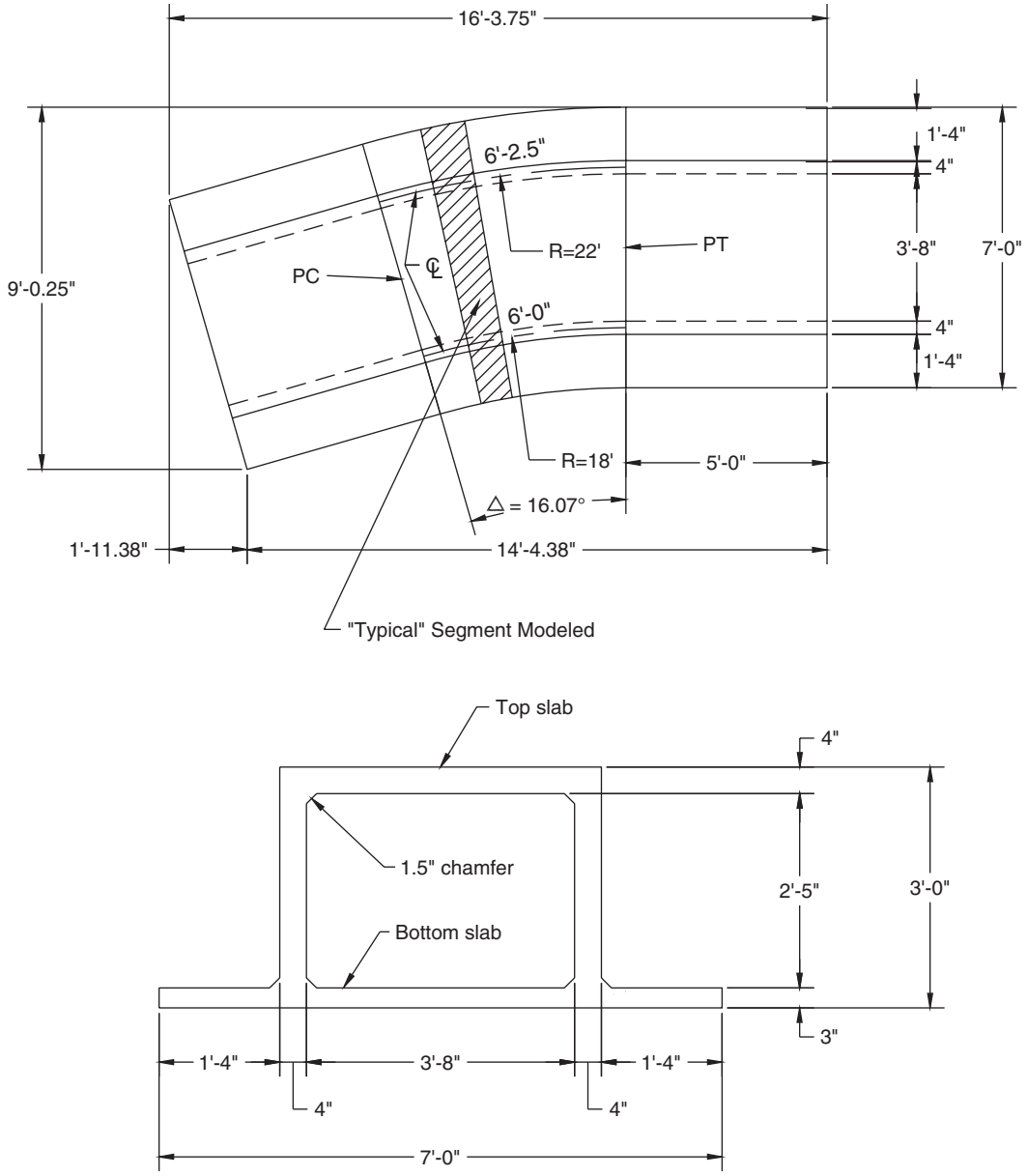

Figure 5-3. Plan and end view of U.T. girder test specimen (from Van Landuyt, 1991).

bottom varied longitudinally. Average thicknesses were calculated, scaled and rounded off to an integral number of inches. At Las Lomas, the centerline distance between interior and exterior webs was 11 feet. This scaled to 3 ft 8 in. The model was constructed with a centerline web-to-web distance of 4 feet so that the radius of each web was a whole number. To save on materials and labor, the cantilevers were shortened slightly from a scaled value of 1 foot 10 inches to 1 ft 4 in. (The actual cantilever length has little effect on web behavior.) The dimensions of the web were considered important. The exact scaled values of 4 in for the thickness and 3 ft for the overall height were maintained (Figure 5-4).

The web radii were chosen to be small enough so that the tendon breakout in the web would occur before failure of any other part of the girder or testing apparatus. If the curve were not sharp enough, anchorage zone failure might have resulted or the strands would have been loaded to an unsafe level. Duct arrangement controlled the design of the curve radius. The capacity to resist lateral shear failure was calculated for each tendon, assuming two failure planes would form and that the maximum concrete strength would be 5000 psi.

$$F_r = 2\sqrt{5000}(2)12''(1.125'') = 3.8k/ft$$

where F_r is the lateral (radially oriented relative to the curve) prestress force.

Therefore a total F_r of 15.2 k/ft was required for all four tendons. A jacking force of 372 kips could be delivered from

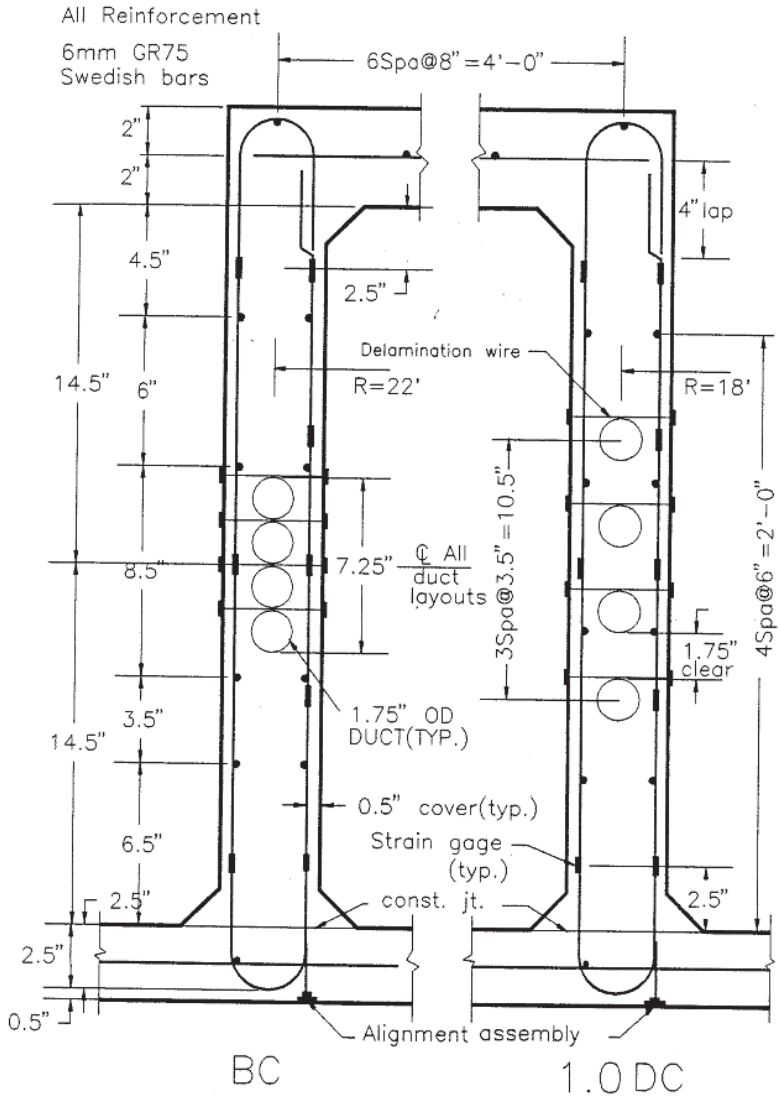

Figure 5-4. Girder #1 cross section in curved region (from Van Landuyt, 1991).

the loading apparatus. An 18-ft radius for the inside of web was selected, as it would permit a total F_r of 20.6 k/ft. This was more than a third larger than the anticipated failure load. The previously determined cell width mandated that the companion web radius be 22 feet. The curve length of 5 feet was chosen for the 18-ft radius. The curved region was the most difficult part of the model to construct and was kept as short as possible. A 5-ft curve was more than twice the clear height of the web and was thought to be sufficient to allow regional transverse bending. A 5-ft straight transition zone on each end insulated the curve from the complex stresses at anchorages.

Las Lomas was reinforced with GR40 #5 stirrups spaced at 15 inches. No standard bars match this on a ⅛ scale. The closest match was 6 mm, 75 ksi bars from Sweden already available in the lab. This is nearly equivalent to a #2 bar. The stirrup spacing needed to be adjusted to reflect the imprecise scaling of stirrup sizes. Equivalent spacing of #6's at 21.3 inches was scaled to 6-mm bars at 7 inches. The spacing was not increased to account for the greater yield strength of the Swedish bar. Stirrup spacing was reduced in the anchorage zones to 5½ inches.

A four-tendon bundle and three other promising arrangements were tested. Only duct positioning varied from web to web; all other details remained the same. Duct size at Las Lomas was not given, although based on the maximum number of strands (28), ducts of approximately 4½-inch O.D. should have been used. Scaling required 1½-inch ducts for the model, but the major manufacturers of post-tensioning duct apparently do not make this size. The nearest available duct size (1.75 inches) was used.

Specimen BC is the duct arrangement similar to the one at Las Lomas. A slight modification was made for the model

(Figure 5-4). A straight vertical formation was used in lieu of the zigzag because it was considered more universal. The relative horizontal offsets between ducts in a zigzag pattern can change from bridge to bridge, depending on the clear distance between the stirrup legs and the diameter of the ducts. No large difference in behavior between the two arrangements was anticipated. The vertical bundle height at Las Lomas was approximately 16 inches; a vertical stacked bundle would have been 17½ inches. All ducts were centered on the web vertical axis.

Specimen 1.0DC follows the Texas State Department of Highway and Public Transportation design of the San Antonio "Y" project with an arrangement that maintained a clear spacing between ducts equal to the diameter of the duct. It is believed that this allows for better consolidation and, more importantly, eliminates the single large discontinuity found at Las Lomas. This arrangement is conservative and would be considered an upper limit beyond which further spacing of ducts would provide no benefit. The scaled vertical spacing was 1.75 inches. All ducts were centered on the web vertical axis.

All test concrete strengths were much greater than the 28-day design strength of 3500 psi. The slab and web concrete had higher overall strengths and faster strength gains as is typical of concrete containing super-plasticizers. The web concrete strength was 5300 psi.

6-mm-diameter hot-rolled bars were used for all reinforcement. Tensile tests on bars conducted at the lab showed average yield strength of 75 ksi.

Galvanized, corrugated, folded metal ducts were used in all instances. The outside ridge-to-outside ridge dimension was 1.75 inches. The inside diameter was 1.60 inches and the gauge was 0.035 inches.

Post-tensioning was applied to the specimens with 7-wire, ½-inch Ø, 270 ksi, low-relaxation strands. Test data provided with the strand showed an actual yield of 276 ksi and ultimate of 289.5 ksi.

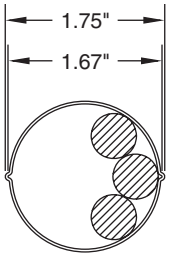

Figure 5-5. Strand positions in curve (from Van Landuyt, 1991).

A loading system was developed to apply gradually increasing load simultaneously to all tendons with an equal force in each tendon. It was necessary to consider how the strand or strands that would constitute a tendon would bear on a duct. The ducts at Las Lomas were nearly filled to capacity with strands. This meant that almost the entire 180 degrees of the duct on the inside of the curve was in contact with the strands. That same type of load distribution could be approximated with a minimum of three ½-inch-diameter strands per duct (Figure 5-5). Given that there were four ducts, a total of twelve strands could be safely stressed to $0.75f_{pu}$ to develop a maximum force of 372 kips.

Regional beam behavior was monitored by deflection of the web relative to the top and bottom slabs. U-shaped frames were mounted to the web face on the outside of the curve (Figure 5-6). The actual attachment points were about 2 inches below the top slab and 2 inches above the bottom

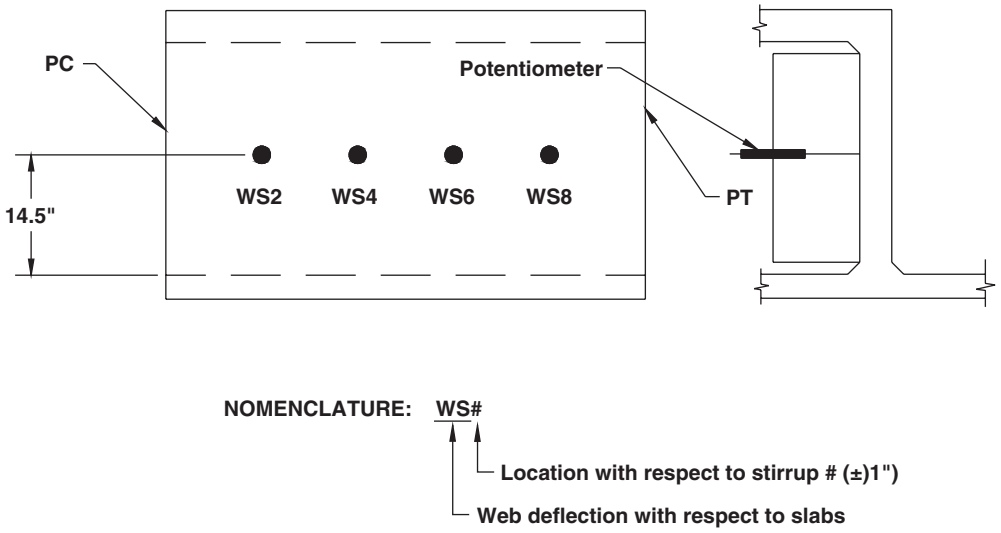

Figure 5-6. Web potentiometer configuration (from Van Landuyt, 1991).

slab. This permitted the construction of only one type of frame, which could be mounted on either web. Ideally, the frame should have been mounted on the slabs. However the deflection anticipated in the first 2 inches is negligible. A single potentiometer was mounted at the mid-height of the frame (which is also the c.g. of the tendon group). A small mirror glued to the specimen provided a smooth surface on which the potentiometer stem could bear.

Mounting the potentiometers on the outside face of the curve meant that deflections should not be influenced by local beam action; regional beam behavior should be solely responsible for measured deflections. Also potentiometers attached to the back face were protected from exploding concrete. The web-slab potentiometer nomenclature is given in Figure 5-6. The description begins with the letters WS to signify that deflections of the web relative to the slab are being measured. The number of the stirrup nearest the potentiometer follows these letters. Web delaminations were measured by wires/potentiometers placed in tubes cast through the webs above and below the duct group. Sudden movements in these measurements were good indicators of imminent failure.

Figure 5-7 is a sketch of how the concrete cracked and failed during the test. Figure 5-8 compares tendon horizontal force versus deflections for the four different webs tested.

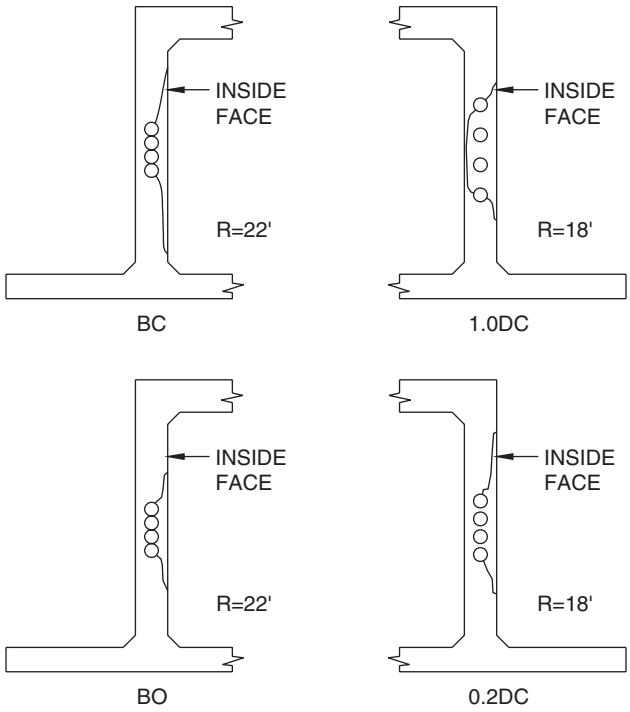

Figure 5-7. Specimen failure plans (from Van Landuyt, 1991).

Finite Element (FE) Model and Analysis

An FE model of Girder BC and 1.0DC was developed for a typical slice of the test model in the curved region, as was shown in Figure 5-3. The cross-section and duct geometry (as was shown in Figures 5-4 and 5-5) were modeled per the test configuration and dimensions. The FE model and boundary conditions are illustrated in Figure 5-9. This shows how a 3-D slice was modeled with horizontal tendon loads applied directly to the inner surfaces of the ducts. The

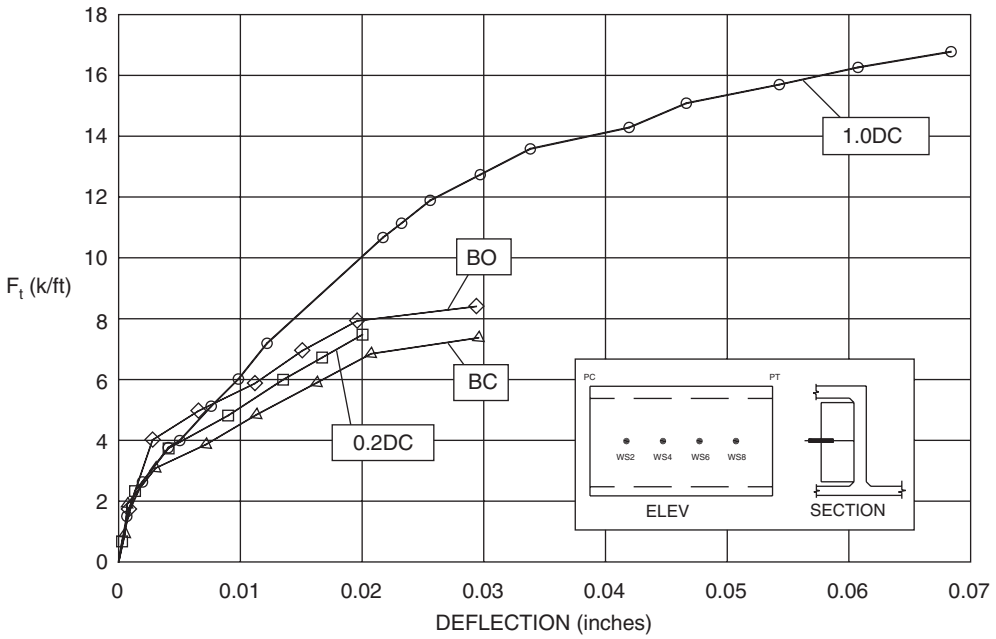

Figure 5-8. Comparison of web deflections relative to slabs at Stirrup #6 (from Van Landuyt, 1991).

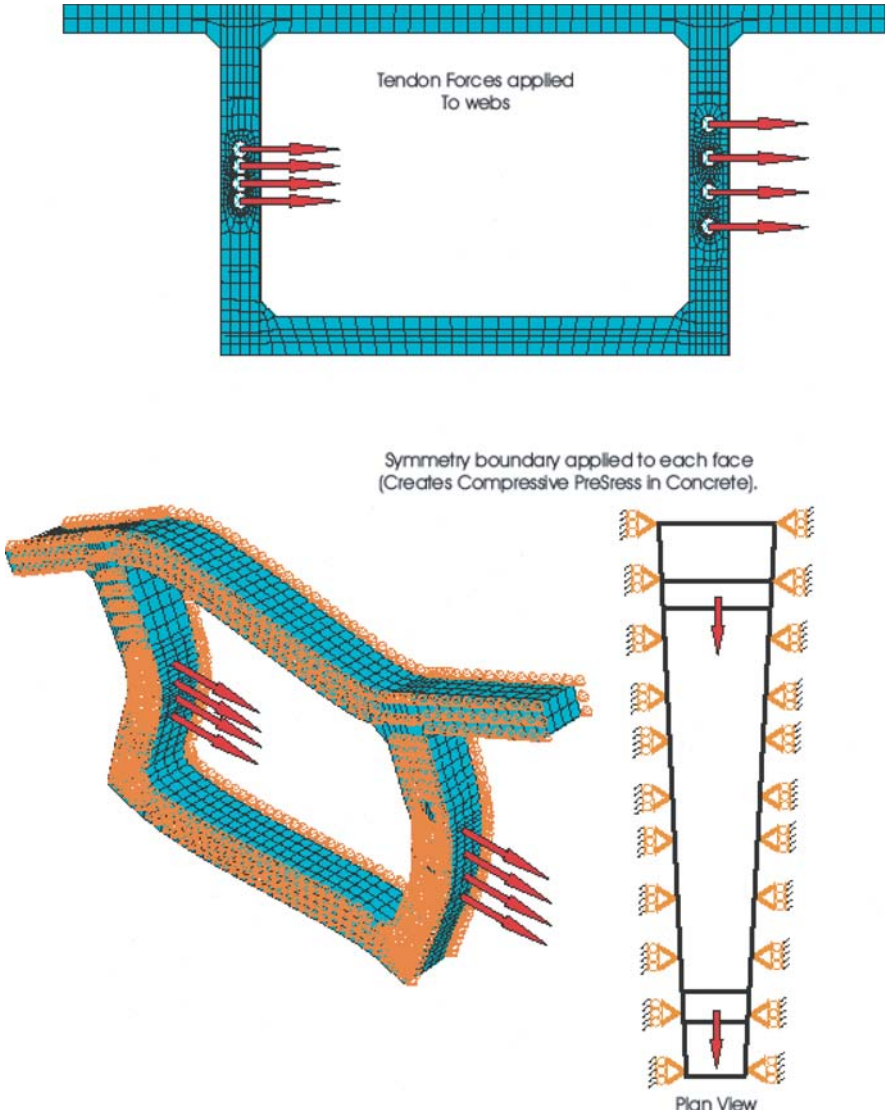

Figure 5-9. Finite element model and boundary conditions.

wedge slice model configuration and "symmetry" boundary conditions allowed horizontal (radial) displacement to occur naturally in the FE model, and this in turn, causes "longitudinal" compression prestress in the concrete in a manner similar to the actual test specimen. What is precisely mathematically represented with such boundary conditions is a wedge-slice of a complete circle, but the boundary conditions are also reasonably accurate for a section of a curve.

The tendon forces were applied in incremental fashion with enough equilibrium iterations and small load increments to achieve solution convergence at every increment. This solution procedure is often referred to as Full-Newton, where upon the next load increment; the structure stiffness is updated, based on the material damage, which has occurred (concrete cracking/crushing and steel yielding). The analysis was run out to large web displacements and significant damage (failure), i.e., well beyond the displacements plotted in Figure 5-8.

A typical deformed shape from the analysis (at the 1.0 DC web displacement of 0.07 inches) is shown in Figure 5-10. The amount of deflection and the sharpness of the flexural curvature is significantly more severe in Girder-BC than in Girder-1.0DC. This agrees with test observations. In the illustration, displacements are magnified by 50.

Figure 5-11 shows the same deformed shape, but with contours of maximum principal strain. In reinforced concrete analysis, these are one of the most effective ways to show damage and deformation distributions in the concrete and rebar. Concrete stress contours are generally not helpful, because after concrete cracks, the stress reduces to nearly zero, so a zero or small tensile stress may be displayed in a zone that is already highly damaged. But maximum principal strains (generally, the maximum tension found in any orientation for a given point in the continuum) can indicate concrete cracking, which occurs at strain of approximately 1.50E-4 to

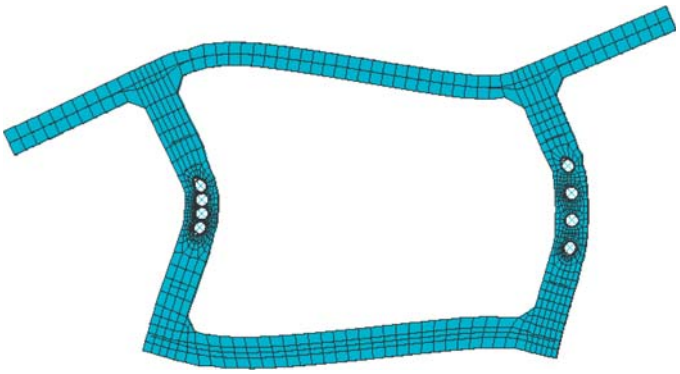

Figure 5-10. Deformed shape (displacements × 50) at 1.0 DC deflection of 0.07 inches.

2.00E-4. Figure 5-11 shows widespread cracking in the vicinity of the ducts and much more severe cracking at the BC configuration than at the 1.0DC.

Figure 5-12 shows similar strain contours, but in an end view at a lower displacement. Here the crack zones are also fully formed, but are easier to see in cross section. Figure 5-13 shows the same deformed shape as Figure 5-12, but viewed in conjunction with principal strains, is used to estimate the extent of cracks. Using this information, and judgment from experience with many similar analyses, actual cracks implied by the analysis are drawn onto the figure. Comparing to Figure 5-7 shows similar trends in the location of the cracking as compared to the test. In making this conclusion, it is assumed that the test also showed other small cracks in the vicinity of the ducts, but the cracks shown in Figure 5-7 were the primary failure planes.

Another significant analysis versus test comparison is shown in Figure 5-14: the lateral force versus deflection at the mid-height of the duct bank relative to the slab. The comparison shows that for both the BC and 1.0DC girder webs, the analysis is simulating the response (initial stiffness and stiffness degradation with accumulating damage) and the lateral force capacity reasonably well.

These comparisons and experience with many similar reinforced concrete analyses indicate that the FE representation and modeling strategy are appropriate for moving on to the prototype models.

Local Analysis of Multicell Box-Girders

For the NCHRP 12-71 project study, there are two basic local model types:

- Multi-cell box (three-cell box with super-elevation/ vertical interior webs, and inclined exterior webs; also ran with vertical exterior webs)
- Single-cell box (prototypical pre-cast box with super-elevation and inclined webs)

The prototype geometry for the multicell box girder was super-elevated since this is how curved girders often occur in practice. In the multicell studies conducted, the only effect of super-elevation was a small difference in the end conditions of

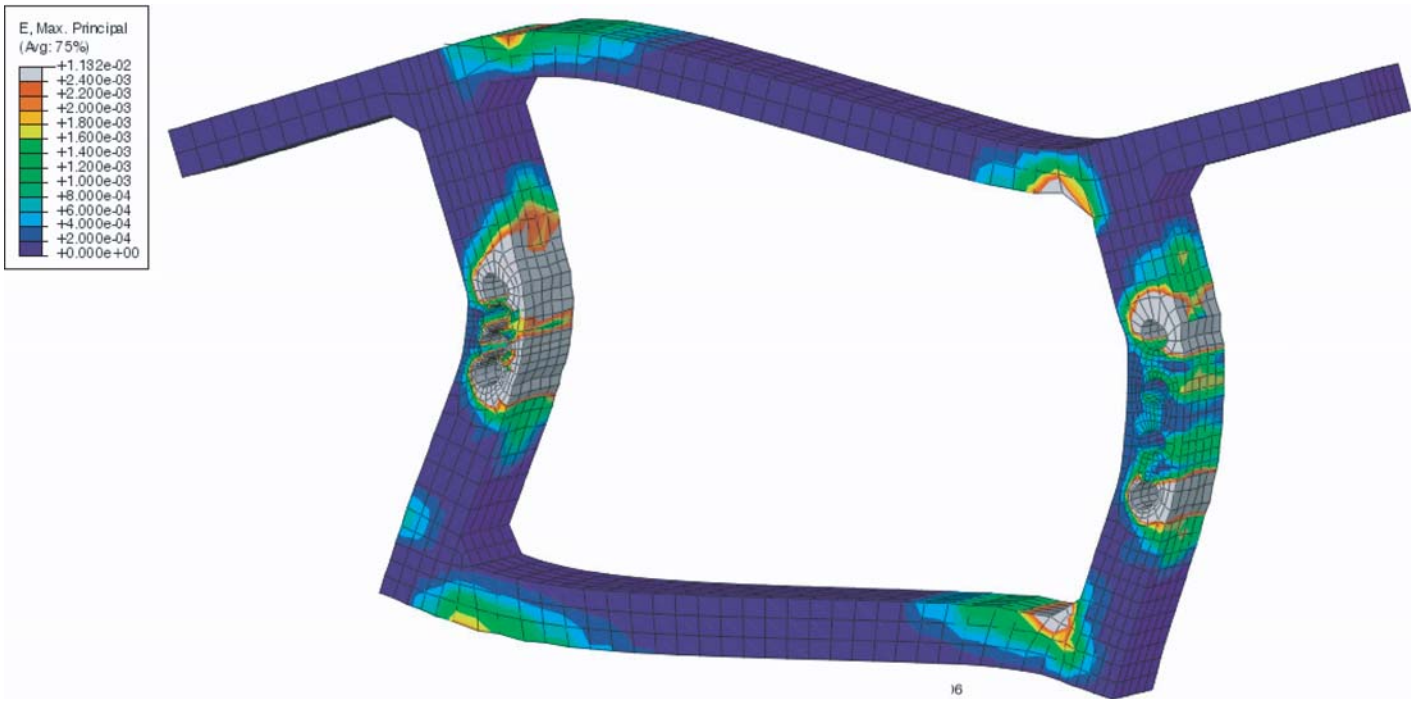

Figure 5-11. Contours of max principle strains at 1.0DC deflections of 0.07 inches.

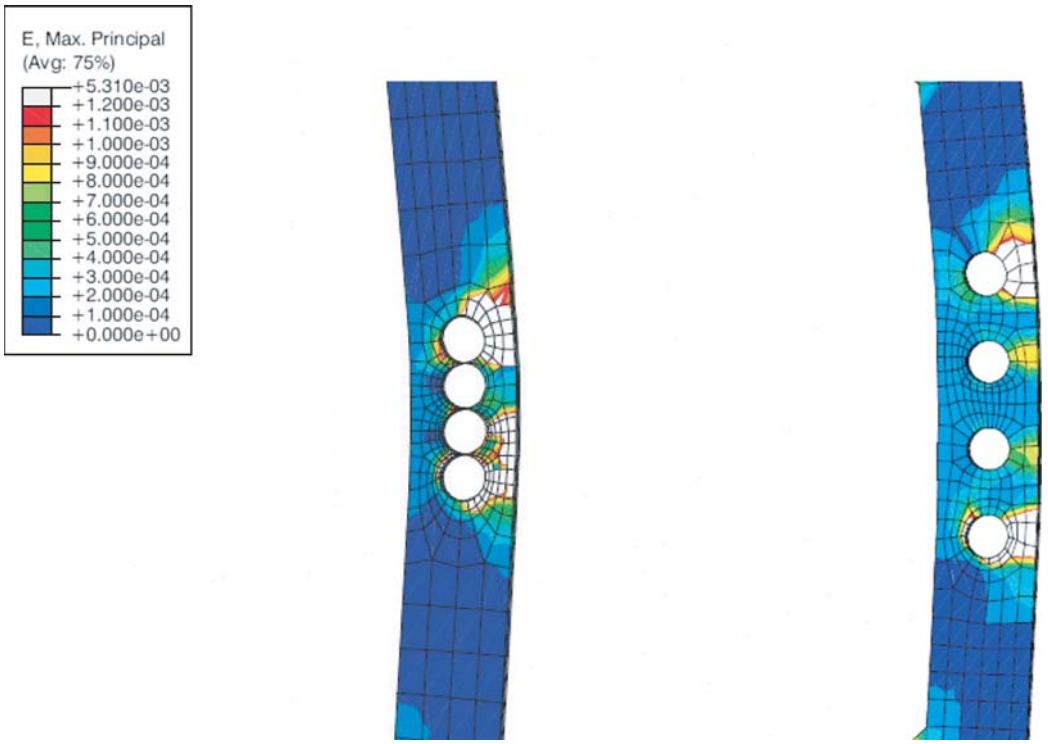

Figure 5-12. Contours for max principle strains at BC deflection of 0.03 inches (displ × 25).

the regional moment calculation in the sloping exterior webs. Though not studied in depth, there was no apparent effect on the behavior of vertical webs caused by super-elevation so it was not included in the single cell section that was studied.

The variables that may significantly influence local behavior are as follows:

- Web depth,
- Web thickness,
- Web slope,
- Cover thickness,
- Number and configuration of tendon ducts,
- Number and configuration of duct ties,
- Stirrups, and
- Concrete material properties, especially assumed tensile strength.

A last variable, P_t/R, is evaluated by the analyses producing Pt/R versus deformation curves. So each analysis includes the full range of P_t/R up to failure. The analysis matrix to study the parameters for the multi-cell series is shown in Table 5-1.

Model Prototype: Three-Cell Cast-In-Place Box Girder

A multi-cell, cast-in-place box configuration was used as shown in Figure 5-15. The basic model (shown in Figure 5-16) uses 3-D elements and a slice, with out-of-page thickness equal to one stirrup spacing. The stirrups (and other rebar) are modeled explicitly (unlike in two dimensions, where the stirrup is smeared). This allows introduction of the out-of-page compression due to prestress. Using this model framework, geometry variabilities were introduced directly into the models—e.g., one web can have one thickness, and another have a different thickness. Also, by using this model prototype, the effects of web slope are included and can be compared. Webs A and D have different slopes and can be compared with B and C, which are vertical. Webs A and D demonstrate the differences related to web sloping away from the radius of curvature versus sloping toward the radius of curvature. (Two additional cases were later added with vertical-web exterior webs to provide additional comparisons.)

The tendon duct arrangements and local reinforcements are shown in Figure 5-17. In configuration Type 4, analyses were run with (4b) and without the center web ties (4a). This refers to the two rebar ties in the middle of the group of ducts. In configuration Type 3, separation of the ducts by 1½ inches was found to provide increased resistance to lateral tendon breakout. Further separation may provide even higher resistance, but it was the opinion of the project team that enforcing even larger separations between the ducts begins to pose a very significant limitation on the effectiveness of the prestressing. Designers need to be allowed some flexibility in duct placement in order to achieve a range of vertical positions of prestressing within the webs, for typical designs.

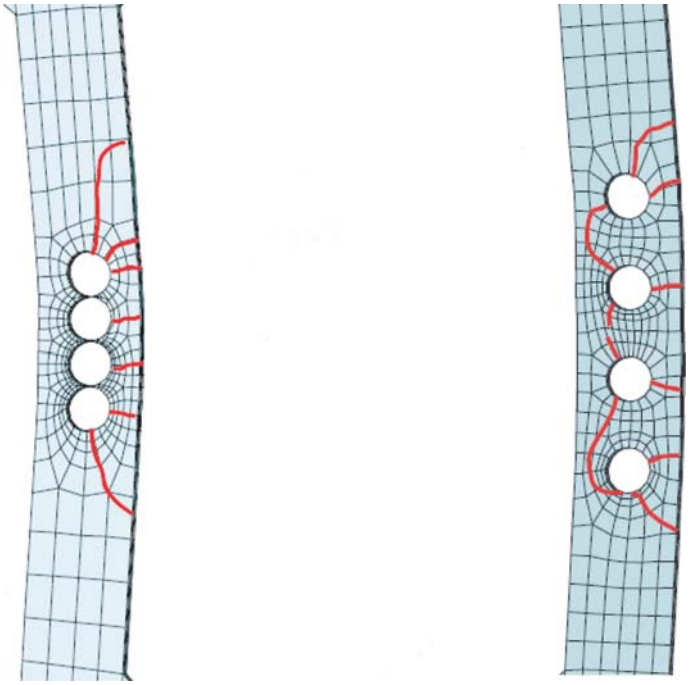

Figure 5-13. Estimated cracking in the webs based on strains (displ. × 25).

The boundary conditions for the models were the same as for the UT Test simulation, which produced reasonable correlation between analysis and test. The model is a sector slice taken from a curve. The dimension longitudinally varies between inside and outside edge, but on average is equal to 1.5 ft. This is also the stirrup spacing for the baseline model. This bridge example is assumed to be on an 800-foot curve radius, so the sector width varies slightly from the inside of the curve (Web D) to the outside (Web A).

The concrete properties were $f_c' = 5{,}000$ psi, and Young's Modulus = 4,030.5 ksi. The rebar was Grade 60. Plots of material stress-strain curves for the concrete and steel are shown in Figure 5-18. Tensile strengths (f_t) for concrete when tested in direct uniaxial tension can show large variations, but most results fall within the range $4\sqrt{f_c'}$ to $6\sqrt{f_c'}$; $5\sqrt{f_c'}$ is considered a reasonable average.

Multicell Models—Analysis Results

The 16 different multicell girder local models were developed, and analyses were completed. The results are shown in this chapter through the following plots and tables. These allow for qualitative and quantitative assessment and comparison of the cases analyzed.

- Lateral Force vs. Deflection of Web Midheight
- Lateral Force vs. Deflection of Web Quarter-height
- Maximum Principal Strain Contours in Concrete at 75%, 100%, 125%, 150% P_c
- Strains in stirrup rebar at 3 locations along duct bank at 75%, 100%, 125%, 150% P_c
- Distortions (change in web width) at three locations along duct bank at 75%, 100%, 125%, 150% P_c

P_c refers to a lateral force applied to the web that will cause theoretical web failure calculated using conventional means and removing various safety factors. This creates a framework for comparing the results of the detailed FE analysis to a baseline capacity. The displacements were measured at the "outside curve" edge of the webs.

Although the four individual webs in each multi-cell model tended to act independently, the local analyses required a decision as to loading of the individual webs. In planning this loading it was found that the interaction of the webs with their end conditions (i.e., the stiffness characteristics of the top and bottom slabs) was important to how the webs behaved. An initial study using the baseline geometry (Model 1M) and all-elastic material properties showed that web mid-height deflections varied as shown when equal loads (1,000 lbs per web) were applied to the webs as indicated in Figures 5-19 and 5-20.

These figures show how the exterior web ends are freer to rotate than the interior webs. For the two extremes of fixed-fixed versus pinned-pinned, the ratios of mid-height moment to applied tendon force (P) would be h/8 versus h/4 or a ratio of one-half. But the web end conditions are neither fixed-fixed nor pinned-pinned. One way to quantify these differences associated with end effects was to apply the tendon forces to a beam model, as shown in the deformed shape plot of Figure 5-21.

This exercise produced the following ratios of web mid-height moments to applied force:

Web

A	B	C	D
0.186h	0.145h	0.147h	0.171h

h = 92.75 in. (7.73 ft.)

Normalizing to the pinned-pinned condition (M = P × h/4) gives ratios of:

0.744 0.580 0.588 0.684

Considered as coefficients, these can be compared with the Caltrans Memo-to-Designers Formula:

$M_u = 0.8(¼)(P_j/R)h_c$

Where P_j is the tendon force (j is for "jacking force")

Thus, for this case, Caltrans uses a continuity factor of 0.8 for design. Based on the work performed for this project, factors of 0.6 for interior webs and 0.7 for exterior webs are proposed.

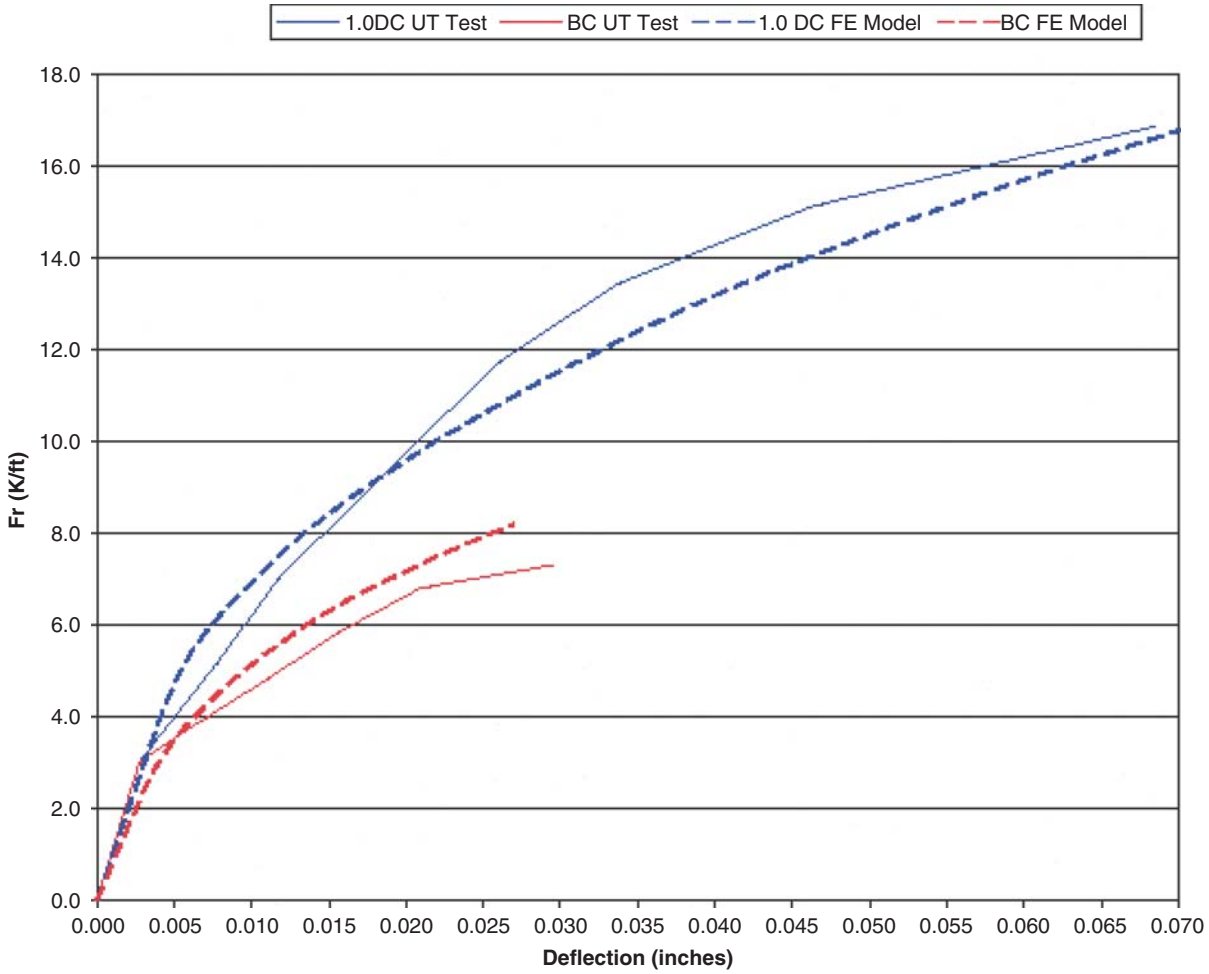

Figure 5-14. Force vs. deflection (FE model compared with U.T. Test).

The overall distribution of these moments to webs agrees well with damage trends observed in the FE analysis, so one finding from the Local Analysis study may be that designers should account for this effect in more detail than to just apply a single formula to calculate mid-height moment demand.

Further study of this using fully nonlinear properties showed that once concrete cracking begins to occur, the differences between webs become even larger. So it was eventually decided to choose a baseline prestress force divided by the four webs, then increase this force for the interior webs, and reduce this force for the exterior webs. Using this as a basis and choosing a prestress force large enough to cause significant damage in all of the parametric models led to the following total applied forces in kips/ft. This is analogous to P_j/R. Of course in some cases, the webs failed prior to reaching this total load.

Web			
A	B	C	D
13 k/ft	17 k/ft	17 k/ft	15 k/ft

In order to establish a baseline for comparison with design calculations, as previously mentioned, P_c is defined as a "Capacity" calculated using conventional means, but removing safety factors, so as to make direct comparison to finite element analyses. For the interior (B or C webs) of the multicell geometry prototype, P_c was calculated as follows.

$\phi M_n = 8.7$ k-ft/ft

Removing the resistance factor $\phi = 0.9$,

$M_n = 9.7$ k-ft/ft

Applying an over-strength factor for rebar strain hardening (which is included in the FE analysis),

$M_o = M_n \times 1.125 = 10.9$ k-ft/ft

The moment-fixity effect is rounded off at 0.6. It is also recognized that the duct forces are not applied at one point in midheight, but are instead, applied at five points distributed along 18 inches of the height. This decreases the moment to

Table 5-1. Parameters for multi-cell girder local response analysis.

Analysis #	Model Type	Web #	Web Thickness	Duct/Tie Config.	Bundle Vert. Pos.	Stirrup Spacing (in.)	Cover Thickness	Concr. Tens. Str. (x√fc`)
1M	Multi-cell	A, D	12	1	midheight	18	3	4
"baseline"		B	12	1	midheight	18	3	4
		C	12	1	midheight	18	3	4
2M	Multi-cell	A, D	12	2a	midheight	18	3	4
		B	12	2a	midheight	18	3	4
		C	12	2a	midheight	18	3	4
3M	Multi-cell	A, D	A-10, D-12	2b	midheight	18	3	4
		B	10	2a	midheight	18	3	4
		C	14	2a	midheight	18	3	4
4M	Multi-cell	A, D	12	2a	1/4 height	18	3	4
		B	12	2a	1/4 height	18	3	4
		C	12	2a	bottom	18	3	4
5M	Multi-cell	A, D	12	2b	midheight	18	3	4
		B	12	2b	midheight	18	3	4
		C	12	2a	midheight	18	3	6
6M	Multi-cell	A, D	12	2a	midheight	12	3	4
		B	12	2a	midheight	12	3	4
		C	12	2a	midheight	18	3	2
7M	Multi-cell	A, D	12	2a	midheight	27	3	4
		B	12	2a	midheight	27	3	4
		C	12	2a	midheight	18	2	4
8M	Multi-cell	A, D	12	2a	midheight	18	2	4
		B	12	2b	midheight	18	2	4
		C	12	2a	midheight	18	4	4
9M	Multi-cell	A, D	12	3a	1/4 height	18	2	4
		B	12	2a	1/4 height	18	2	4
		C	12	2a	bottom	18	2	4
10M	Multi-cell	A, D	12	3a	midheight	27	3	4
		B	12	3a	midheight	27	3	4
		C	12	3a	midheight	18	2	4
11M	Multi-cell	A, D	A-10, D-12	4a	midheight	18	3	4
		B	10	4a	midheight	18	3	4
		C	14	4b	midheight	18	3	4
12M	Multi-cell	A, D	12	4a	Midheight	18	3	2
		B	12	4a	midheight	18	3	4
		C	12	4b	midheight	18	3	6
13M	Multi-cell	A, D	12	4a	midheight	27	3	4
		B	12	4a	midheight	27	3	4
		C	12	4a	midheight	18	2	4
14M	Multi-cell	A, D	12	4b	1/4 height	18	3	4
		B	12	4b	1/4 height	18	3	4
		C	12	4b	bottom	18	3	4
2m-Vert	Multi-cell	A, D	12	2a	midheight	18	3	4
		B	12	2a	midheight	18	3	4
		C	12	2a	midheight	18	3	4
11M-Vert	Multi-cell	A, D	A-10, D-12	4a	midheight	18	3	4
		B	10	4a	midheight	18	3	4
		C	14	4b	midheight	18	3	4

88.4% of that caused by a single point load at midheight. So the baseline P_c becomes

$P_c = [10.9/(h/4)]/0.6/0.884 = 10.6$ k/ft

This is used as "100%" in the results tables and plots. But for the exterior webs, the "100%" force is less, because the load is applied in the proportions previously listed. The result of all this is to proportion loads so that webs will be "failing" more-or-less simultaneously, therefore maintaining proper flexural stiffnesses in webs and flanges at all loading stages.

The results of all the multi-cell analyses are shown in Tables 5-1, 5-2, 5-3, and 5-4 and figures. The figures are shown in Appendix E-b and are numbered as Figures E-b-1, E-b-2, etc.

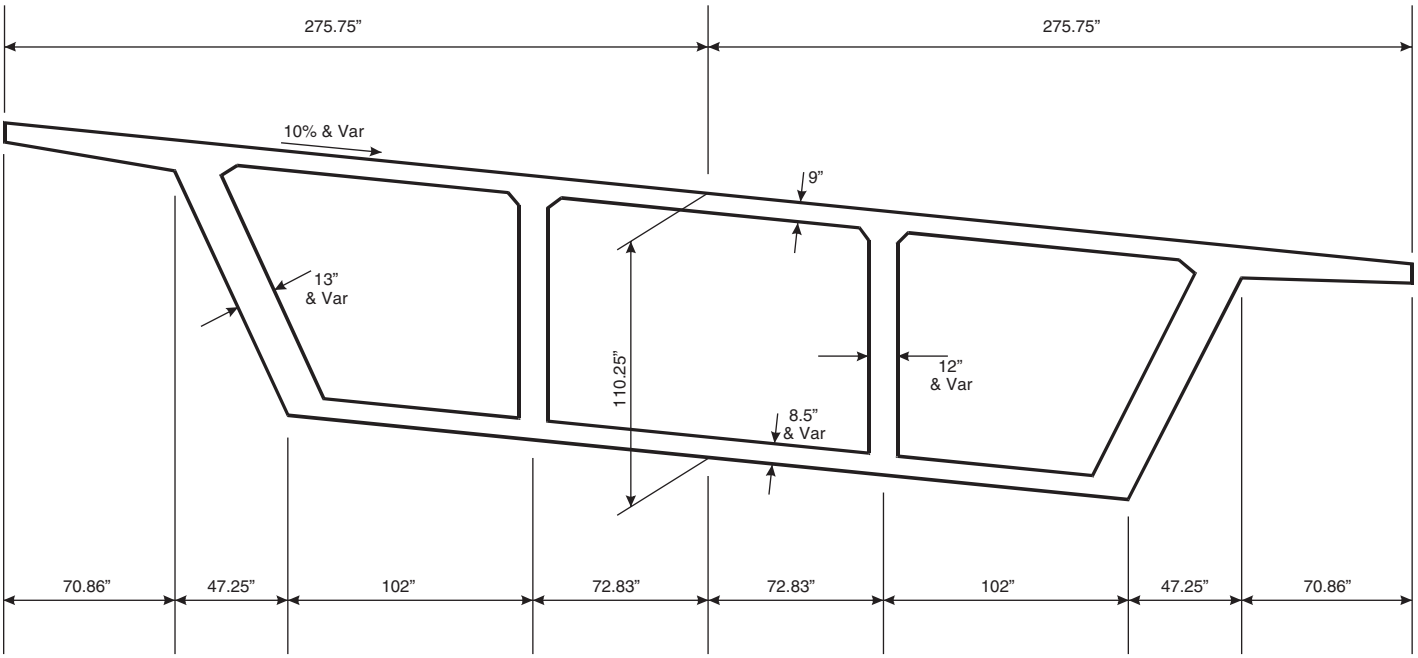

I-405 - 55 HOV Connector O/C
General Cross-Section (inches)

Figure 5-15. Multicell girder cross-section geometry.

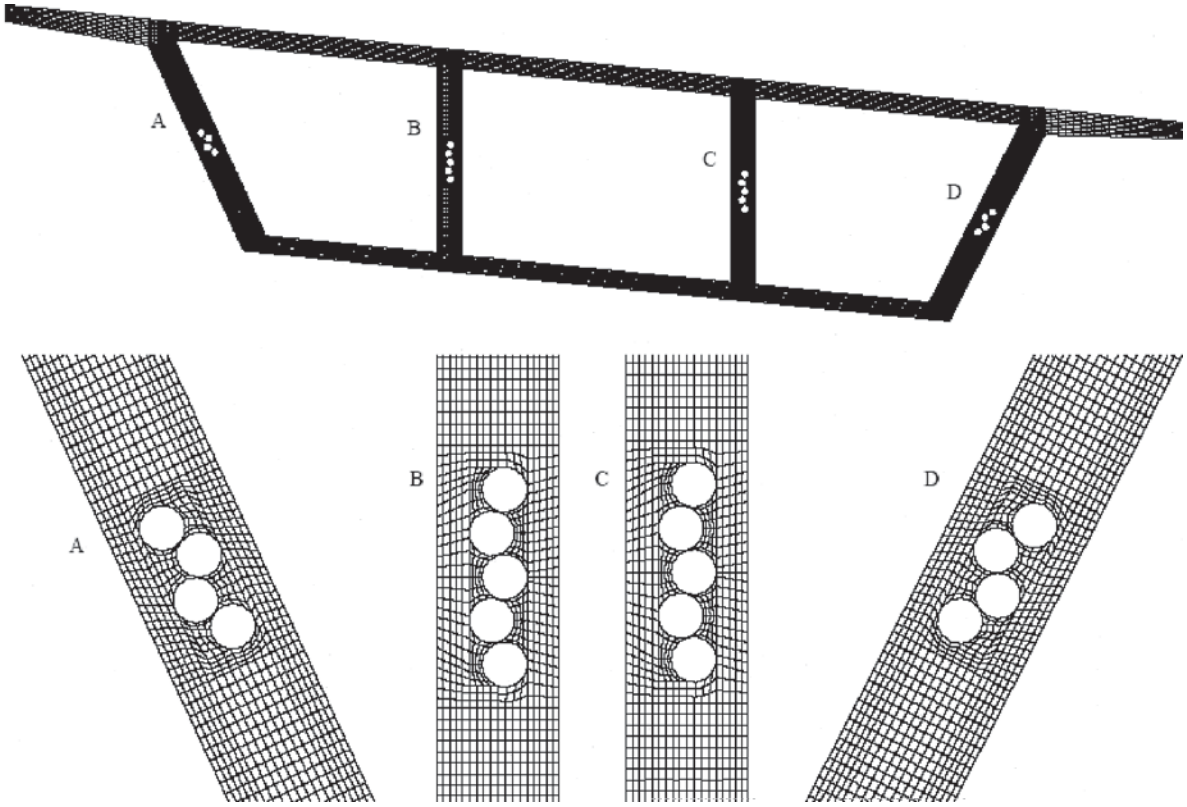

Figure 5-16. Example finite element mesh for multicell local analysis prototype. All duct diameters are 4½”.

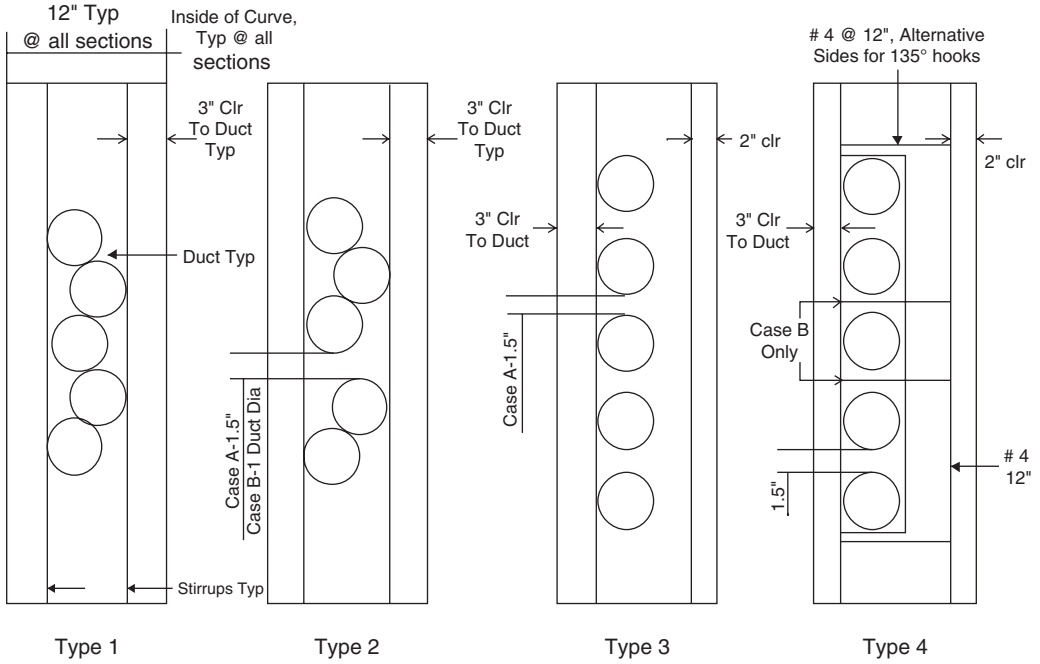

Figure 5-17. Tendon duct and local reinforcement for multicell box local analysis prototypes (note that this figure is an idealization of bar placements that are implemented in the FE analysis).

The maximum principal strain contours illustrate the general level of damage to the concrete surrounding the tendon ducts (maximum tensile strain regardless of orientation).

The following strain thresholds are important quantities to compare to when viewing these results.

$\varepsilon_{11} = 1.6 \times 10^{-4}$ first visible cracking (micro-cracking occurs at about half of this strain)
2.0×10^{-3} first rebar yield
1.0×10^{-2} 1% strain in rebar; typically wide open cracks/sometimes spalling concrete

In Table 5-4, delaminations ("distortion") information is provided at "Duct 1," "Duct 3," and "Duct 5." This refers to a measure across the bottom edge, top edge, and centerline of the duct assembly.

Discussion of Results

The analysis results have been used to compare the web design parameters. The first general observation is the comparison of the midheight cases with the "¼ height" and "bottom" cases. It was generally observed that when the ducts occur near the bottom of the web (either "quarter-height" or "bottom" as was tested in Configurations 4M and 14M) the force at "failure" is substantially lower than when the ducts are placed at the midheight, i.e., on average as much as 25% to 40% lower when comparing these cases with similar cases. The reason for this is a tendency toward lateral shear failure of the overall web. When the ducts are located at the midheight, the lateral shear is divided equally between the top and bottom of the web. But when the ducts move down, the bottom of the web carries most of the lateral shear, and this is a different mechanism than the failure modes observed for tendon ducts at mid-height. So the "quarter-height" cases can be compared to each other (and the "bottom" cases), but should not be compared directly with the "midheight" cases. "P_c" only applies to the "midheight" cases.

For purposes of interpreting and comparing the results, the following damage criteria should be considered:

- Stirrup rebar strain exceeding yield (i.e., 0.2% strain for Grade 60 steel); note that for Load Factor Design, concrete reinforcement is designed to yield at the ultimate member forces.
- Visible concrete cracking occurs at strains of approximately 0.016%, but this is not necessarily web failure; concrete with maximum principal strains of 0.3% can be considered to be heavily cracked. Concrete with strains in excess of 1.0% will generally show wide-open cracks and potential spalling from the section.
- Significant distortion or delamination (change of width of the webs) would also represent an upper bound on serviceable capacity for webs; the delamination is evidence of a local splitting or lateral shear failure within the web. It was arbitrarily assumed that a crack width of ⅛" is an

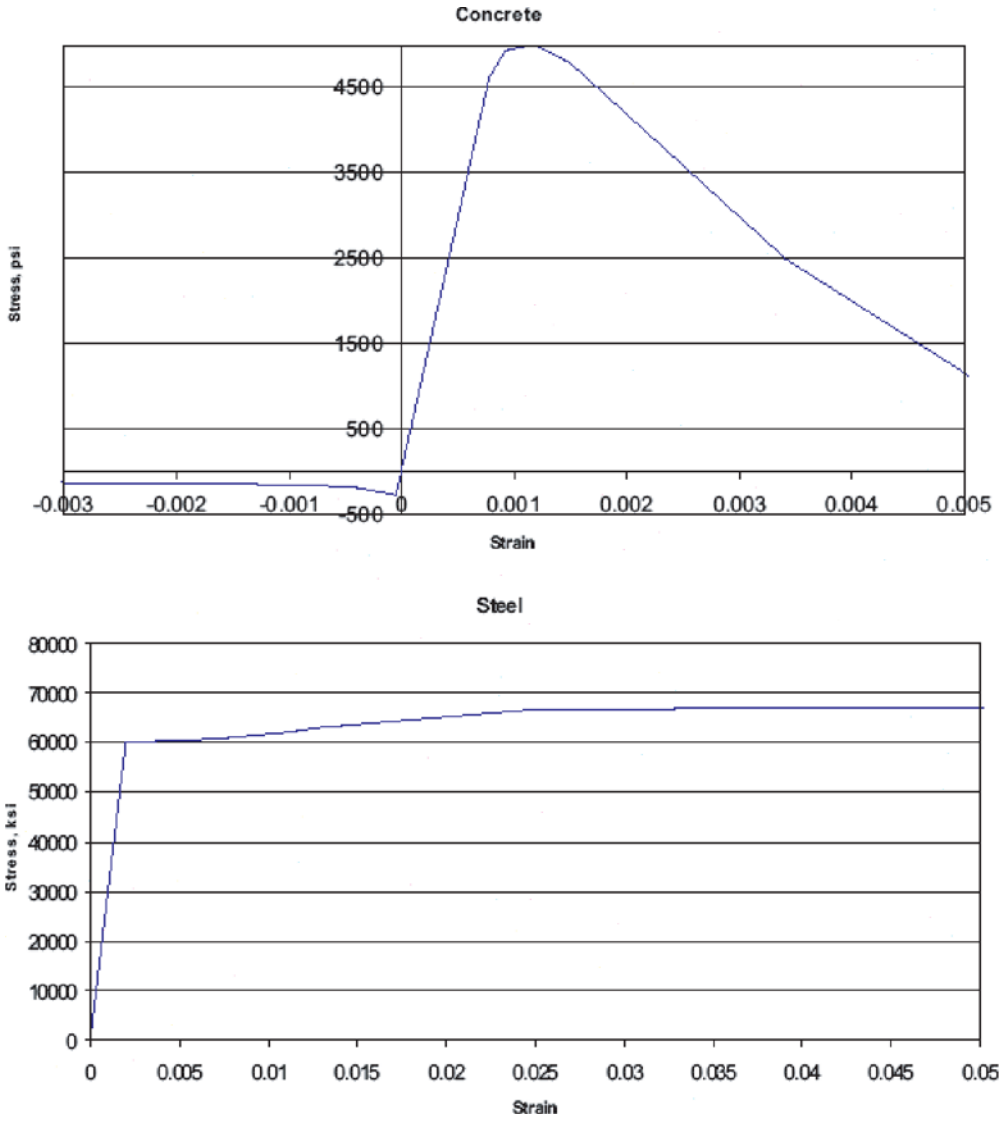

Figure 5-18. Stress vs. strain curves concrete and steel in local FE analysis.

indicator of such a failure. For 12" webs, this represents a distortion of 0.06 inches, and a distortion ratio (average strain through the section) of 0.5%. For sections with web ties, this means the web ties have yielded; for sections without web ties, the section is at a web splitting or a web lateral shear failure condition.

Two of the criteria, Stirrup Yield and Web Delamination, have been summarized in Tables 5-5 and 5-6. These are the total forces (sum of all tendon ducts in the web) applied when any part of the stirrup reaches yield, and when the web distortion reaches 0.06 inch.

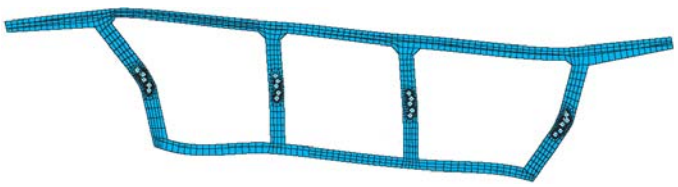

Figure 5-19. Deformed shape of typical cross-section with the same force applied to each web.

Using these criteria and the results tables and plots has resulted in the following observations.

Web Depth

This parameter was varied indirectly by subjecting the webs to wide ranges of moments and horizontal shears. Based on observations of the analysis results, web depth can be adequately accounted for by considering and designing for web moments.

Web Thickness

Web thickness was varied in Model 3M (A – 10 inches, B – 10 inches, C – 14 inches), and similarly in Model 11M.

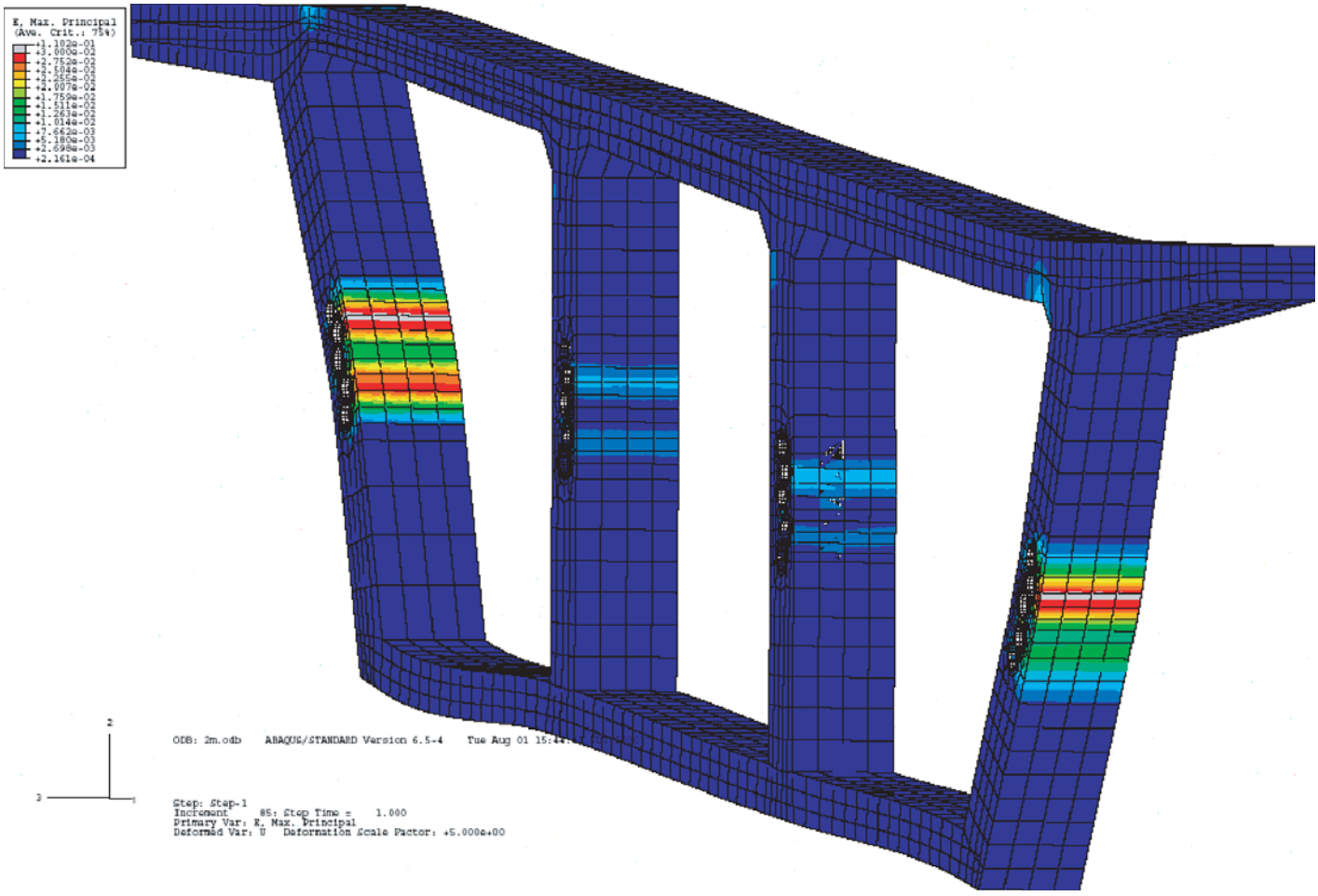

Figure 5-20. Deformed shape/strain contour when the same force is applied to each web.

Model 11M included web ties. The results compared with their respective baselines are shown in Table 5-7.

These results demonstrate significant influence on resistance to lateral bending and tendon pullout caused by web thickness. Stirrups yielded sooner, and concrete damage and web delamination was more extensive with the thinner webs.

For stirrup yield, capacity formulae based on regional flexure considerations appear to be appropriate for design. Differences in stirrup yield and especially web delamination were also significantly influenced when the web ties were added because the web ties tended to eliminate the web delamination failure mode. Moving the ducts toward the curve outside face within the webs also contributed to resistance against delamination and local lateral shear damage.

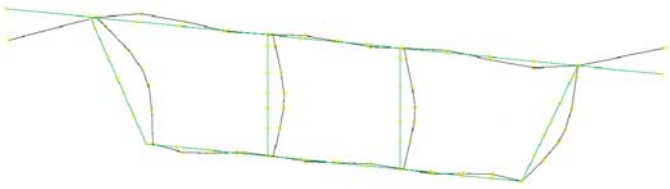

Figure 5-21. Tendon forces applied to a beam model of typical cross-section.

Web Slope

As described earlier, the sloped webs in this analysis series were found to be significantly weaker (30–40%) than the vertical webs, but part of this difference was caused by being exterior webs rather than interior. Exterior webs have more flexible end conditions at their connection with the top and bottom slab, and this produces larger mid-height moments.

Comparison of Webs A to D for the inclined webs show that Web A is generally weaker than D by about 10%, due to orientation of slope relative to the direction of the tendon force.

In order to examine the differences between sloped webs and vertical webs more directly, two additional analyses were performed with exterior webs converted to vertical webs. The strain contour and Force versus Deflection plots are included in Appendix F. Models 2M and 11M were chosen for these comparisons because these have the baseline values for all properties, but they investigate duct-tie configurations 2a and

Table 5-2. Deflections.

Model #	Percent Capacity	Web A Mid	Web A Quarter	Web B Mid	Web B Quarter	Web C Mid	Web C Quarter	Web D Mid	Web D Quarter
1m	75%	0.0290	0.0287	0.0360	0.0262	0.0271	0.0210	0.0199	0.0139
	100%	0.0830	0.0686	0.0962	0.0555	0.0797	0.0420	0.0554	0.0225
	125%	0.1851	0.1553	0.2249	0.1371	0.1981	0.1115	0.1390	0.0625
	150%	0.4067	0.3567	0.5017	0.3382	0.4859	0.3083	0.3379	0.1867
2m	75%	0.0309	0.0340	0.0242	0.0262	0.0237	0.0259	0.0254	0.0216
	100%	0.0872	0.0891	0.0702	0.0690	0.0673	0.0672	0.0673	0.0573
	125%	0.1966	0.2026	0.1702	0.1629	0.1676	0.1623	0.1566	0.1366
	150%	0.4455	0.4509	0.3821	0.3756	0.4080	0.3897	0.3477	0.3067
3m	75%	0.0554	0.0520	0.0411	0.0403	0.0225	0.0293	0.0309	0.0266
	100%	0.1524	0.1395	0.1323	0.1191	0.0615	0.0792	0.0863	0.0751
	125%	0.3711	0.3367	0.3314	0.2972	0.1571	0.1974	0.2103	0.1841
	150%	2.2610	2.2670	1.6490	1.5490	0.9640	1.2280	0.9860	0.6550
4m	75%	0.2148	0.3214	0.2289	0.3171	0.1890	0.2885	0.2141	0.2803
	100%	0.8136	1.2218	0.9112	1.2538	0.7589	1.1392	0.8323	1.0922
	125%	2.3248	3.5099	2.7380	3.7348	2.2520	3.3725	2.4692	3.2460
	150%	11.1900	16.3600	11.3300	15.5600	9.9500	15.1500	12.4100	14.2900
5m	75%	0.0251	0.0269	0.0190	0.0202	0.0172	0.0195	0.0179	0.0142
	100%	0.0665	0.0687	0.0518	0.0539	0.0409	0.0481	0.0511	0.0415
	125%	0.1385	0.1408	0.1103	0.1114	0.0938	0.0986	0.1082	0.0870
	150%	0.2707	0.2731	0.2248	0.2240	0.1954	0.1983	0.2109	0.1726
6m	75%	0.0352	0.0386	0.0278	0.0304	0.0506	0.0385	0.0257	0.0231
	100%	0.1240	0.1290	0.1051	0.1048	0.1610	0.1313	0.0887	0.0840
	125%	0.3047	0.3182	0.2684	0.2603	0.3685	0.3123	0.2182	0.2071
	150%	0.7176	0.7433	0.6550	0.6354	0.8475	0.7286	0.5231	0.4981
7m	75%	0.0279	0.0298	0.0220	0.0230	0.0207	0.0225	0.0206	0.0170
	100%	0.0789	0.0799	0.0583	0.0606	0.0548	0.0587	0.0596	0.0486
	125%	0.1674	0.1702	0.1295	0.1325	0.1283	0.1305	0.1332	0.1074
	150%	0.2980	0.3033	0.2425	0.2393	0.2493	0.2427	0.2385	0.1935
8m	75%	0.0313	0.0337	0.0217	0.0253	0.0214	0.0253	0.0235	0.0202
	100%	0.0922	0.0916	0.0545	0.0660	0.0621	0.0680	0.0671	0.0558
	125%	0.2020	0.2030	0.1338	0.1560	0.1639	0.1630	0.1563	0.1285
	150%	0.4180	0.4180	0.2815	0.3252	0.3478	0.3461	0.3340	0.2714
9m	75%	0.1442	0.1983	0.1270	0.1825	0.1067	0.1682	0.1481	0.1654
	100%	0.5575	0.7819	0.5310	0.7502	0.4394	0.6840	0.5756	0.6430
	125%	1.6680	2.3691	1.6878	2.3781	1.3931	2.1697	1.7823	1.9963
	150%	9.7190	13.7340	8.8200	12.3520	7.6240	11.8020	11.0610	11.3050
10m	75%	0.0230	0.0254	0.0178	0.0197	0.0178	0.0195	0.0156	0.0122
	100%	0.0591	0.0627	0.0397	0.0480	0.0390	0.0463	0.0427	0.0363
	125%	0.1350	0.1428	0.0892	0.1096	0.0924	0.1098	0.0990	0.0847
	150%	0.2458	0.2636	0.1778	0.2091	0.1755	0.2090	0.1939	0.1626
11m	75%	0.0388	0.0390	0.0253	0.0273	0.0183	0.0213	0.0195	0.0154
	100%	0.1024	0.1019	0.0683	0.0765	0.0453	0.0566	0.0575	0.0491
	125%	0.2601	0.2544	0.1764	0.1961	0.1160	0.1450	0.1534	0.1270
	150%	1.1300	1.2390	0.7370	0.7760	0.6300	0.6890	0.5420	0.3130
12m	75%	0.0212	0.0236	0.0168	0.0181	0.0161	0.0180	0.0153	0.0113
	100%	0.0493	0.0537	0.0355	0.0414	0.0343	0.0412	0.0407	0.0328
	125%	0.1051	0.1118	0.0761	0.0864	0.0705	0.0860	0.0991	0.0748
	150%	0.1949	0.2089	0.1515	0.1688	0.1332	0.1642	0.1939	0.1454
13m	75%	0.0190	0.0202	0.0161	0.0169	0.0162	0.0175	0.0154	0.0117
	100%	0.0372	0.0392	0.0285	0.0319	0.0288	0.0327	0.0324	0.0256
	125%	0.0750	0.0780	0.0533	0.0610	0.0541	0.0627	0.0630	0.0516
	150%	0.1201	0.1258	0.0986	0.1089	0.1059	0.1164	0.1122	0.0903

Table 5-2. (Continued).

Model #	Percent Capacity	Web A Mid	Web A Quarter	Web B Mid	Web B Quarter	Web C Mid	Web C Quarter	Web D Mid	Web D Quarter
14m	75%	0.1016	0.1346	0.0841	0.1233	0.0842	0.1228	0.1207	0.1239
	100%	0.3100	0.4193	0.2772	0.4126	0.2657	0.3889	0.3656	0.3779
	125%	0.8000	1.0955	0.7350	1.0775	0.7158	1.0229	0.9539	0.9897
	150%	2.1159	2.8840	1.8586	2.7535	1.9289	2.7251	2.5100	2.6583
2MVert	75%	0.0153	0.0160	0.0170	0.0172	0.0162	0.0171	0.0154	0.0162
	100%	0.0338	0.0318	0.0400	0.0343	0.0398	0.0348	0.0319	0.0302
	125%	0.0913	0.0748	0.0896	0.0731	0.1033	0.0796	0.0806	0.0665
	150%	0.1824	0.1475	0.1917	0.1481	0.2198	0.1664	0.1831	0.1401
11MVert	75%	0.0314	0.0295	0.0245	0.0254	0.0146	0.0182	0.0191	0.0206
	100%	0.0686	0.0594	0.0474	0.0479	0.0255	0.0320	0.0325	0.0355
	125%	0.1449	0.1190	0.1026	0.0977	0.0489	0.0614	0.0677	0.0697
	150%	0.2706	0.2221	0.2076	0.1937	0.0935	0.1189	0.1365	0.1337

4a/b. Direct comparisons of Force versus Deflection are shown in Figures 5-22a and 5-22b below.

These figures show the vertical webs to be stiffer and stronger than the sloping webs, but show that the differences in force capacity (strength) are negligibly small. A comparison of the occurrence of rebar yield and web delamination is shown in Table 5-8.

Cover Thickness

Cover thickness was varied in Models 7M, 8M, and 13M. Table 5-9 summarizes sample strength comparisons.

The conclusion reached is that cover thickness influences lateral pullout resistance, but is not the only driver of pullout resistance. The results of the parameter study were influenced by the fact that when the cover is reduced, for the same overall web thickness, the moment arm for the stirrups is increased, and this is an off-setting influence on pullout resistance. As will be discussed further in the conclusions, it appears appropriate to check cover concrete thickness for resistance to initial cracking, but not to include cover concrete tensile strength in the calculation of regional transverse bending strength.

Number and Configuration of Tendon Ducts

This was evaluated by comparing Configurations 1, 2, and 3 (from Figure 5-17), which involve comparing Models 1M vs. 2M, 3M-D vs. 2M-D, 5M vs. 2M, and 10M-C vs. 7M-C. Results are shown in Table 5-10.

Clearly, when the ducts are spread apart, the performance significantly improves. Roughly 20% resistance force improvement was demonstrated by separating the 5-duct bundle into two bundles (Config. 2A versus Config. 1), and an additional 4% improvement was demonstrated by spreading the bundles farther apart (4.5" versus 1.5" separation). So in general, a prudent recommendation is to require a maximum of 3 ducts per bundle. When the individual ducts were separated (i.e., Config. 3A) and moved toward the curve's outside edge of the web, performance further improved. In fact, as measured by the delamination criteria, Configuration 3A exceeded 200% P_c, so the improvement in delamination performance was very large. The influence on stirrup yield performance by spreading individual ducts apart was only 5%, and it is often impractical for designers to spread individual ducts apart due to lack of space in the web and due to requirements on location of C.G. of the tendon group.

Number and Configuration of Duct Ties

This was evaluated by comparing Configurations 4A and 4B, to Configurations 1, 2, and 3. This is covered by comparing Model/Webs 11M-D to 10M-D, 12M-B to 10M-B, 13M-A-D to 10M-A-D, 12M-C to 12M-B, and 14M-B, D to 9M-B. This comparison is shown in Table 5-11.

The conclusions from these comparisons are that web/duct ties make a significant contribution to the resistance to lateral tendon breakout.

Stirrups

Stirrup spacing was evaluated by comparing Model-Webs 6M-A, B, and D to 2M-A, B, and D, comparing 7M-A, B, D to 2M-A, B, D, and comparing 13M-A, B, D to 12M-A, B, D. These comparisons are shown in Table 5-12.

This indicates that web section strength is significantly influenced by the stirrup spacing only when web/duct tie reinforcement is NOT used or when the web-splitting/lateral shear-failure does not occur. In other words, if the failure

Table 5-3. Stirrup strain (%) adjacent to mid-height of ducts (Duct 1 – bottom, Duct 3 – middle, Duct 5 – top).

		Web A			Web B			Web C			Web D		
	Percent	Duct 1	Duct 3	Duct 5	Duct 1	Duct 3	Duct 5	Duct 1	Duct 3	Duct 5	Duct 1	Duct 3	Duct 5
Model #	Capacity												
1m	75%	0.0002	0.0003	0.0002	0.0002	0.0005	0.0004	0.0002	0.0004	0.0002	0.0002	0.0003	0.0002
	100%	0.0007	0.0011	0.0005	0.0006	0.0017	0.0010	0.0005	0.0015	0.0006	0.0006	0.0011	0.0005
	125%	0.0015	0.0023	0.0013	0.0012	0.0045	0.0016	0.0012	0.0033	0.0013	0.0013	0.0026	0.0013
	150%	0.0026	0.0057	0.0018	0.0017	0.0104	0.0026	0.0020	0.0085	0.0026	0.0024	0.0071	0.0019
2m	75%	0.0002	0.0002	0.0002	0.0002	0.0002	0.0002	0.0002	0.0002	0.0002	0.0002	0.0002	0.0001
	100%	0.0007	0.0003	0.0003	0.0003	0.0005	0.0008	0.0003	0.0012	0.0003	0.0006	0.0004	0.0003
	125%	0.0013	0.0008	0.0006	0.0007	0.0013	0.0018	0.0008	0.0018	0.0008	0.0013	0.0019	0.0007
	150%	0.0026	0.0015	0.0012	0.0018	0.0021	0.0039	0.0019	0.0083	0.0014	0.0024	0.0019	0.0012
3m	75%	0.0003	0.0003	0.0002	0.0003	0.0002	0.0003	0.0002	0.0001	0.0001	0.0003	0.0005	0.0001
	100%	0.0009	0.0008	0.0005	0.0012	0.0008	0.0008	0.0004	0.0004	0.0003	0.0010	0.0012	0.0003
	125%	0.0023	0.0019	0.0013	0.0027	0.0019	0.0018	0.0010	0.0009	0.0006	0.0018	0.0032	0.0009
	150%	0.0209	0.0186	0.0207	0.0225	0.0153	0.0218	0.0178	0.0170	0.0172	0.0242	0.0244	0.0164
4m	75%	0.0011	0.0019	0.0007	0.0008	0.0013	0.0014	0.0009	0.0015	0.0010	0.0016	0.0013	0.0003
	100%	0.0025	0.0029	0.0025	0.0019	0.0045	0.0080	0.0027	0.0068	0.0046	0.0056	0.0021	0.0011
	125%	0.0093	0.0235	0.0090	0.0065	0.0153	0.0246	0.0107	0.0171	0.0158	0.0197	0.0048	0.0021
	150%	0.0789	0.0978	0.0787	0.0793	0.0756	0.0994	0.0870	0.0796	0.0876	0.1241	0.0923	0.0653
5m	75%	0.0002	0.0002	0.0001	0.0002	0.0001	0.0002	0.0001	0.0001	0.0001	0.0003	0.0003	0.0001
	100%	0.0007	0.0003	0.0003	0.0007	0.0004	0.0003	0.0003	0.0003	0.0002	0.0007	0.0012	0.0002
	125%	0.0015	0.0009	0.0006	0.0016	0.0009	0.0006	0.0009	0.0008	0.0003	0.0014	0.0020	0.0005
	150%	0.0029	0.0015	0.0012	0.0033	0.0015	0.0012	0.0019	0.0017	0.0007	0.0025	0.0040	0.0010
6m	75%	0.0003	0.0002	0.0002	0.0002	0.0002	0.0002	0.0007	0.0006	0.0004	0.0004	0.0004	0.0001
	100%	0.0016	0.0009	0.0004	0.0007	0.0010	0.0004	0.0018	0.0016	0.0011	0.0014	0.0004	0.0003
	125%	0.0041	0.0022	0.0015	0.0014	0.0027	0.0012	0.0042	0.0036	0.0023	0.0028	0.0026	0.0008
	150%	0.0099	0.0065	0.0037	0.0027	0.0026	0.0031	0.0110	0.0029	0.0054	0.0081	0.0020	0.0017
7m	75%	0.0002	0.0002	0.0001	0.0002	0.0002	0.0002	0.0002	0.0002	0.0002	0.0002	0.0002	0.0001
	100%	0.0006	0.0006	0.0003	0.0005	0.0005	0.0003	0.0005	0.0005	0.0003	0.0006	0.0006	0.0003
	125%	0.0013	0.0012	0.0005	0.0010	0.0010	0.0007	0.0010	0.0010	0.0007	0.0013	0.0013	0.0007
	150%	0.0026	0.0017	0.0010	0.0017	0.0019	0.0013	0.0017	0.0019	0.0013	0.0023	0.0019	0.0014
8m	75%	0.0002	0.0002	0.0002	0.0002	0.0001	0.0002	0.0001	0.0001	0.0001	0.0003	0.0003	0.0001
	100%	0.0009	0.0008	0.0003	0.0003	0.0004	0.0003	0.0004	0.0004	0.0004	0.0008	0.0009	0.0003
	125%	0.0019	0.0016	0.0005	0.0008	0.0010	0.0007	0.0012	0.0010	0.0008	0.0015	0.0019	0.0008
	150%	0.0040	0.0035	0.0012	0.0015	0.0022	0.0017	0.0024	0.0020	0.0017	0.0024	0.0046	0.0018
9m	75%	0.0010	0.0005	0.0002	0.0007	0.0009	0.0006	0.0008	0.0008	0.0004	0.0013	0.0006	0.0001
	100%	0.0042	0.0022	0.0010	0.0029	0.0042	0.0025	0.0027	0.0036	0.0022	0.0062	0.0013	0.0003
	125%	0.0147	0.0083	0.0019	0.0101	0.0133	0.0105	0.0100	0.0118	0.0070	0.0203	0.0038	0.0012
	150%	0.0747	0.0664	0.0559	0.0708	0.0742	0.0753	0.0721	0.0713	0.0688	0.1066	0.0592	0.0514
10m	75%	0.0001	0.0001	0.0001	0.0001	0.0001	0.0001	0.0001	0.0001	0.0001	0.0002	0.0001	0.0001
	100%	0.0004	0.0004	0.0003	0.0002	0.0002	0.0002	0.0002	0.0001	0.0002	0.0008	0.0003	0.0002
	125%	0.0009	0.0009	0.0007	0.0003	0.0003	0.0005	0.0004	0.0003	0.0007	0.0016	0.0006	0.0004
	150%	0.0016	0.0016	0.0011	0.0008	0.0007	0.0012	0.0008	0.0007	0.0013	0.0027	0.0014	0.0008
11m	75%	0.0002	0.0002	0.0002	0.0002	0.0001	0.0002	0.0001	0.0001	0.0001	0.0003	0.0001	0.0001
	100%	0.0006	0.0005	0.0004	0.0003	0.0002	0.0005	0.0002	0.0001	0.0002	0.0008	0.0002	0.0002
	125%	0.0016	0.0013	0.0011	0.0008	0.0005	0.0012	0.0004	0.0002	0.0005	0.0021	0.0006	0.0005
	150%	0.0103	0.0091	0.0109	0.0108	0.0048	0.0117	0.0098	0.0042	0.0096	0.0154	0.0070	0.0086

Table 5-3. (Continued).

		Web A			Web B			Web C			Web D		
	Percent	Duct 1	Duct 3	Duct 5	Duct 1	Duct 3	Duct 5	Duct 1	Duct 3	Duct 5	Duct 1	Duct 3	Duct 5
Model #	Capacity												
12m	75%	0.0001	0.0001	0.0001	0.0001	0.0001	0.0001	0.0001	0.0001	0.0001	0.0002	0.0001	0.0001
	100%	0.0002	0.0003	0.0003	0.0002	0.0002	0.0002	0.0002	0.0001	0.0002	0.0008	0.0002	0.0002
	125%	0.0005	0.0008	0.0007	0.0004	0.0004	0.0005	0.0004	0.0003	0.0005	0.0017	0.0007	0.0006
	150%	0.0009	0.0013	0.0014	0.0009	0.0008	0.0010	0.0008	0.0005	0.0009	0.0034	0.0013	0.0011
13m	75%	0.0001	0.0001	0.0001	0.0001	0.0001	0.0001	0.0001	0.0001	0.0001	0.0002	0.0001	0.0001
	100%	0.0002	0.0002	0.0003	0.0002	0.0001	0.0002	0.0001	0.0001	0.0002	0.0006	0.0002	0.0002
	125%	0.0006	0.0005	0.0006	0.0003	0.0002	0.0004	0.0002	0.0002	0.0003	0.0011	0.0004	0.0003
	150%	0.0009	0.0008	0.0009	0.0006	0.0005	0.0007	0.0005	0.0005	0.0007	0.0017	0.0007	0.0005
14m	75%	0.0005	0.0005	0.0002	0.0001	0.0001	0.0004	0.0002	0.0001	0.0003	0.0011	0.0002	0.0001
	100%	0.0017	0.0015	0.0009	0.0004	0.0007	0.0021	0.0010	0.0004	0.0013	0.0034	0.0008	0.0002
	125%	0.0045	0.0048	0.0019	0.0011	0.0013	0.0063	0.0032	0.0014	0.0032	0.0111	0.0011	0.0004
	150%	0.0125	0.0143	0.0046	0.0017	0.0022	0.0182	0.0113	0.0036	0.0081	0.0273	0.0018	0.0012
2MVert	75%	0.0001	0.0001	0.0001	0.0002	0.0001	0.0001	0.0001	0.0001	0.0001	0.0001	0.0001	0.0001
	100%	0.0003	0.0003	0.0002	0.0005	0.0004	0.0003	0.0004	0.0004	0.0003	0.0003	0.0003	0.0002
	125%	0.0010	0.0009	0.0006	0.0009	0.0010	0.0008	0.0011	0.0010	0.0006	0.0008	0.0010	0.0007
	150%	0.0019	0.0017	0.0011	0.0019	0.0021	0.0016	0.0023	0.0020	0.0015	0.0020	0.0021	0.0016
11MVert	75%	0.0002	0.0001	0.0002	0.0002	0.0001	0.0002	0.0001	0.0001	0.0001	0.0001	0.0001	0.0001
	100%	0.0006	0.0002	0.0007	0.0002	0.0002	0.0006	0.0002	0.0002	0.0002	0.0002	0.0002	0.0003
	125%	0.0013	0.0007	0.0014	0.0006	0.0005	0.0011	0.0003	0.0003	0.0004	0.0005	0.0005	0.0006
	150%	0.0024	0.0015	0.0026	0.0013	0.0011	0.0019	0.0006	0.0006	0.0008	0.0011	0.0011	0.0012

mode is tending toward local duct pullout, stirrups are not a very effective deterrent against this failure mode. But if the duct layout and duct ties are properly detailed to eliminate the local pullout failure mode, the stirrup spacing does define the web "regional" beam strength.

Concrete Material Properties, Especially Assumed Tensile Strength

This was evaluated by comparing Model-Webs 5M-C to 2M-C, 6M-C to 2M-C, 12M-D to 11M-D, and 12M-C to 12M-B. This comparison is shown in Table 5-13.

So the web section strength tends to be significantly influenced by the concrete strength only when the section is prone to web-splitting/local-lateral shear-failures, i.e., when vulnerable duct placement is used or web/duct tie reinforcement is NOT used. When web/duct tie reinforcement is used, concrete tensile strength has little effect on the section strength. This tends to further underscore the importance of providing web/duct tie reinforcement; because of the various parameters involved in reinforced concrete design, concrete tensile strength has wide variability, and low reliability. Thus designers should be directed toward design rules that will ensure good performance regardless of variabilities in concrete tensile strength.

Local Analysis of Single-Cell Box Girders

Model Prototype: Single-Cell CIP Box Girder

A single-cell box configuration was used as shown in Figure 5-23, with the tendon duct arrangements and local reinforcements shown in Figure 5-16 and further illustrated in Figure 5-23. The duct and tie configurations are referred to as #6 and #6a, to differentiate from the configurations of the multi-cell. The only difference between these is that #6 has no duct ties, and #6a has the two rebar ties as shown. The basic model uses 3D elements and a slice, with out-of-page thickness equal to one stirrup spacing. The stirrups (and other rebar) are modeled explicitly (unlike in 2D, where the stirrup is smeared). This allows introduction of the out-of-page compression due to prestress. Using this model framework, geometry variabilities were introduced directly into the models—e.g., one web can have one thickness and another have a different thickness. Webs 1 and 2 demonstrate the differences related to web sloping away from the radius of curvature versus sloping toward the radius of curvature.

Web 1 - left, Web 2 - right. (Duct/Tie configuration "6". "6a" would include horizontal crossties.)

Similar to the multi-cell analysis series, in order to establish a baseline for comparison with design calculations, P_c was

Table 5-4. Distortion (web thickness change) across the mid-height of ducts (Duct 1 – bottom, Duct 3 – middle, Duct 5 – top).

		Web A			Web B			Web C			Web D		
Model #	Percent Capacity	Duct1	Duct 3	Duct 5	Duct1	Duct 3	Duct 5	Duct1	Duct 3	Duct 5	Duct1	Duct 3	Duct 5
1m	75%	0.0020	0.0029	0.0016	0.0029	0.0088	0.0020	0.0020	0.0078	0.0010	0.0020	0.0116	0.0016
	100%	0.0033	0.0092	0.0041	0.0368	0.0283	0.0039	0.0039	0.0303	0.0029	0.0041	0.0251	0.0035
	125%	0.0075	0.0209	0.0078	0.0254	0.0693	0.0107	0.0078	0.0732	0.0078	0.0062	0.0251	0.0073
	150%	0.0101	0.0409	0.0150	0.0508	0.1387	0.0234	0.0156	0.1621	0.0244	0.0089	0.0591	0.0133
2m	75%	0.0016	0.0012	0.0014	0.0010	0.0049	0.0020	0.0010	0.0039	0.0020	0.0034	0.0032	0.0014
	100%	0.0026	0.0035	0.0018	0.0020	0.0146	0.0029	0.0020	0.0137	0.0039	0.0067	0.0098	0.0019
	125%	0.0051	0.0943	0.0044	0.0010	0.0342	0.0059	0.0068	0.0332	0.0059	0.0158	0.0221	0.0053
	150%	0.0113	0.1010	0.0087	0.0029	0.0742	0.0146	0.0293	0.0791	0.0117	0.0443	0.0488	0.0089
3m	75%	0.0019	0.0013	0.0010	0.0029	0.0029	0.0020	0.0020	0.0049	0.0020	0.0024	0.0033	0.0011
	100%	0.0023	0.0031	0.0032	0.0098	0.0117	0.0020	0.0039	0.0107	0.0039	0.0064	0.0087	0.0017
	125%	0.0052	0.0055	0.0087	0.0244	0.0342	0.0059	0.0078	0.0264	0.0107	0.0112	0.0242	0.0052
	150%	0.1803	0.1789	0.1843	0.1748	0.3154	0.1875	0.2803	0.4268	0.2910	0.2535	0.3563	0.2105
4m	75%	0.0019	0.0170	0.0021	0.0078	0.0127	0.0049	0.0078	0.0137	0.0059	0.0104	0.0110	0.0022
	100%	0.0048	0.0133	0.0042	0.0293	0.0596	0.0039	0.0264	0.0459	0.0068	0.0380	0.0437	0.0083
	125%	0.0249	0.0081	0.0074	0.0947	0.2266	0.0010	0.0752	0.1211	0.0117	0.0918	0.1244	0.0292
	150%	0.9973	0.8594	0.8428	1.1494	1.7051	0.9990	1.1553	1.5244	1.1211	1.0413	1.2327	0.9574
5m	75%	0.0014	0.0013	0.0021	0.0020	0.0029	0.0020	0.0010	0.0029	0.0020	0.0034	0.0024	0.0006
	100%	0.0013	0.0025	0.0026	0.0068	0.0059	0.0029	0.0020	0.0059	0.0029	0.0065	0.0037	0.0016
	125%	0.0042	0.0045	0.0056	0.0186	0.0146	0.0049	0.0049	0.0176	0.0049	0.0133	0.0059	0.0029
	150%	0.0065	0.0088	0.0093	0.0361	0.0312	0.0107	0.0117	0.0371	0.0098	0.0253	0.0130	0.0046
6m	75%	0.0016	0.0019	0.0013	0.0029	0.0039	0.0020	0.0059	0.0117	0.0039	0.0026	0.0032	0.0014
	100%	0.0044	0.0149	0.0020	0.0068	0.0186	0.0029	0.0225	0.0381	0.0107	0.0075	0.0117	0.0028
	125%	0.0080	0.0174	0.0046	0.0146	0.0479	0.0098	0.0547	0.0801	0.0234	0.1099	0.0321	0.0105
	150%	0.0193	0.0282	0.0110	0.0391	0.1055	0.0186	0.1113	0.1660	0.0537	0.0447	0.0764	0.0140
7m	75%	0.0021	0.0007	0.0014	0.0020	0.0039	0.0010	0.0029	0.0049	0.0020	0.0027	0.0040	0.0014
	100%	0.0021	0.0036	0.0034	0.0059	0.0088	0.0029	0.0049	0.0098	0.0049	0.0082	0.0073	0.0025
	125%	0.0035	0.0064	0.0046	0.0117	0.0195	0.0068	0.0156	0.0244	0.0088	0.0184	0.0169	0.0052
	150%	0.0068	0.0130	0.0093	0.0283	0.0391	0.0146	0.0303	0.0498	0.0195	0.0358	0.0369	0.0109
8m	75%	0.0014	0.0014	0.0011	0.0020	0.0020	0.0020	0.0029	0.0010	0.0010	0.0040	0.0037	0.0012
	100%	0.0010	0.0049	0.0029	0.0029	0.0049	0.0029	0.0029	0.0098	0.0029	0.0083	0.0057	0.0022
	125%	0.0039	0.0077	0.0056	0.0078	0.0137	0.0049	0.0244	0.0303	0.0068	0.0197	0.0174	0.0047
	150%	0.0075	0.0167	0.0103	0.0156	0.0321	0.0107	0.0527	0.0625	0.0176	0.0478	0.0438	0.0084
9m	75%	-0.0001	0.0014	0.0013	0.0049	0.0117	0.0039	0.0029	0.0098	0.0029	0.0031	0.0032	0.0011
	100%	0.0012	0.0015	0.0031	0.0215	0.0361	0.0078	0.0078	0.0352	0.0059	-0.0040	0.0089	0.0035
	125%	-0.0140	-0.0261	0.0055	0.0801	0.1162	0.0059	0.0352	0.1143	0.0146	-0.0002	0.0296	0.0111
	150%	0.7518	0.6562	0.6789	0.9424	1.1504	0.7197	0.7256	1.1426	0.8164	0.7270	0.9038	1.8598

Table 5-4. (Continued).

Model #	Percent Capacity	Web A			Web B			Web C			Web D		
		Duct1	Duct 3	Duct 5	Duct1	Duct 3	Duct 5	Duct1	Duct 3	Duct 5	Duct1	Duct 3	Duct 5
10m	75%	0.0014	0.0019	0.0013	0.0010	0.0020	0.0020	0.0010	0.0029	0.0010	0.0021	0.0013	0.0016
	100%	0.0026	0.0035	0.0013	0.0020	0.0039	0.0020	0.0010	0.0039	0.0029	0.0035	0.0025	0.0024
	125%	0.0041	0.0046	8.0000	0.0049	0.0088	0.0049	0.0020	0.0117	0.0049	0.0061	0.0062	0.0031
	150%	0.0060	0.0095	9.0000	0.0127	0.0176	0.0078	0.0059	0.0225	0.0088	0.0082	0.0146	0.0064
11m	75%	0.0015	0.0010	0.0015	0.0020	0.0020	0.0010	0.0010	0.0020	0.0010	0.0019	0.0016	0.0008
	100%	0.0560	0.0010	0.0021	0.0029	0.0029	0.0010	0.0010	0.0039	0.0020	0.0033	0.0021	0.0024
	125%	0.0036	0.0033	0.0032	0.0049	0.0078	0.0029	0.0029	0.0107	0.0049	-0.0090	0.0086	0.0049
	150%	0.0809	0.0963	0.0978	0.0977	0.1387	0.0781	0.1211	0.1963	0.1328	0.0939	0.1518	0.1160
12m	75%	0.0014	0.0014	0.0014	0.0008	0.0008	0.0008	0.0020	0.0020	0.0020	0.0018	0.0018	0.0018
	100%	0.0020	0.0020	0.0020	0.0016	0.0016	0.0016	0.0039	0.0039	0.0039	0.0030	0.0030	0.0030
	125%	0.0041	0.0041	0.0041	0.0041	0.0041	0.0041	0.0078	0.0078	0.0078	0.0038	0.0038	0.0038
	150%	0.0078	0.0078	0.0078	0.0093	0.0093	0.0093	0.0127	0.0127	0.0127	0.0071	0.0071	0.0071
13m	75%	0.0015	0.0017	0.0008	0.0010	0.0020	0.0020	0.0000	0.0020	0.0020	0.0014	0.0014	0.0017
	100%	0.0023	0.0026	0.0021	0.0020	0.0029	0.0020	0.0000	0.0029	0.0020	0.0026	0.0027	0.0017
	125%	0.0022	0.0027	0.0021	0.0039	0.0068	0.0029	0.0000	0.0068	0.0039	0.0041	0.0058	0.0028
	150%	0.0047	0.0045	0.0021	0.0078	0.0137	0.0059	0.0000	0.0117	0.0059	0.0059	0.0117	0.0017
14m	75%	0.0018	0.0018	0.0012	0.0010	0.0022	0.0004	0.0010	0.0020	0.0020	0.0016	0.0022	0.0011
	100%	0.0030	0.0029	0.0015	0.0042	0.0043	0.0065	0.0010	0.0049	0.0059	0.0013	0.0053	0.0019
	125%	0.0072	-0.0008	0.0017	0.0097	0.0109	0.0086	-0.0010	0.0059	0.0117	0.0060	0.0104	0.0047
	150%	0.0228	-0.0302	0.0064	0.0268	0.0279	-0.0193	-0.0195	0.0146	0.0098	-0.0168	0.0364	0.0140
2MVert	75%	0.0015	0.0028	0.0020	0.0020	0.0029	0.0010	0.0010	0.0029	0.0020	0.0021	0.0029	0.0020
	100%	0.0021	0.0057	0.0020	0.0059	0.0088	0.0020	0.0010	0.0088	0.0029	-0.0017	0.0050	-0.0233
	125%	0.0065	0.0204	0.0059	0.0000	0.0000	0.0039	0.0049	0.0264	0.0000	0.0046	0.0175	0.0074
	150%	0.0132	0.0397	0.0109	0.0332	0.0488	0.0068	0.0117	0.0557	0.0117	0.0074	0.0371	0.0163
11MVert	75%	0.0010	0.0010	0.0010	0.0010	0.0020	0.0010	0.0020	0.0020	0.0010	0.0022	0.0010	0.0019
	100%	0.0000	0.0020	0.0000	0.0020	0.0029	0.0010	0.0039	0.0039	0.0029	0.0024	0.0030	0.0019
	125%	0.0000	0.0039	0.0010	0.0039	0.0049	-0.0013	0.0059	0.0068	0.0049	0.0050	0.0069	0.0038
	150%	0.0000	0.0107	0.0020	0.0068	0.0146	0.0000	0.0127	0.0107	0.0088	0.0091	0.0148	0.0068

defined as a "Capacity" calculated using conventional means, but removing resistance factors. This provided the best direct comparison to finite element analyses. For the webs of the single-cell geometry prototype, P_c was calculated as follows:

h = 9.67 feet

$\phi M_n = 42.1$ k-ft/ft

Removing the safety factor $\phi = 0.9$,

$M_n = 46.8$ k-ft/ft

Applying an over-strength factor for rebar strain hardening (which is included in the FE analysis),

$M_o = M_n \times 1.125 = 52.6$ k-ft/ft

As described earlier, moment-fixity effects were approximately 0.6 for interior webs and 0.7 for exterior webs. Since there were only three ducts distributed vertically, the increase to capacity caused by load distribution was small, so no capacity increase was applied for this. So the baseline P_c became

$P_c = [52.6/(h/4)]/0.7 = 31.1$ k/ft

Table 5-5. Lateral prestress force at stirrup yield (0.2% strain) for stirrups on inside of curve.

	Total Force (in % of Pc and in K/ft)							
Model #	Web A	Web A	Web B	Web B	Web C	Web C	Web D	Web D
1M	119.55%	9.93	107.36%	11.38	111.04%	11.77	122.41%	11.18
2M	141.66%	11.77	128.85%	13.66	128.67%	13.64	129.38%	11.82
3M	121.11%	10.06	118.77%	12.59	144.72%	15.34	134.24%	12.26
4M	-	6.24	-	8.59	-	8.57	-	7.42
5M	134.96%	11.21	133.11%	14.11	150.47%	15.95	126.25%	11.53
6M	105.54%	8.77	118.54%	12.57	105.75%	11.21	117.92%	10.77
7M	140.98%	11.71	154.06%	16.33	153.87%	16.31	147.93%	13.51
8M	124.72%	10.36	148.49%	15.74	145.38%	15.41	129.86%	11.86
9M	-	7.28	-	9.59	-	9.58	-	7.75
10M	157.23%	13.06	162.45%	17.22	161.60%	17.13	142.01%	12.97
11M	131.45%	10.92	141.51%	15.00	148.15%	15.70	126.77%	11.58
12M	160.55%	13.34	165.81%	17.58	165.58%	17.55	135.53%	12.38
13M	180.74%	15.01	184.97%	19.61	184.00%	19.50	166.09%	15.17
14M	-	8.65	-	10.47	-	11.81	-	8.48
2MVert	151.05%	12.55	148.79%	15.77	145.06%	15.38	151.69%	13.85
11MVert	140.59%	11.68	152.49%	16.16	165.41%	17.53	167.19%	15.27

- Percentages not shown for cases other than ducts placed at midheight

This was used as "100%" in the results tables and plots. The results of the single-cell analyses are shown in Tables 5-14, 5-15, 5-16, and 5-17, and the figures in the remainder of this chapter. The figures are included in Appendix Fa and are numbered (Fig. B-1, B-2, etc.). The maximum principal strain contours illustrate the general level of damage to the concrete surrounding the tendon ducts (maximum tensile strain regardless of orientation).

Single-Cell Models – Analysis Results

The results of the 10 different single-cell box-girder local models allow for qualitative and quantitative assessment and comparison of the cases analyzed.

- Lateral Force vs. Deflection of Web Mid-height
- Lateral Force vs. Deflection of Web Quarter-height

Table 5-6. Lateral prestress force at web delamination of 0.5% (0.06" for 12" web).

Model #	% Pc	Web A Total Force (K/ft)	Deflection (in)	% Pc	Web B Total Force (K/ft)	Deflection (in)	% Pc	Web C Total Force (K/ft)	Deflection (in)	% Pc	Web D Total Force (K/ft)	Deflection (in)
1M	165.03%	13.708	3.440	121.05%	12.831	0.193	118.90%	12.604	0.156	155.08%	14.163	0.425
2M	130.38%	10.830	0.249	143.12%	15.170	0.301	142.06%	15.059	0.305	159.45%	14.563	0.446
3M	136.29%	11.321	0.568	120.84%	12.809	0.278	123.99%	13.143	0.148	124.87%	11.405	0.190
4M	-	9.458	1.573	-	10.620	0.914	-	10.677	0.787	-	9.337	0.853
5M	200% *	16.613	0.830	184.92%	19.601	0.513	172.64%	18.300	0.384	200% *	18.266	0.688
6M	162.10%	13.464	3.103	131.33%	13.921	0.332	114.65%	12.153	0.257	142.79%	13.041	0.365
7M	200% *	16.613	0.753	173.24%	18.364	0.407	161.42%	17.111	0.346	179.26%	16.372	0.429
8M	200% *	16.613	14.363	178.17%	18.886	1.810	142.28%	15.082	0.274	167.97%	15.341	1.032
9M	-	10.058	1.504	-	10.939	0.602	-	11.042	0.528	-	10.767	1.181
10M	200% *	16.613	10.122	200% *	21.200	7.139	200% *	21.200	7.533	200% *	18.266	3.868
11M	145.14%	12.056	0.519	137.96%	14.624	0.259	138.95%	14.729	0.183	140.55%	12.836	0.235
12M	200% *	16.613	7.883	200% *	21.200	7.160	200% *	21.200	5.334	200% *	18.266	3.725
13M	200% *	16.613	2.717	200% *	21.200	2.575	200% *	21.200	2.697	200% *	18.266	2.230
14M	-	16.830	9.277	-	20.186	6.473	-	27.218	15.109	-	16.288	6.762
2MVert	166.40%	13.822	0.289	158.62%	16.814	0.250	153.77%	16.299	0.248	171.58%	15.670	0.315
11MVert	200% *	16.613	10.559	200% *	21.200	8.047	200% *	21.200	6.917	200% *	18.266	7.757

* Never reached delamination limit, so the delamination at 200% of P_c is shown

Table 5-7. Effect of web thickness – thin webs.

Model-Web	Force at stirrup yield (kips/ft)		Difference
2M-A vs. 3M-A	11.77 vs.	10.06	-15% change between 12” vs. 10”
2M-B vs. 3M-B	13.66 vs.	12.59	-8% change between 12” vs. 10”
2M-C vs. 3M-C	13.64 vs.	15.34	12% change between 12” vs. 14”
12M-A vs. 11M-A	13.34 vs.	10.92	-18% change between 12” vs. 10”
12M-B vs. 11M-B	17.58 vs.	15.00	-15% change between 12” vs. 10”
Model-Web	**Force at web delam. (kips/ft)**		**Difference**
2M-B vs. 3M-B	15.17 vs.	12.81	-16% change between 12” vs. 10”
12M-A* vs. 11M-A	16.61 vs.	12.06	-27% change between 12” vs. 10”
12M-B* vs. 11M-B	21.20 vs.	14.62	-31% change between 12” vs. 10”

* Never reached delamination limit

- Maximum Principal Strain Contours in Concrete at 75%, 100%, 125%, and 150% P_c
- Strains in stirrup rebar at 3 locations along duct bank at 75%, 100%, 125%, and 150% P_c
- Distortions (change in web width) 3 locations along duct bank 75%, 100%, 125%, and 150% P_c

Detailed results are included in Appendix F-a.

Discussion of Results

Analyses of these models showed similar trends as the multi-cell model analyses, and there were no surprises as to the performance of the sections. As expected, the sections with duct ties performed better than those without. Having the double row of tendons was found to concentrate the local damage area within the web, but having the 20-inch web thickness with local reinforcement was quite adequate to accommodate this.

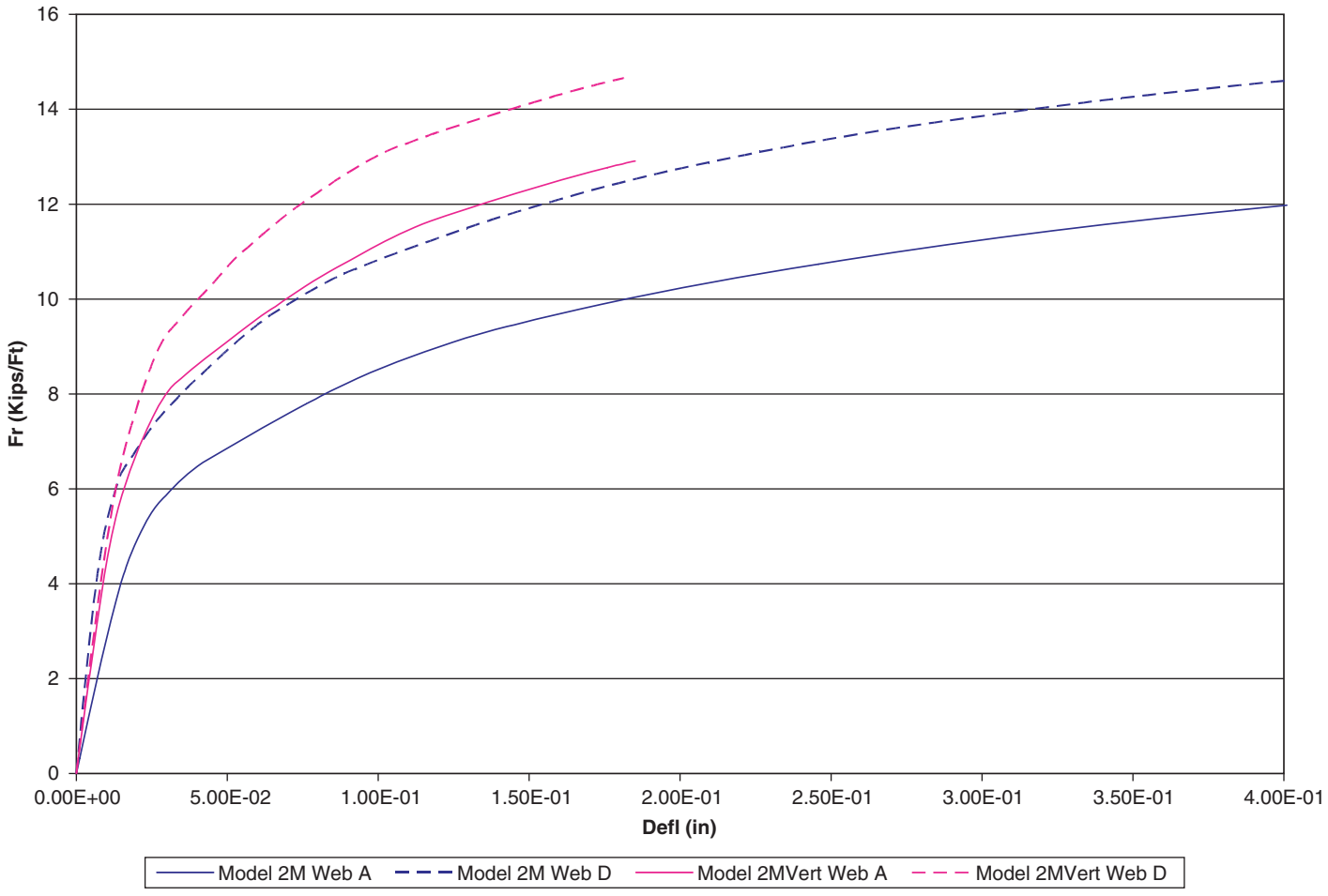

Figure 5-22a. Model 2M and 2MVert force vs. deflection comparison for Webs A and D (quarter height).

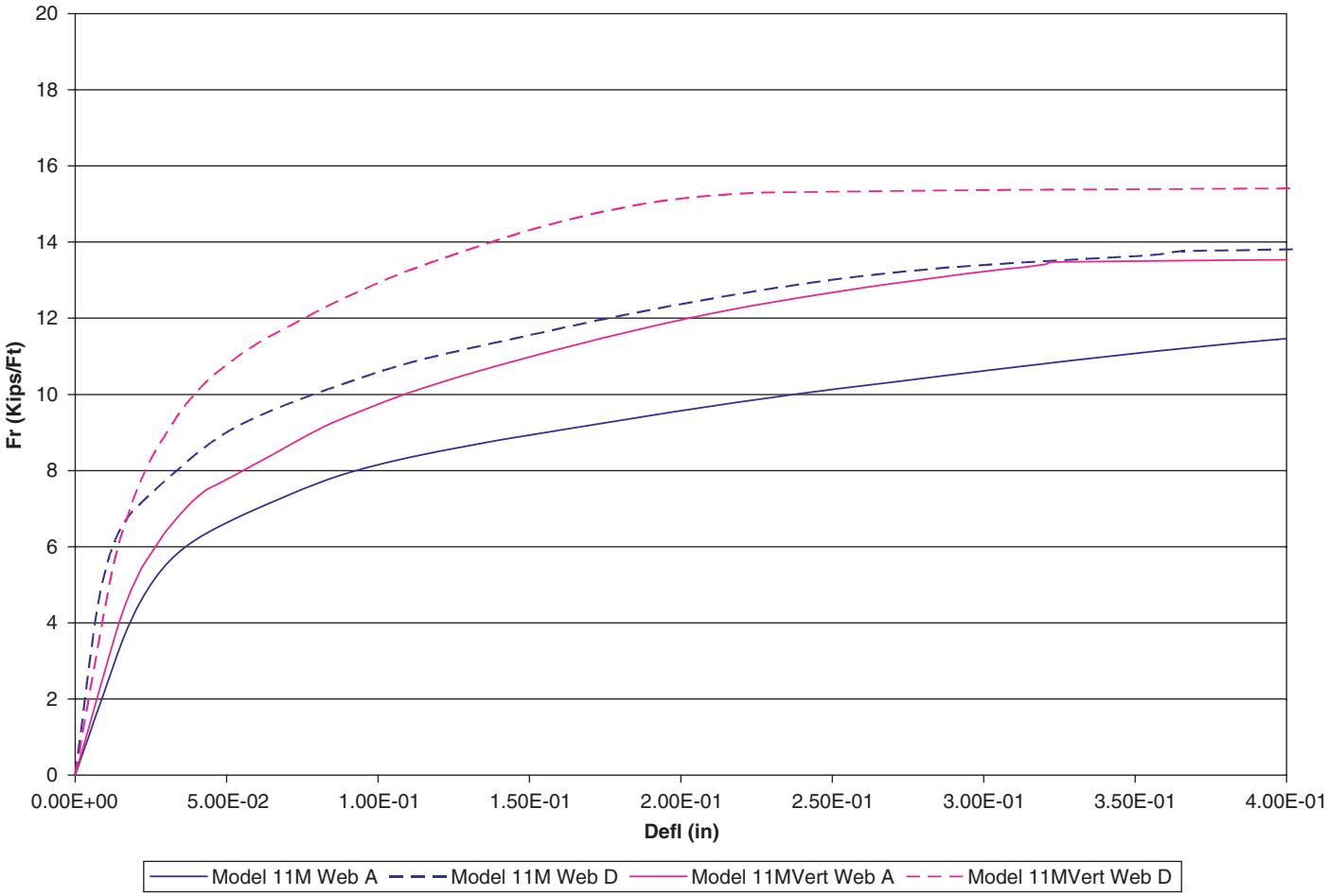

Figure 5-22b. Model 11M and 11MVert force vs. deflection comparison for Webs A and D (mid height).

Table 5-8. Effect of web slope – thin webs.

Model-Web	Force at stirrup yield (kips/ft)			Difference
2M-A vs. 2Mvert-A	11.77	vs.	12.55	7% change with vertical web
2M-D vs. 2Mvert-D	11.82	vs.	13.85	17% change with vertical web
11M-A vs. 11Mvert-A	10.92	vs.	11.68	7% change with vertical web
11M-D vs. 11Mvert-D	11.58	vs.	15.27	32% change with vertical web

Model-Web	Force at web delam. (kips/ft)			Difference
2M-A vs. 2Mvert-A	10.83	vs.	13.82	28% change with vertical web
2M-D vs. 2Mvert-D	14.56	vs.	15.67	8% change with vertical web
11M-A vs. 11Mvert-A*	12.06	vs.	16.61	38% change with vertical web
11M-D vs. 11Mvert-D*	12.84	vs.	18.27	42% change with vertical web

* Never reached delamination limit

Table 5-9. Effect of cover thickness – thin webs.

Model-Web	Force at stirrup yield (kips/ft)			Difference
8M-A vs. 2M-A	10.36	vs.	11.77	14% change between 2" vs. 3"
8M-C vs. 2M-C	15.41	vs.	13.64	-11% change between 4" vs. 3"
8M-D vs. 2M-D	11.86	vs.	11.82	-0.3% change between 2" vs. 3"
Model-Web	**Force at web delam. (kips/ft)**			**Difference**
8M-C vs. 2M-C	15.08	vs.	15.06	-0.2% change between 4" vs. 3"
8M-D vs. 2M-D	15.34	vs.	14.56	-5% change between 2" vs. 3"

Qualitative evidence can also be obtained by examining the strain plots in the Appendixes for the models where cover thickness was varied.

Table 5-10. Effect of different duct configurations – thin webs.

Model-Web	Force at stirrup yield (kips/ft)			Difference
1M-A vs. 2M-A	9.93	vs.	11.77	19% change - Config. 1 vs. 2A
1M-B vs. 2M-B	11.38	vs.	13.66	20% change - Config. 1 vs. 2A
1M-C vs. 2M-C	11.77	vs.	13.64	16% change - Config. 1 vs. 2A
3M-D vs. 2M-D	12.26	vs.	11.82	-4% change - Config. 2B vs. 2A
5M-B vs. 2M-B	14.11	vs.	13.66	-3% change - Config. 2B vs. 2A
10M-C vs. 7M-C	17.13	vs.	16.31	-5% change - Config. 3A vs. 2A
Model-Web	**Force at web delam. (kips/ft)**			**Difference**
1M-B vs. 2M-B	12.83	vs.	15.17	18% change - Config. 1 vs. 2A
1M-C vs. 2M-C	12.60	vs.	15.06	19% change - Config. 1 vs. 2A
5M-B vs. 2M-B	19.60	vs.	15.17	-23% change - Config. 2B vs. 2A
10M-C* vs. 7M-C	21.20	vs.	17.11	* change - Config. 3A vs. 2A

* Never reached delamination limit

Similar to the multi-cell studies, the analysis results can be used to compare the web design parameters. For purposes of interpreting the 3D finite element analysis results, the following damage limit criteria are suggested:

- Stirrup rebar strain exceeding yield (i.e., 0.2% strain for Grade 60 steel); for Load Factor Design, concrete reinforcement is designed to yield; yield should be considered an upper bound criteria for unfactored loads.
- Visible concrete cracking occurs at strains of approximately 0.016%, but this is not necessarily web failure; concrete with maximum principal strains of 0.3% can be considered to be heavily cracked. Concrete with strains in excess of 1.0% will generally show wide-open cracks and potential spalling from the section.
- Significant distortion or delamination (change of width of the webs) also represents an upper limit on capacity for webs; the delamination is evidence of a local splitting or lateral shear failure within the web; it was again assumed that an upper bound on crack width of 1/16" is an indicator of such a failure. For 20" webs, this represents a distortion ratio (average strain through the section) of 0.3%. For sections with web ties, this means the web ties have yielded; for sections without web ties, the section is at a web splitting or a cover concrete spalling condition.

One of the criteria, Stirrup Yield, has been summarized in Table 5-18. These are the total forces (sum of all tendon ducts in the web) applied when any part of the stirrup reaches yield.

Using these criteria, and examining the results tables and plots resulted in the following observations.

Web Slope

Similar to the multi-cell series, the inside radius web, sloping toward the center of the curve, was found to be roughly 10% stronger than the outside radius web, sloping away from the center of the curve. Further study indicated a possible reason for this was that loading the inside radius web (Web 2) created positive transverse moment in the top slab adjacent to the web (tension on the bottom of the slab), whereas loading Web 1 created negative moment. The slab resistance to

Table 5-11. Effect of duct tie arrangements – thin webs.

Model-Web	Force at stirrup yield (kips/ft)			Difference
10M-B vs. 12M-B	17.22	vs.	17.58	2% change - Config. 3A vs. 4A
10M-C vs. 12M-C	17.13	vs.	17.55	2% change - Config. 3A vs. 4B
10M-A vs. 13M-A	13.06	vs.	15.01	15% change - Config. 3A vs. 4A
10M-B vs. 13M-B	17.22	vs.	19.61	14% change - Config. 3A vs. 4A
10M-C vs. 13M-C	17.13	vs.	19.50	14% change - Config. 3A vs. 4A
10M-D vs. 13M-D	12.97	vs.	15.17	17% change - Config. 3A vs. 4A
12M-B vs. 12M-C	17.58	vs.	17.55	-0.2% change - Config. 4A vs. 4B
9M-B vs. 14M-B	9.59	vs.	10.47	9% change - Config. 2A vs. 4B
Model-Web	**Force at web delam. (kips/ft)**			**Difference**
9M-B vs. 14M-B	10.94	vs.	20.19	85% change - Config. 2A vs. 4B

Table 5-12. Effect of stirrup spacing – thin webs.

Model-Web	Force at stirrup yield (kips/ft)			Difference
6M-A vs. 2M-A	8.77	vs.	11.77	34% change with 50% more stirrup steel
6M-B vs. 2M-B	12.57	vs.	13.66	9% change with 50% more stirrup steel
6M-D vs. 2M-D	10.77	vs.	11.82	10% change with 50% more stirrup steel
7M-B vs. 2M-B	16.33	vs.	13.66	-16% change with 33% less stirrup steel
7M-D vs. 2M-D	13.51	vs.	11.82	-13% change with 33% less stirrup steel
13M-A vs. 12M-A	15.01	vs.	13.34	-11% change with 33% less stirrup steel
13M-B vs. 12M-B	19.61	vs.	17.58	-10% change with 33% less stirrup steel
13M-D vs. 12M-D	15.17	vs.	12.38	-18% change with 33% less stirrup steel
Model-Web	Force at web delam.(kips/ft)			Difference
6M-B vs. 2M-B	13.92	vs.	15.17	9% change with 50% more stirrup steel
6M-D vs. 2M-D	13.04	vs.	14.56	12% change with 50% more stirrup steel
7M-B vs. 2M-B	18.36	vs.	15.17	-17% change with 33% less stirrup steel
7M-D vs. 2M-D	16.37	vs.	14.56	-11% change with 33% less stirrup steel

these moments was stronger (about 2 times stronger, based on typical deck reinforcing) in positive moment than in negative moment, and this translated to more strength in the associated web.

Cover Thickness

Cover thickness was varied in Model 6S, where increases for Webs 1 and 2 were by 50% and 75%, respectively. Table 5-19 summarizes the relevant strength comparisons.

The local concrete damage was less severe with thicker cover, but the comparisons for stirrup yield were inconclusive because (1) for 2-inch cover and above, cover failure did not control the failure mode, and (2) when the cover was less, the "moment arm" between the stirrups was more, and this increased capacity rather than decreasing it.

Number and Configuration of Tendon Ducts

The only variation studied in the single-cell case was the positioning of the duct group (studied in Configurations 2S and 10S). The number and relative position of the ducts to each other was held constant. But it was again observed that, when the ducts occurred near the bottom of the web (either "quarter-height" or "bottom" as tested in Configurations 4M and 14M), the force at "failure" was substantially lower than when the ducts were placed at the mid-height, i.e., on average as much as 25% to 40% lower when comparing these cases to similar cases. The reason for this was a tendency toward lateral shear failure of the overall web, and a tendency toward flexural damage in the top slab, thus weakening the whole system. When the ducts were located at the mid-height, the lateral shear was divided equally between the top and bottom of the web. But when the ducts moved down, the bottom of the web carried most of the lateral shear. This is a different mechanism than the failure modes observed for tendon ducts at mid-height, but one that still warrants consideration in design.

Number and Configuration of Duct Ties

This was evaluated by comparing duct tie Configuration 6a, which had duct ties, to Configuration 6, which had no duct

Table 5-13. Effect of concrete strengths – thin webs.

Model-Web	Force at stirrup yield (kips/ft)			Difference
2M-C vs. 5M-C	13.64	vs.	15.95	17% change with 50% larger concr. strength
2M-C vs. 6M-C	13.64	vs.	11.21	-18% change with 50% smaller concr. strength
12M-B vs. 12M-C	17.58	vs.	17.55	-0.2% change with 50% larger concr. strength
Model-Web	Force at web delam. (kips/ft)			Difference
2M-C vs. 5M-C	15.06	vs.	18.30	22% change with 50% larger concr. strength
2M-C vs. 6M-C	15.06	vs.	12.15	-19% change with 50% smaller concr. strength

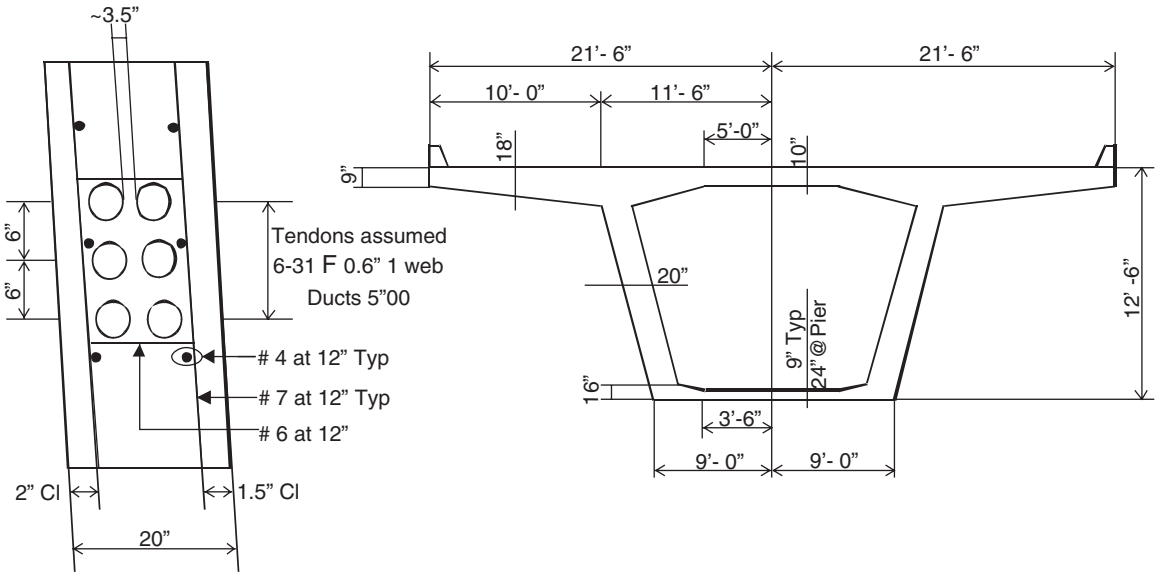

Figure 5-23. Tendon duct and local reinforcement for the local analysis prototype for a single-cell box.

ties. Table 5-20 compares Model/Webs 7S to 1S, 8S to 3S, and 9S-1 to 5S-1.

These comparisons show that, for the wider web (20 inches) and double row of tendon ducts, the ties do not make a significant difference in the force to cause stirrup yield, but they make a large difference in the delamination-damage that can occur within the web. Delaminations (width changes in the web) are reduced by 24 to 31% with duct ties as compared to without duct ties.

Stirrups

Stirrup spacing was evaluated by comparing Model-Webs 4S-1 to 1S-1, 5S-1 to 1S-1, and 9S-1, 2 to 7S-1, 2. The results are shown in Table 5-21.

The web section strength tends to be significantly influenced by the stirrup spacing for this geometry also, perhaps even more so than for the multi-cell geometry. Again, stirrup spacing is a driver of web "regional" beam strength.

Table 5-14. Single-cell box variations/parameter study.

Analysis #	Model Type	Web #	Web-ties	Web Thickness	Duct/Tie Config.*	Bundle Vert. Pos.	Stirrup Spacing(in.)	Cover Thickness	Concr. Tens. Str. (x√fc`)
1S	Single-cell	1	N	20	6	midheight	12	1.5"/2"	4
"baseline"		2	N	20	6	midheight	12	1.5"/2"	4
2S	Single-cell	1	N	20	6	1/4 height	12	1.5"/2"	4
		2	N	20	6	bottom	12	1.5"/2"	4
3S	Single-cell	1	N	20	6	midheight	12	1.5"/2"	4
		2	N	20	6	midheight	12	1.5"/2"	6
4S	Single-cell	1	N	20	6	midheight	8	1.5"/2"	4
		2	N	20	6	midheight	12	1.5"/2"	2
5S	Single-cell	1	N	20	6	midheight	18	1.5"/2"	4
		2	N	20	6	midheight	12	1.5"/2"	4
6S	Single-cell	1	N	20	6	midheight	12	2.5"/3"	4
		2	N	20	6	midheight	12	3:/3.5"	4
7S	Single-cell	1	Y	20	6a	midheight	12	1.5"/2"	4
		2	Y	20	6a	midheight	12	1.5"/2"	4
8S	Single-cell	1	Y	20	6a	midheight	12	1.5"/2"	2
		2	Y	20	6a	midheight	12	1.5"/2"	6
9S	Single-cell	1	Y	20	6a	midheight	18	1.5"/2"	4
		2	Y	20	6a	midheight	8	1.5"/2"	4
10S	Single-cell	1	Y	20	6a	1/4 height	12	1.5"/2"	4
		2	N	20	6a	bottom	12	1.5"/2"	4

Table 5-15. Deflections (inches) measured at mid-height of webs on backside.

Model #	Percent Capacity	Web 1 Mid	Web 1 Quarter	Web 2 Mid	Web 2 Quarter
1S	75%	0.176	0.174	0.179	0.158
	100%	0.404	0.402	0.418	0.360
	125%	1.076	1.090	1.208	0.978
	150%	2.496	2.499	2.903	2.224
2S	75%	0.888	1.251	0.724	1.068
	100%	2.340	3.365	1.924	2.852
	125%	4.521	6.484	3.647	5.410
	150%	26.702	36.174	22.345	31.707
3S	75%	0.156	0.152	0.135	0.131
	100%	0.366	0.357	0.338	0.307
	125%	0.918	0.906	0.871	0.778
	150%	2.239	2.161	2.246	1.868
4S	75%	0.272	0.274	0.314	0.256
	100%	0.678	0.681	0.764	0.609
	125%	1.805	1.775	2.050	1.570
	150%	4.030	3.904	4.542	3.445
5S	75%	0.140	0.140	0.159	0.137
	100%	0.295	0.298	0.351	0.293
	125%	0.685	0.701	0.961	0.722
	150%	1.728	1.815	2.526	1.835
6S	75%	0.195	0.190	0.192	0.170
	100%	0.462	0.457	0.463	0.405
	125%	1.212	1.204	1.288	1.066
	150%	2.805	2.691	2.974	2.362
7S	75%	0.168	0.168	0.174	0.154
	100%	0.372	0.377	0.400	0.355
	125%	0.953	0.987	1.056	0.923
	150%	2.286	2.335	2.600	2.169
8S	75%	0.205	0.192	0.155	0.154
	100%	0.435	0.420	0.357	0.341
	125%	1.095	1.046	0.866	0.846
	150%	2.588	2.447	2.127	1.996
9S	75%	0.146	0.148	0.182	0.151
	100%	0.320	0.335	0.472	0.365
	125%	0.849	0.915	1.409	1.011
	150%	2.102	2.292	3.413	2.463
10S	75%	0.808	1.131	0.659	0.972
	100%	2.301	3.242	1.877	2.785
	125%	4.462	6.274	3.493	5.187
	150%	23.358	31.548	19.232	27.371

Concrete Material Properties, Especially Assumed Tensile Strength

The effect of concrete strength was evaluated by comparing Model-Webs 3S-2 to 1S-2, 4S-2 to 1S-2, and 8S-1, 2 to 7S-1, 2. The results are shown in Table 5-22.

So, repeating the trend observed in the multi-cell analysis, the web section strength tends to be only marginally influenced by the concrete strength, and mostly this influence occurs when web/duct tie reinforcement is NOT used. When web/duct tie reinforcement is used, concrete tensile strength has less effect on the section strength. Of the various parameters involved in reinforced concrete design, concrete tensile strength has wide variability, and low reliability, so designers should use design rules that will ensure good performance, regardless of variabilities in concrete tensile strength.

Conclusions from Local Analyses

General Observations on Capacity

Using the capacity definitions described in this section (P_c, developed based on regional transverse bending considerations), it was found that all of the multi-cell box-girders achieved this target capacity. The baseline (Model 1M) interior webs achieved it marginally (i.e., stirrup yield was reached at 107% of P_c), while stronger details that use spreading apart the ducts, adding duct ties, or moving the ducts toward the curve-outside-face of the web reached as high as 185% of P_c. The variations in force to cause local duct bank breakout (either local shearing or web delamination) were even larger, depending on the detailing used, so the detailing significantly influences resistance to lateral pullout. For the single-cell example, with the 20-inch webs and double row of ducts, the finite element analysis showed capacities that were mostly lower than the hand-calculated regional transverse bending capacity (i.e., stirrup yield was reached at a range from 52% P_c up to 100% P_c), but this is explained by the fact that, for the thicker web, failures were dominated by local lateral shearing.

Summary of Influences from Detailing Parameters

- **Web Depth** can be adequately accounted for by considering and designing for web moments.
- **Web Thickness** significantly influences resistance to regional transverse bending and tendon pullout. For stirrup yield, capacity formulae based on regional flexure considerations appear to be appropriate for design.
- **Web Slope.** Sloped webs were found to be significantly weaker (roughly 30%) than the vertical webs, but much of this difference is caused because these are exterior webs rather than interior ones. Exterior webs have more flexible end conditions at their connection with the top and bottom slab, and this produces larger mid-height moments. Comparison of Webs A to D for the inclined webs show that Web A is generally weaker than D by about 10%. It is believed this is due to the difference in positive bending versus negative bending strength of the top slab. Lateral force for Web D applies positive moment

Table 5-16. Stirrup strain (%) on curve inside - face.

		Web 1			Web 2		
	Percent	Duct 2	Duct 4	Duct 6	Duct 2	Duct 4	Duct 6
Model #	Capacity						
1S	75%	0.00166	0.00137	0.00097	0.00150	0.00150	0.00150
	100%	0.00421	0.00222	0.00173	0.00310	0.00310	0.00310
	125%	0.01851	0.01023	0.00275	0.01506	0.01506	0.01506
	150%	0.04107	0.03204	0.01021	0.04032	0.04032	0.04032
2S	75%	0.01429	0.00345	0.00187	0.00680	0.00311	0.00188
	100%	0.03765	0.01701	0.00450	0.02543	0.01638	0.00724
	125%	0.07417	0.04288	0.01750	0.04969	0.03558	0.02096
	150%	0.24986	0.15104	0.06873	0.21465	0.10079	0.05699
3S	75%	0.00152	0.00127	0.00090	0.00158	0.00097	0.00049
	100%	0.00376	0.00218	0.00176	0.00326	0.00236	0.00164
	125%	0.01529	0.00902	0.00279	0.01341	0.00712	0.00421
	150%	0.04083	0.03034	0.00937	0.03334	0.02640	0.01838
4S	75%	0.00332	0.00190	0.00134	0.00165	0.00172	0.00175
	100%	0.01269	0.00563	0.00244	0.00361	0.00580	0.00520
	125%	0.03219	0.02447	0.00713	0.01271	0.02075	0.02036
	150%	0.06683	0.05776	0.01953	0.03541	0.04853	0.04659
5S	75%	0.00126	0.00112	0.00076	0.00140	0.00141	0.00110
	100%	0.00189	0.00177	0.00137	0.00244	0.00332	0.00187
	125%	0.00942	0.00452	0.00200	0.01017	0.01499	0.00759
	150%	0.02689	0.01755	0.00329	0.03406	0.03425	0.03028
6S	75%	0.00178	0.00137	0.00109	0.00150	0.00132	0.00113
	100%	0.00642	0.00204	0.00190	0.00415	0.00284	0.00215
	125%	0.02163	0.00915	0.00323	0.01628	0.01319	0.00910
	150%	0.04799	0.02955	0.00911	0.03942	0.03223	0.02922
7S	75%	0.00159	0.00135	0.00092	0.00160	0.00140	0.00124
	100%	0.00329	0.00215	0.00160	0.00525	0.00335	0.00259
	125%	0.01451	0.01098	0.00257	0.01872	0.01541	0.00807
	150%	0.03987	0.03238	0.00851	0.04636	0.04096	0.02690
8S	75%	0.00162	0.00149	0.00134	0.00154	0.00106	0.00059
	100%	0.00387	0.00339	0.00277	0.00407	0.00243	0.00158
	125%	0.01690	0.01528	0.01066	0.01612	0.00684	0.00332
	150%	0.04019	0.03653	0.02766	0.04088	0.02560	0.01352
9S	75%	0.00129	0.00110	0.00072	0.00207	0.00174	0.00151
	100%	0.00207	0.00178	0.00129	0.00841	0.00630	0.00387
	125%	0.01140	0.00698	0.00196	0.02662	0.02184	0.01958
	150%	0.03106	0.02321	0.00373	0.06473	0.05138	0.04844
10S	75%	0.01253	0.00783	0.00210	0.00703	0.00380	0.00184
	100%	0.03730	0.02768	0.00920	0.02789	0.01708	0.00750
	125%	0.07189	0.05973	0.02640	0.05278	0.03636	0.01851
	150%	0.23078	0.19175	0.09182	0.19842	0.09676	0.04984

Table 5-17. Distortion (web thickness changes – inches) at mid-height of ducts.

Model #	Percent Capacity	Web A Duct 2	Web A Duct 4	Web A Duct 6	Web B Duct 2	Web B Duct 4	Web B Duct 6
1S	75%	0.0126	0.0104	0.0026	0.0128	0.0247	0.0095
	100%	0.0351	0.0297	0.0053	0.0442	0.0630	0.0316
	125%	0.0732	0.0666	0.0179	0.0987	0.1464	0.0876
	150%	0.1398	0.1446	0.0673	0.1702	0.3469	0.2093
2S	75%	0.0169	0.0278	0.0064	0.0472	0.0849	0.0226
	100%	0.0635	0.0779	0.0303	0.1207	0.2037	0.0671
	125%	0.1959	0.2289	0.1114	0.2546	0.4035	0.1122
	150%	0.4625	0.4472	0.2166	0.4946	0.7850	0.2093
3S	75%	0.0165	0.0084	0.0031	0.0051	0.0108	0.0034
	100%	0.0348	0.0277	0.0092	0.0176	0.0455	0.0137
	125%	0.0658	0.0512	0.0196	0.0374	0.0875	0.0412
	150%	0.1347	0.1356	0.0813	0.1102	0.2152	0.1084
4S	75%	0.0245	0.0141	0.0039	0.0339	0.0496	0.0332
	100%	0.0569	0.0392	0.0132	0.0928	0.1219	0.0903
	125%	0.1079	0.0971	0.0463	0.1995	0.2876	0.2064
	150%	0.2377	0.2341	0.1441	0.4056	0.5930	0.4169
5S	75%	0.0077	0.0094	0.0031	0.0112	0.0223	0.0087
	100%	0.0247	0.0212	0.0058	0.0356	0.0521	0.0250
	125%	0.0459	0.0462	0.0133	0.0862	0.1145	0.0600
	150%	0.0734	0.0898	0.0346	0.1594	0.3204	0.1824
6S	75%	0.0158	0.0129	0.0021	0.0106	0.0235	0.0048
	100%	0.0366	0.0328	0.0077	0.0406	0.0632	0.0175
	125%	0.0935	0.0748	0.0302	0.0965	0.1555	0.0424
	150%	0.1985	0.2021	0.1147	0.2057	0.3781	0.1055
7S	75%	0.0106	0.0093	0.0026	0.0104	0.0217	0.0075
	100%	0.0213	0.0237	0.0053	0.0274	0.0479	0.0153
	125%	0.0425	0.0405	0.0085	0.0573	0.0939	0.0261
	150%	0.0567	0.0824	0.0253	0.1254	0.2166	0.0563
8S	75%	0.0936	0.0157	0.0069	0.0106	0.0173	0.0052
	100%	0.0207	0.0273	0.0164	0.0246	0.0503	0.0127
	125%	0.0413	0.0574	0.0461	0.0442	0.0872	0.0250
	150%	0.0735	0.1541	0.0933	0.0922	0.1443	0.2584
9S	75%	0.0057	0.0095	0.0032	0.0390	0.0227	-0.0218
	100%	0.0189	0.0190	0.0062	0.0298	0.0480	0.0126
	125%	0.0345	0.0361	0.0139	0.0630	0.1241	0.0217
	150%	0.0386	0.0645	0.0274	0.1379	0.3115	0.0543
10S	75%	0.0132	0.0250	0.0064	0.0399	0.0661	0.0072
	100%	0.0124	0.0600	0.0154	0.0800	0.1449	0.0163
	125%	0.0751	0.1321	0.0279	0.1604	0.2918	0.0202
	150%	0.1939	0.2563	0.0306	0.2885	0.5176	0.0376

Table 5-18. Force at stirrup yield (0.2% strain).

	Total Force (K/ft)	
Model #	Web 1	Web 2
1S	25.83	28.18
2S	16.05	17.88
3S	26.21	28.6
4S	20.1	26.17
5S	31.18	28.77
6S	24.16	28.04
7S	26.21	26.64
8S	26.12	27.95
9S	29.87	23.78
10S	16.09	18.38

to the top slab, and the positive moment reinforcement is approximately 2 times that of the negative moment reinforcement.

- **Cover Thickness.** Inside face duct cover influences lateral pullout resistance, but is not the only driver of pullout resistance. The results of the parameter studies are influenced by the fact that when the cover is reduced, for the same overall web thickness, the moment arm for the stirrups is increased, which is an offsetting influence on pullout resistance. It appears appropriate to check cover concrete thickness for resistance to initial cracking, but not to include cover concrete tensile strength in calculating regional transverse bending strength.
- **Number and Configuration of Tendon Ducts.** When ducts are spread apart, the performance significantly improves. Roughly 20% resistance force improvement was demonstrated by separating the 5-duct bundle into two bundles, and an additional 4% improvement was demonstrated by spreading the bundles farther apart (4.5 inches versus 1.5 inches of separation). It is believed prudent to require a maximum of 3 ducts per bundle. When individual ducts were separated and moved toward the curve's outside face of the web, performance further improves. When measured by the delamination/local-lateral shear criteria, Duct Configuration 3A exceeded 200% P_c, so the improvement in delamination performance was very large. However, it is often impractical for designers to spread individual ducts apart due to lack of space in the web and due to requirements on location of the C.G. of the tendon group.
- **Number and Configuration of Duct Ties** contribute significantly to resistance to lateral tendon breakout.
- **Stirrups.** Regional transverse bending strength is directly tied to stirrup area, but it controls the design only when web/duct tie reinforcement is NOT used or when the web-splitting/lateral shear-failure does not occur. In other words, if the failure mode is tending toward local duct breakout, stirrups are not a very effective deterrent against this failure mode. But if the duct layout and duct ties are properly detailed to eliminate the local pullout failure mode, the stirrup spacing does define the web "regional" beam strength.
- **Concrete Material Properties, Especially Assumed Tensile Strength.** Web section strength can be significantly influenced by concrete tensile strength only when the section is prone to web-splitting/local-lateral shear-failures, i.e., when vulnerable duct placement is used or web/duct tie reinforcement is NOT used. When web/duct tie reinforcement is used, concrete tensile strength has little effect on the section strength. Thus designers should be directed toward design rules that will ensure good performance, regardless of variabilities in concrete tensile strength.

Recommendations for Web Capacity Design

Web capacity design for lateral tendon force resistance should be a three-step calculation: Regional flexure check, local-lateral shear/breakout check, and cover concrete cracking check

Regional Transverse Bending

The regional mechanism is the web acting as a vertical beam loaded laterally near its center. Fundamentally, the calculation follows the equation:

M_u = (Load Factor)(Moment Fixity Factor)(¼)(Pj/R) h_c

This equation (a modified version of the Caltrans Equation) and the corresponding stirrup spacing should be evaluated for each web of a box-girder separately—not for the total box divided by the number of webs. The radius is different for each web, and it was found that the moment fixity factor is also different. AASHTO LRFD currently applies a load factor of 1.2 to the Pjack tendon force, which is judged to be reasonable. Appropriate moment fixity factors are 0.6 for interior webs and 0.7 for exterior webs.

The stirrup sizing and spacing should then be calculated using Ultimate Strength design such that

$$\phi M_n \geq M_u$$

Table 5-19. Effect of cover thickness – thick webs.

Model-Web	Force at Stirrup Yield (kips)	Difference
6S-1 vs. 1S-1	24.16 vs. 25.83	7% increase with 3" vs. 2"
6S-2 vs. 1S-2	28.04 vs. 28.18	0% increase with 3.5" vs. 2"

Table 5-20. Effect of duct ties – thick webs.

Model-Web	Force at Stirrup Yield (kips) (and delamination at 100%P_c)	Difference
7S-1 vs. 1S-1	26.21 vs. 25.83	2% incr. with Duct ties
	(0.024" vs. 0.035")	(31% less delamination)
7S-2 vs. 1S-2	26.64 vs. 28.18	-5% change with Duct ties
	(0.048" vs. 0.063")	(24% less delamination)
8S-2 vs. 3S-2	27.95 vs. 28.60	-2% change with Duct ties
	(0.050" vs. 0.046")	(little change in delamination)
9S-1 vs. 5S-1	29.87 vs. 31.18	-4% change with Duct ties
	(0.019" vs. 0.025")	(24% less delamination)

However, the V_s stress in the stirrups due to vertical shear in the web should be added to the stress due to flexure in the sizing and spacing of the stirrups. At the midheight of the web, on the inside-curve side of the web, these stresses are directly additive.

Local Lateral Shear Check

The local lateral shear mechanism involves the complex behavior that develops in the concrete and stirrup region immediately adjacent to the duct bank. This may be checked by the following equations developed by the University of Texas (Van Landuyt, 1991):

For a strip of web 1 foot long, the applied lateral shear demand along a plane d_{eff} long is

$$V_d = P_j/R \div 2$$

V_c capacity of the cover-beam along this plane may be taken as

$$V_c = \phi 24 d_{eff} \sqrt{f_c'}$$

Where $\phi = 0.75$ (reduced due to uncertainties in concrete quality within the cover-beam)

When the spacing between ducts is greater than or equal to the duct diameter

$$d_{eff} = d_c + (Duct\ Diam.)/4 + \sum s/2$$

or

$$d_{eff} = t_w - (Duct\ Diam)/2$$

whichever is least.

where

s = space between ducts (assume 0 if s < 1.5" or for single ducts)
t_w = thickness of web

When the spacing between ducts is less than the duct diameter or for single ducts

$$d_{eff} = d_c + (Duct\ Diam)/4$$

where d_c = cover over the ducts

Figure 5-24 shows what is intended by the above equations for d_{eff}.

There has been discussion within the industry as to selecting d_{eff} (some refer to this as the "lateral shearing plane depth"). Some say this should be no greater than d_c (the cover concrete depth) due to uncertainties in the concrete interaction with the ducts, but the local analyses conducted here allow for the extra width of ¼ of a duct diameter.

If this lateral shear is exceeded, the most effective design remedy is the addition of duct-tie reinforcement.

Table 5-21. Effect of stirrup spacing – thick webs.

Model-Web	Force at stirrup yield (kips)	Difference
4S-1 vs. 1S-1	20.1 vs. 25.83	29% increase with 50% more stirrup steel
5S-1 vs. 1S-1	31.18 vs. 25.83	21% decrease with 33% less stirrup steel
9S-1 vs. 7S-1	29.87 vs. 26.21	14% decrease with 50% less stirrup steel
9S-2 vs. 7S-2	23.78 vs. 26.64	21% increase with 50% more stirrup steel

Table 5-22. Effect of material strength – thick webs.

Model-Web	Force at stirrup yield (kips)	Difference
3S-2 vs. 1S-2	28.60 vs. 28.18	2% increase with 50% larger concrete tensile strength
4S-2 vs. 1S-2	26.17 vs. 28.18	7% decrease with 50% smaller concrete. strength
8S-1 vs. 7S-1	26.12 vs. 26.21	0% change with 50% smaller concrete. strength
8S-2 vs. 7S-2	27.95 vs. 26.64	5% increase with 50% larger concrete. strength

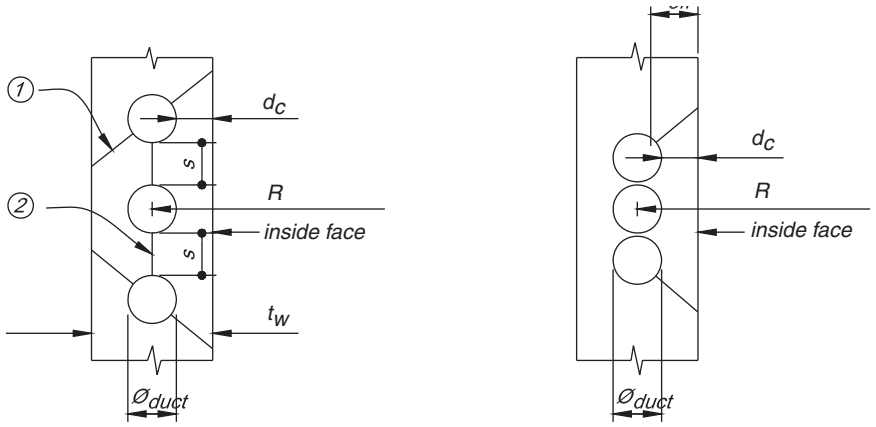

For "s" ≥ $\varnothing_{duct}$

d_{eff} = lesser of:

① $d_{eff} = t_w - \frac{\varnothing_{duct}}{2}$

② $d_{eff} = d_c + \frac{\varnothing_{duct}}{4} + \frac{\Sigma_s}{2}$

For Single Ducts or for "s" < $\varnothing_{duct}$

$$d_{eff} = d_c + \frac{\varnothing_{duct}}{4}$$

Figure 5-24. Definition of d_{eff} (after Van Landuyt, 1991).

Cover Concrete Cracking Check

Evaluating the cracking of the cover concrete is a check that is made to ensure serviceability because it is recommend that the lateral tendon forces be completely carried by the strength elements of the above two checks. But this serviceability check remains critical to achieving a good design, because significant cover cracks running along the tendons should be avoided for long-term structure durability.

The flexure on the cover beam involves a complex mechanism because it is uncertain what the level of adhesion is of the cover concrete to the duct bank and to the concrete surrounding the duct bank. Assuming there is no adhesion between the metal duct and the web concrete in the radial direction of the duct, the flexure calculation proceeds as follows. The cover-beam acts as a vertical beam "built-in" or fixed at top and bottom. Thus the following moments are produced:

$$M_{ends} = \frac{wL^2}{12} = (\mathrm{Pj/R}/L)L^2/12$$

$$M_{center} = \frac{wL^2}{24}$$

L is the height of the duct bank

$$\mathrm{I} = \frac{bd_c^3}{12}$$

and $\phi M_n \geq M_u$

Where M_n is defined by an allowable tensile stress for concrete of $5\sqrt{f_c'}$, and $\phi = 0.55$. The allowable tensile stress should also be reduced by the tensile stress in the concrete at the critical point due to regional transverse bending. Although this may appear quite conservative in terms of choice of tensile strength and choice of ϕ, once cracking begins within the interior of the cover concrete near the top and bottom of the duct bank, the moment at the center of the duct banks quickly becomes

$$M_{center} = \frac{wl^2}{8}$$

So these factors and conservative tensile strengths are judged appropriate to prevent this progressive cracking mechanism from occurring.

Other Local Detailing Guidelines

A further guideline, which has come out of the local analysis work and from examination of some local breakout failures in various bridges and test structures, is to limit the number of ducts of a sub-bundle to no more than three. Sub-bundles should then be separated by either a duct-tie rebar or by a minimum of ⅓ of one duct diameter (for example, 1½ inches for the analyses performed here).

Duct ties should be well anchored with hooks around stirrup reinforcement. A generic duct tie detail is shown in Figure 5-25.

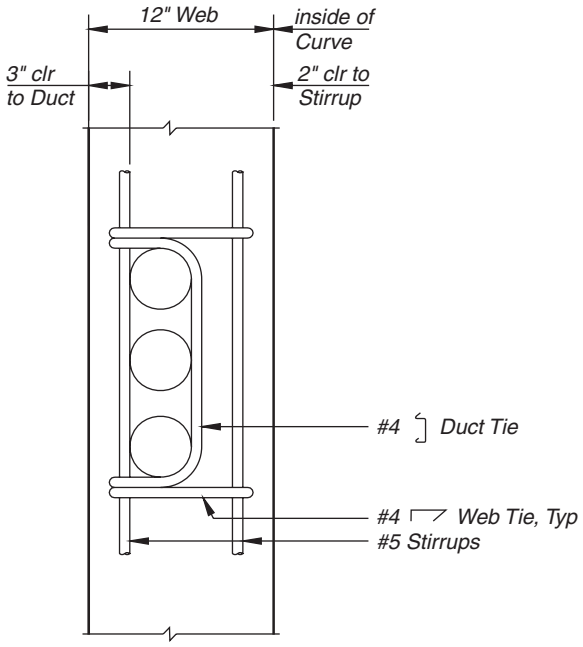

Figure 5-25. Generic web and duct tie detail.

Construction Tolerances

Designers should consider the practical aspects of construction tolerances when checking and implementing their designs. Construction tolerances should be held to industry standards—it is not the point of this design recommendation to modify these, but designers may wish to consider conservatively allowing for field variations in web width and in rebar placement of up to ±0.5 inch when evaluating issues of web regional transverse bending strength, local breakout resistance, and, particularly, cover-beam strength. Dimensional changes of 0.5 inch can make considerable difference in the stresses in the web concrete and reinforcing steel.

The following is an example of how design and construction issues can affect conditions for lateral tendon breakout. As a box-girder gets deeper, the stirrup cage gets deeper. As the stirrup cage gets deeper, it becomes more flexible laterally, especially in areas of low lateral shear demand where designers often specify stirrup spacing as large as 24 inches. During the web and soffit pour, the stirrup cage has been shown to deflect laterally within the web form due to unbalanced concrete placement, vibration process, and duct float. Duct float, in combination with sloped exterior webs, can often lead to a substantial reduction in concrete cover between the stirrup cage and the interior face of the web. This may be mitigated somewhat by rebar spacer requirements at midheight of webs to help control stirrup movement during the pour, but the designer should be aware of possible variations in the actually constructed dimensions.

Several conditions can aggravate the chances for lateral tendon breakout, including

1. Reduction of cover over the duct or rebar, which can affect resistance to breakout.
2. Excessive wobble of the ducts, which can result in either reduced resistance to breakout or locally elevated lateral forces.
3. Out-of-plane forces in a vertically curved tendon due to wedging of the stand.
4. Pressure from grout leakage due to poor quality duct (excessive flexibility), damaged duct, or improperly sealed duct.
5. Distortion of empty ducts acted on by adjacent stressed ducts.
6. Local curvature in ducts near anchorage zones or blisters

The specified load and resistance factors (1.2 and 0.75) reflect the assumption that construction tolerances are reasonably well controlled. If this may not be the case, the designer may wish to consider one of the following three options.

1. Use higher load factors and/or lower resistance factors. Some engineers familiar with the potential problems have recommended ϕ factors be reduced from 0.75 to 0.55 for local lateral shear failure. Load factors could also be raised above 1.2 to say 1.5.
2. Use dimensions that include an allowance for misplacement of the duct, rebar, or forms. As suggested above, critical dimensions could be reduced by 0.5 inch or even 1.0 inch
3. When in doubt, provide web and duct tie reinforcement

Tendon breakout failures can be expensive to repair. Although the recommended design specifications should provide an adequate factor of safety in most cases, the designer is ultimately responsible for assessing the likely conditions in the field.

CHAPTER 6

Conclusions

Several critical issues relative to the design of concrete box-girder bridges were identified at the beginning of the project. Methods exercised in this study that were intended to address these issues consisted of a survey of the state of practice, a review of published literature, analytical studies of global and local response, discussions of the experienced research team that attempted to reach a consensus on critical design requirements, and a review by an advisory panel with expertise in this area of study.

Several conclusions were drawn from the research conducted in this project. In many cases, these conclusions have translated into recommended AASHTO LRFD Specification provisions as presented in Appendix A. Analysis guidelines were also developed to assist designers in performing response analysis. These are provided in Appendix C. Other conclusions found that current design practice was adequate and did not require a change. The following paragraphs discuss conclusions relative to the critical issues defined at the beginning of the project.

- **Applicability.** Curved concrete box-girder bridges are used throughout the United States. Most modern bridges of this type are prestressed. A review of the state of practice in the United States found that both single- and multi-cell box-girder bridges are widely used. The predominate construction type in some West Coast states is multi-cell box-girder bridges cast-in-place on falsework. This type is also widely used throughout the United States. Single-cell box-girder bridges are also common, but tend to dominate the type of box-girder construction used on the East Coast. East Coast construction also uses more precast segmental construction than is used on the West Coast where cast-in-place construction is more dominant, even when segmental methods are used. Some states do not use this type of bridge on a regular basis. Curved spread box beams are an emerging structure type, but are not widely used at this time.

  Both single- and multi-cell concrete box-girder bridges are covered by this project. They may be cast-in-place or precast and may be constructed segmentally or on falsework.
- **Appropriate levels of analysis and design.** Selecting the type of global analysis that should be used for curved concrete box-girder bridges is one of the most important issues addressed by this project. Published research shows that these types of bridges are most accurately analyzed using 3-D finite element or similar techniques. Unfortunately, these analysis methods are tedious and in general not practical for production design work. Also, in many cases, more simplified analysis methods will produce acceptable results. To determine the range of applicability of various analysis methods, a detailed global analysis study was undertaken.

  The first step was to identify a more simplified 3-D analysis approach that would yield results comparable to the more detailed finite element technique. This was accomplished with the grillage analogy approach. In this method, the bridge is simulated as a grillage of beam elements in the longitudinal and transverse direction. Guidelines for preparing the computer model, performing the analysis, and interpreting results were developed and are included in Appendix C. From the designer's point of view, this analysis method has advantages over the finite element approach. Besides being a smaller and less computationally intense analytical model, the grillage analogy produces results in terms of the structural members commonly considered by the designer. This makes it easier to design these elements, whereas the finite element approach would involve considerable post processing of analytical results to accomplish the same goal.

  Second, the limits of applicability of three analytical approaches were assessed. The three methods considered were
  1. Plane Frame Analysis. This allows the bridge to be analyzed as if it were straight.
  2. Spine Beam Analysis. This is a space frame analysis in which the superstructure is modeled as a series of

straight, chorded beam elements located along the centerline of the superstructure.

3. Full 3-D Analysis. This includes several different sophisticated approaches that include the grillage analogy described above as well as the finite element and other sophisticated approaches.

Extensive parameter studies were performed that included the effects of structural framing (simply supported or continuous), span lengths, radius of curvature, cross section (including bridge width), and bearing configuration on the response of bridges. These studies included both grillage analysis and spine beam analysis for which plane frame analysis constituted the case of a bridge with a very large radius. These studies showed that the radius-to-span length ratio as represented by the central angle between two adjacent supports was the dominant parameter that determined the accuracy of the various analysis methods. The span length-to-width ratio (aspect ratio) of the superstructure also had a minor effect. Based on these parameter studies, the following limits for the various types of analysis are recommended:

1. For central angles less than or equal to 12 degrees, plane frame analysis is acceptable.
2. For central angles between 12 and 46 degrees and an aspect ratio above 2.0, spine beam analysis is required.
3. For central angles between 12 and 46 degrees and an aspect ratio less than 2.0, sophisticated 3-D analysis is required.
4. For central angles greater than 46 degrees, sophisticated 3-D analysis is required.
5. For all bridges with otherwise unusual plan geometry, sophisticated 3-D analysis is recommended.

- **Section properties and member stiffness.** The section properties and member stiffnesses that should be used in the spine beam analysis and the grillage analogy analysis are critical and are discussed in the analysis guidelines presented in Appendix C. For the spine beam analysis, the cross-sectional area and the three rotational moments of inertia are important. In the case of the grillage analogy, all six section properties of each beam member are required. Special formulae for some of these section properties are used to simulate various aspects of the behavior of a curved concrete box-girder bridge. This in turn requires special interpretation of some of the results.
- **Critical position of live loads.** The number and position of the live load lanes in the transverse direction as well as their position along the longitudinal axis of the bridge are critical for curved concrete box-girder bridges. Given the number of possible load positions, it will be desirable to use the live load generating capabilities of sophisticated commercially available software to rigorously envelope the live load response. This can be a daunting task if such software is not used. Fortunately, the whole-width design approach as described in the LRFD specifications was shown to yield conservative results when used in conjunction with the plane or spine beam approaches. This will greatly simplify the effort of the designer in determining live load response. When using this approach, it is important to distinguish between the longitudinal response along each of the webs and the effect of torsion across the whole section. When torsional response is being assessed by the whole-width design approach, the number of live load lanes should be reduced to the actual number of lanes that can fit on the cross-section and adjusted by the multiple presence factor and dynamic load factor (for truck loading only).

  When a 3-D model of the bridge (either a spine beam or grillage analogy model) is being used, it is important to consider the transverse position of prestress tendons. The length of the various tendons will have an effect on friction losses and tendons will also produce a transverse response in the bridge superstructure.

  Vehicular effect may be assessed using the method prescribed in the LRFD Bridge Design Specifications. Other load conditions such as centrifugal forces, breaking or acceleration forces, wind, etc. should be determined according to the LRFD Specifications and then applied to the spine beam model. If the plane frame approach is being used, these loads may be analyzed in the same manner as if the bridge were straight. The effect of bridge superelevation can usually be ignored.
- **Torsion design.** The design of concrete box sections for torsion is covered in the current AASHTO LRFD Specifications. However, some clarification of these requirements is in order. These were discussed in the review of published literature included in Chapter 3.

  Torsion demands usually translate to additional lateral shear demands in the webs of concrete box-girders. These may be determined from both the spine beam and grillage analogy methods.

  In the case of the spine beam analysis, the torsion demands are taken directly from the torsion forces generated in the spine beam. These forces must be transformed into shear flow around the perimeter of the box section. This shear flow will increase the effective shear in one web while decreasing it in another. Webs should be designed for the combined flexural and torsional shear.

  In the case of the grillage analogy, the effects of torsion on web shear are partially accounted for because each web is explicitly included in the analytical model. However, because of the way torsional stiffness of the superstructure is distributed to the individual longitudinal members of the grillage model, the total effect of torsion on the entire cross section is not completely accounted for by the longitudinal member shear demands. To correct for this deficiency, it is

necessary to consider the torsional forces in each of the longitudinal members at a given longitudinal location in the grillage model and apply the sum of these torsions to the entire cross section to obtain residual shear flow about the perimeter of the section. This is done in a manner similar to that used for the spine beam. When this residual shear flow is combined with the flexural shear in the extreme longitudinal members, the correct demands to be used for web shear design are obtained.

The procedures to be used for torsion design for both the spine beam and grillage analogy analysis methods are illustrated in the example problem included in Appendix B.

- **Tendon breakout.** Extensive analytical studies were performed to investigate lateral bursting stresses in curved concrete box-girder bridges with internal prestress tendons. The first step in these studies was to verify that the nonlinear finite element models used could accurately predict lateral tendon breakout behavior observed in experimental studies performed at the University of Texas. The results of the analyses compared well with the experimental results so that there is confidence that both the experimental and analytical results have yielded accurate results.

  Based on parameter studies conducted using these verified nonlinear finite element techniques and the results of the University of Texas studies, modifications to the specifications for considering in-plane force are recommended. These include

  1. *A method for assessing the local lateral shear resistance to pullout.* These provisions are the recommendations from the University of Texas, which were further verified by the nonlinear finite element parameter studies conducted as part of this study. They also include provisions for considering the effect of construction tolerances, which have been shown by past failures to have a significant effect on web performance and are discussed in Chapter 5.
  2. *A method for checking flexural cracking of the unreinforced concrete cover over the inside of the prestress tendons.* This is a new requirement that applies only to vertically stacked tendons. It is included to prevent maintenance, architectural, and structural problems that can arise due to longitudinal cracking of the web. The results are used to determine the need for web and duct tie reinforcement. Vertical duct stacks are limited to three tendons high and concrete cover over the inside of the ducts should be maximized. Generic web and duct tie reinforcement details are included in the commentary.
  3. *A method for calculating the regional transverse bending moments within a web*. These moments result from the regional transverse bending of a web between the top and bottom slab of the bridge due to lateral prestress forces. When combined with global forces such as flexural shear and torsion, regional transverse bending can result in the need for more stirrup reinforcement in the webs. Regional transverse bending also exacerbates flexural cracking of the concrete cover as described in Item 2 above.

- **Consideration of stresses at critical locations.** Several critical stresses should be considered in the design of curved concrete box-girder bridges. These include

  1. *Axial stresses in the top and bottom slabs and the webs.* These stresses result from vertical flexure of the bridge between supports and the primary and secondary effects of longitudinal prestressing. Regional transverse bending of the superstructure may also occur and should be considered when determining these stresses. Because the web lengths vary in a curved bridge, moments and flexural shears in each web may also vary. This effect is best captured in the grillage analogy approach. To best capture it with the spine beam approach, prestress tendons should be located at their correct transverse positions with respect to the bridge centerline.
  2. *Shear stresses in the webs.* These stresses result from the flexural and torsional behavior of the superstructure. Torsion results in shear flow around the perimeter of the cross section that should be combined with the flexural shear. In continuous superstructures or between the joints in precast superstructures, these shear forces result in diagonal tension stresses that can combine with the flexural tensile stresses resulting from regional transverse bending. Stirrup design may be accomplished by combining the reinforcing requirements for each of these actions. At the joints in precast bridges, the shear is carried by a shear friction mechanism.
  3. *Transverse stresses in the cross section.* These stresses can generally be determined using the same methods used for a straight bridge. They govern the design of the deck and soffit. The transverse deck and soffit reinforcing must also participate in carrying the shear flow generated by torsion, but because concrete is often sufficient for this purpose, this is often not a significant consideration in design.
  4. *Flexural and lateral shear stresses in the vicinity of prestress tendons.* Complex stresses are developed in the webs of curved concrete box-girders due to the lateral forces developed by the curvature of prestress tendons. Simplified methods for assessing these effects have been developed and are included in the recommended LRFD specifications and commentary.

  Because design for the above forces is often optimized, it is prudent to evaluate these forces at several longitudinal locations along the length of the bridge. Prestress forces and path location, web and slab thicknesses, and the size and spacing of stirrups can be designed accordingly.

- **Bearing load and bearing movement considerations.** Both the spine beam and grillage analogy methods of analysis will accurately predict elastic bearing forces if used according to the criteria outlined in the proposed AASHTO LRFD Bridge Design Specifications and Commentary and the Analysis Guidelines included in Appendix C. Because of the curvature of the structure, the bearing forces at any longitudinal position along the bridge will vary across the width of the bridge.

  In addition to this, both field experience and time-dependent analysis show that the bearing forces will change over time. The extent of this change is not accurately determined by currently available time-dependent software because of the treatment of torsion creep in these programs, but software that takes into account axial creep is thought to give conservative results. In lieu of a time-dependent analysis, elastically determined abutment dead load torsions should be increased by 20%. It is recommended that bearing force capacities be designed to accommodate both initial and long-term conditions.

  Methods for addressing bearing design when bearing forces are excessive (i.e., either too high or too low) may include, but not be limited to, one or more of the following:
  1. Size individual bearings to accommodate the calculated range of bearing forces.
  2. Specially design bearings so that they will not be displaced if the applied load goes into tension or very low compression.
  3. Provide ballast in the superstructure to ensure that the envelope of bearing forces is within an acceptable range.
  4. Reshore the structure at its bearing locations prior to setting the bearings and then release the shoring after the bearings are set.
  5. Use an outrigger diaphragm to increase the eccentricity of the individual bearings.
  6. Place the bearing group eccentric to the centerline of the superstructure in order to make the individual bearing forces more equal.
  7. Select bridge framing to better control bearing forces. Balancing the center and end span lengths can mitigate bearing problems.

  Considering the curvature of long bridges in a spine beam analysis can mitigate excessive design movements at the bearings due to temperature change and possibly eliminate the need for interior expansion joints. Care should be taken that bearing travel is through the center of movement so that binding of the shear keys does not occur. Prestress shortening may occur along a slightly different orientation.
- **Diaphragms.** Current AASHTO LRFD provisions require that diaphragms be used for curved box-girder bridges with a radius of less than 800 feet, but also allows that they be omitted if justified by analysis or tests. Analytical grillage analogy and finite element studies performed as part of this project demonstrated that interior diaphragms have a minimal effect on the global response of a curved concrete box-girder bridge with a 400-ft radius and 300-ft span lengths. Therefore, it is proposed that the requirement that interior diaphragms be included in bridges with a radius less than or equal to 800 feet be eliminated. It is recommended that end diaphragms still be used at all supports.
- **Post-tensioning sequence.** Because the curvature of tendons can increase the transverse bending of the super structure and result in tensions on the inside of the curve and compression on the outside of the curve, it is recommended that at least one tendon on the inside of the curve be stressed first.

  With respect to varying the final distribution of prestress forces across the width of the bridge, there does not seem to be any significant advantage in doing this. Although webs to the inside of the curve are shorter and thus theoretically subject to less dead load and live load bending forces, decreasing prestress forces for this web will be overcome by the transverse bending of the bridge that will put the inside web in tension. Thus it is thought to be important to model tendons in their correct transverse position for analysis, but a relatively even distribution of prestress forces is desirable. It is theoretically more important for the designer to consider the incidental distribution of prestress forces as allowed by some construction specifications.
- **Skew effects.** Analytical studies were performed to consider the effect of skew at the abutments on the overall response of the bridge. It is commonly known that skew will affect the shears in the web near the obtuse corner of a skewed abutment support. The point of the study was to determine if bridge curvature altered the relationship between the relative response of a skewed and non-skewed abutment. Two skew cases were studied. One case was where the skew occurred at only one of the abutments and the other case was where both abutments were skewed but in opposite directions. The second case is the likely orientation of a curved bridge that crosses over an obstruction that is linear in orientation. In both cases, it was found that the relationship between the response of a non-skewed support and the skewed support followed the same relationship as for a straight bridge. Thus, it was concluded that existing skew correction factors apply to curved concrete box-girder bridges analyzed by the spine beam method.

  The effect of skew on interior supports was not studied nor were the effects of different abutment skew configurations. In all cases, a grillage analogy analysis would capture any effect of skew. This method should be used to analyze any curved concrete box-girder bridges with large skew angles at the interior supports or abutment skew configurations that vary significantly from those studied.

- **Lateral restraint issues.** Horizontal curvature may result in force demands in the lateral direction at the supports if lateral restraint is present and is modeled as rigid elements for computer analysis. Such may be the case for supports consisting of integrally cast abutments or piers. In these cases, lateral restraint should be modeled as the stiffness of the restraining element under consideration. In the case of bearings, however, steel or concrete shear keys usually provide lateral restraint. These are usually provided with a small transverse gap to prevent binding. This gap is large enough to prevent lateral restraint and, for gravity load purposes, should be modeled as a lateral force release. The key to properly considering lateral restraint is to accurately model the actual condition and to use either spine beam or grillage analogy analysis.
- **Thermal effects.** Thermal movement and prestress shortening will result in movements in different directions at the expansion joints in curved structures. This difference should be reflected in a properly conducted spine beam or grillage analysis. Bearings should be capable of travel through the center of movement, although normal gaps provided in shear keys will allow for slight variations in movement.
- **Time-dependent effects.** Because of the interaction between bending moment and torsion in curved bridges, consideration of time-dependent effects is important. However, rigorous 3-D analysis to determine the time-dependent effects of torsion is not present in commercially available software. This requires a reliance on the time-dependent software available. Fortunately, torsion creep is expected to mitigate the effect that has been observed at the bearings, and thus this software will tend to yield conservative results for bearing force redistribution. It can be used for design purposes until improved software is developed.

  Vertical construction cambers can use the results from currently available time-dependent software. In fact, many design engineers interviewed claim to have had good results from 2-D time-dependent analysis. However the bending of tall columns and twisting of the superstructure had to be approximated using elastic 3-D spine beam analysis.

  In the case of curved bridges, horizontal cambers may be required for segmental construction. A curved concrete box-girder bridge with relatively tall piers in California that was constructed by the segmental cantilever method required a horizontal camber of approximately 3 inches at the pier. In other words, the pier had to be constructed 3 inches out of plumb.
- **Construction methods.** The effect of construction methods on the behavior of curved box-girder bridges is critical. However, the analysis methods studied apply to staged construction analysis as well as cast-in-place on falsework construction. The same parameters can be used to select the most appropriate analysis method except that time-dependent analysis should be used. Commercially available software does not consider torsion creep, but should yield generally conservative results and is adequate for design until more sophisticated software is developed.
- **External post-tensioning deviators.** The use of precast construction results in less weight and quicker onsite assembly and is thus increasing in popularity. Deviation blocks or saddles for external prestress tendons in curved precast concrete box-girder bridges may be designed in the same manner as for straight bridges using strut-and-tie methods or as recommended by an experimental study at the University of Texas (Beaupre et al., 1988). For LRFD design of deviators, a load factor of 1.7 should be used for the prestress deviator force and capacity reduction (ϕ) factors should be 0.9 for direct tension and flexure and 0.85 for shear. It is recommended that reinforcing bar sizes in deviation saddles be limited to #5s to ensure the proper development of this reinforcement.

  It is recommended that deviation saddles in tightly curved bridges be continuous across the bottom soffit. Another consideration for curved bridges is that straight segments of tendons cannot rub against the interior of the webs. If necessary, the designer should include extra deviation blocks or saddles to prevent this from happening. A deviation saddle design example, which is reproduced from the University of Texas report, is included in Appendix B.
- **Friction loss/wobble.** The current formulae for determining prestress losses due to friction and wobble apply to curved bridges if the 3-D effects of angle change and tendon length are considered. It is necessary to explicitly consider the difference in tendon length in individual webs and thus prestress tendons should be modeled in their actual transverse location in a 3-D spine beam or grillage analogy analysis. Friction losses should be based on a tendon curved in space when a curved bridge is being designed using 2-D analysis techniques.
- **Web and flange thickness limits.** It is recommended that webs and flanges be designed based on structural and constructability considerations. No minimum thickness requirements are recommended by this study.

References/Bibliography

Al-Rifaie, W. N., and Evans, H. R. (1979) *An Approximate Method for the Analysis of Box-girder Bridges that are Curved in Plan*, Proc., International Association of Bridges and Structural Engineering (IABSE), pp. 1–21.

AASHTO (1996) *Standard Specifications for Highway Bridges*, 16th Edition with Interims, American Association of State Highway and Transportation Officials, Washington, D.C.

AASHTO (1999) *Guide Specifications for Design and Construction of Segmental Concrete Bridges*, 2nd Edition with Interims, American Association of State Highway and Transportation Officials, Washington, D.C.

AASHTO (2003a) *Guide Specifications for Horizontally Curved Steel Girder Highway Bridges*, American Association of State Highway and Transportation Officials, Washington, D.C.

Abendroth, R. E., Klaiber, F. W., and Shafer, M. W. (1995) "Diaphragm Effectiveness in Prestressed-Concrete Girder Bridges," *Journal of Structural Engineering*, Vol. 121, No. 9, pp. 1362–1369.

AASHTO (2003b), *Guide Specifications for Horizontally Curved Highway Bridges*, American Association of State Highway and Transportation Officials, Washington, D.C.

AASHTO (2004), *AASHTO LRFD Bridge Design Specifications,* 2nd Edition with Interims, American Association of State Highway and Transportation Officials, Washington, D.C.

Aneja, I. K., and Roll, F. (1971) "A Model Analysis of Curved Box-Beam Highway Bridges," *Journal of the Structural Division,* Vol. 97, No. 12, pp. 2861–2878.

ASCE Committee on Construction Equipment and Techniques (1989) "Concrete Bridge Design and Construction in the United Kingdom," *Journal of Construction Engineering and Management*, Vol. 115, No. 4, pp. 618–635.

Aslam, M., and Godden, W. G. (1973) "Model Studies of Curved Box-girder Bridges," *UC/SESM 73-5*, Dept. of Civil Engineering, California Univ., Berkeley, CA.

Aslam, M., and Godden, W. G. (1975) "Model Studies of Multicell Curved Box-Girder Bridge," *J. Eng. Mech. Div.,* Vol. 101, No. 3, pp. 207–222.

Bazant, Z. P., and El Nimeiri, M. E. (1974) "Stiffness Method for Curved Box-girders at Initial Stress," *Journal of the Structural Division*, Vol. 100, No. 10, pp. 2071–2090.

Beaupre, R. J., Powell, L. C., Breen, J. E., and Kreger, M. E. (1988) "Deviation Saddle Behavior and Design for Externally Post-Tensioned Bridges," *Research Report 365-2*. Center for Transportation Research, University of Texas at Austin, Austin, TX.

Branco, F. A., and Martins, L. (1984) *Temperature Distribution in Curved Concrete Box-girder Bridges,* Proc., Int. Conf. on Computer-Aided Analysis and Design of Concrete Structures, Pineridge, Swansea, U.K. pp. 1213–1223.

Bridge Design System (BDS) (1986) A Computer Program for Analysis and Design of Multi-Cell Box-girder Bridges, ECC, 1986

Buragohain, D. N., and Agrawal, B. L. (1973) "Analysis of Curved Box-girder Bridges," *Journal of the Structural Division* Vol. 99, No. 5, pp. 799–819.

Caltrans (1996) Bridge Memo to Designers Manual, Memo 11-31, Curved Post-Tensioned Bridges, California Department of Transportation, Sacramento, CA.

Canadian Standards Association (CSA) (1988) (Updated 2000), *Design of Highway Bridges*, CAN/CSA-S6-88, Rexdale, ON.

Cazaly, and Huggins, (1964) *Design Handbook*, Canadian Prestressed Concrete Institute, Canada.

Chang, S. T., and Gang, J. Z. (1990) "Analysis of Cantilever Decks of Thin-Walled Box-girder Bridges, *Journal of Structural Engineering*, Vol. 116, No. 9, pp. 2410–2418.

Chang, S. T., and Zheng, F. Z. (1987) "Negative Shear Lag in Cantilever Box-girder with Constant Depth," *Journal of Structural Engineering,* Vol. 113, No. 1, pp. 20–35.

Choudhury, D., and Scordelis, A. C. (1988) "Structural Analysis and Response of Curved Prestressed Concrete Box-girder Bridges," *Transportation Research Record 1180*, Transportation Research Board, National Research Council, Washington, D.C., pp. 72–86.

Chu, K. J., and Pinjarkar, S. G. (1971) *Analysis of Horizontally Curved Box-Girder Bridges*, *Journal of the Structural Division*, ASCE, 97(10), 2481–2501.

Collins, M. P., and Mitchell, D. (1980) "Shear and Torsion Design of Prestressed and Non-Prestressed Concrete Beams," *Journal of the Prestressed Concrete Institute*, Vol. 25, No. 5, pp. 32–100.

Computers and Structures, Inc. (1998) "SAP2000 – Integrated Finite Element Analysis and Design of Structures," CSI, Berkeley, CA.

Cordtz, K. (2004) Design of Curved Post-Tensioned Bridges for Lateral Prestress Forces, David Evans Associates, Roseville, CA.

Danesi, R. F., and Edwards, A. D. (1982) *Bending, Torsion, and Distorsion of Prestressed Concrete Box Beams of Deformable Cross Section: A Comparison of Experimental and Theoretical Results*, Proceedings Institution of Civil Engineers, London, U.K. Vol. 73(Part 1), pp. 789–810.

Danesi, R. F., and Edwards, A. D. (1983) *The Behavior up-to-Failure of Prestressed Concrete Box Beams of Deformable Cross Section Sub-*

jected to Eccentric Loads, Proceedings Institution of Civil Engineers, London, Vol. 75(Part 2), pp. 49–75.

Evans, H. R., and Al-Rifaie, W. N. (1975) *An Experimental and Theoretical Investigation of the Behavior of Box-girders Curved in Plan*, Proc., Inst. Civ. Eng., Vol. 59, No. 2, pp. 323–352.

Fam, A. R. M., and Turkstra, C. J. (1976) "Model Study of Horizontally Curved Box-girder," *Journal of the Structural Division*, ASCE, Vol. 102, No. 5, pp 1097–1108.

Fu, C. C., and Tang, Y. (2001) *Torsional Analysis for Prestressed Concrete Multiple Cell Box*, *ASCE Journal of Engineering Mechanics*, Vol. 127, No. 1, pp. 45–51.

Fu, C. C., and Yang, D. (1996) "Design of Concrete Bridges with Multiple Box Cells due to Torsion Using Softened Truss Model," *ACI Structural Journal*, Vol. 93, No. 6, pp. 696–702.

Goodall, J. K. (1971) *Torsional Stiffness of Multicellular Box Sections*, Proceedings, Conference on Development of Bridge Design and Construction, Lockwood, London, U.K.

Grant, C. (1993) *Shear Flow in Multicell Sections*, Proceedings, Institution of Mechanical Engineers, London, Vol. 207, No. 4, pp. 247–253.

Hasebe, K., Usuki, S., and Horie, Y. (1985) *Shear Lag Analysis and Effective Width of Curved Girder Bridges*, J. Eng. Mech., Vol. 111, No. 1, pp. 87–92.

Heins, C. P., Bonakdarpour, B. P., and Bell, L. C. (1972) "Multi-Cell Curved Girder Model Studies," J. Struct. Div., Vol. 98, No. 4, pp. 831–843.

Hsu, T. T. C. (1997) *ACI Shear and Torsion Provisions for Prestressed Hollow Girders*, ACI Structural Journal, Vol. 94, No. 6, pp. 787–799.

Ibrahim, A. M. M., et al. (2005) *Torsional Analysis and Design of Curved Bridges with Single Columns - LFD vs. LRFD Approach*, Paper presented at the Western Bridge Engineers Conference, Portland, OR.

Lim, P. T., Kilford, J. T., and Moffatt, K. R. (1971) *Finite Element Analysis of Curved Box-girder Bridges,* Developments in Bridge Design and Construction, U.K., pp. 264–286.

Lopez, A., and Aparico, A. C. (1989), *Nonlinear Behavior of Curved Prestressed Box-Girder Bridges*, IABSE Periodica, Zurich, Vol. 132, No. 1, pp. 13–28.

Maisal, B. I., and Roll, F. (1974) *Methods for Analysis and Design of Concrete Box Beam with Side Cantilevers*, Cement and Concrete Association, London, UK.

Marti, P. (1999) "How to Treat Shear in Structural Concrete," *ACI Structural Journal*, Vol. 96, No. 3.

Menn, C. (1990) *Curved Girder Bridges*, Chapter 7.6, Prestressed Concrete Bridges, ISBN 3-7643-2414-7, Birkhauser Verlag, Basel.

Meyer, C. (1970) *Analysis and Design of Curved Box-girder Bridges*, Structural Engineering and Structural Mechanics Report No. UC SESM 70-22, University of California, Berkeley, CA.

Meyer, C., and Scordelis, A. C. (1971) Analysis of Curved Folded Plate Structures, *Journal of the Structural Division*, Vol. 97, No. 10, pp. 2459–2480.

Nakai, H., and Heins, C. P. (1977) "Analysis Criteria for Curved Bridges," *Journal of the Structural Division*, ASCE, Vol. 103, No. 7, pp 1419–1427.

Okeil, A. M., and El-Tawil, S. (2004) "Warping Stresses in Curved Box-girder Bridges: Case Studies," *Journal of Bridge Engineering*, Vol. 9, No. 5, ASCE.

Oleinik, J. C., and Heins, C. P. (1975) "Diaphragms for Curved Box Beam Bridges," *Journal of Structural Engineering*, Vol. 101, No. 10, pp. 2161–2178.

Ontario Ministry of Transportation and Communication (1983; updated 1998) *Ontario Highway Bridge Design Code, OHBDC*, 2nd Edition, Downview, ON.

Ozakea, M., and Tavsi, N. (2003) "Analysis and Shape Optimization of Variable Thickness Box-girder Bridges in Curved Platform," *Electronic Journal of Structural Engineering International*, Vol. 3, Queensland, AUS.

Perry, S. H., Waldron, P., and Pinkney, M. W. (1985) *Design and Construction of Model Prestressed Concrete Bifurcated Box-Girder Bridges*, Proceedings Institution of Civil Engineers, London, U.K., Vol. 2, No. 79, pp. 439–454.

Pinkney, M. W., Perry, S. H., and Waldron, P. (1985) *Elastic Analysis and Experimental Behavior to Collapse of 1:12 Scale Prestressed Concrete Bifurcated Bridges*, Proceedings Institution Civil Engineers, London, U.K., Vol. 2, No. 79, pp. 454–481.

Podolny, W. Jr. (1985) "The Cause of Cracking in Post-Tensioned Concrete Box-girder Bridge and Retrofit Procedures," *PCI Journal*, March-April 1985, Precast Concrete Institute, Chicago, Illinois.

Rabizadeh, R. O., and Shore, S. (1975) *Dynamic Analysis of Curved Box-Girder Bridges*, Journal Structural Division, ASCE, Vol. 110, No. 9, pp. 1899–1912.

Rahai, A. (1996) "Nonlinear analysis of Box-Girder Bridges Under Thermal Loads," *Journal of Science and Technology*, London, U.K., Vol. 8, No. 32, pp. 206–217.

Rahal, K. N., and Collins, M. P. (1996) "Simple Model for Predicting Torsional Strength of Reinforced and Prestressed Concrete Sections," *ACI Structural Journal*, Vol. 93, No. 6, pp. 658–666.

Rahal, K. N., and Collins, M. P. (2003) "Experimental Evaluation of ACI and AASHTO-LRFD Design Provisions for Combined Shear and Torsion," *ACI Structural Journal*, Vol. 100, No. 3, pp. 277–282.

Rasmussen, L. J. (1996) *Plastic Behavior of Deformable Reinforced Concrete Box Sections Under Eccentric Load*, PhD Thesis, Department of Civil Engineering, University of Queensland, Brisbane, AUS.

Rasmussen, L. J., and Baker, G. (1998) *Stress Resultant Plasticity Model for the Analysis of Reinforced Concrete Shell and Box Structures*, Proceedings Institution of Civil Engineers, London, Vol. 128, No. 2, pp. 177–187.

Rasmussen, L. J., and Baker, G. (1999) "Large Scale Experimental Investigation of Deformable RC Box Sections," *Journal of the Structural Division*, ASCE, Vol. 125, No. 3, pp. 227–235.

Reilly, R. J. (1972) "Stiffness Analysis of Grids Including Warping," *Journal of the Structural Division*, ASCE, Vol. 98, No. 7, pp. 1511–1523.

Rogowsky, D. M. and Marti, P. (1991) *Detailing for Post-Tensioning*, VSL International Ltd., Bern, Switzerland.

Schlaich, J., and Scheef, H. (1982) *Concrete Box-Girder Bridges*, ISBN 3 85748 031 9, Switzerland.

Scordelis, A. C., Elfgren, L. G., and Larsen, P. K. (1977) "Ultimate Strength of Curved RC Box-girder Bridge," *Journal of the Structural Division*, Vol. 103, No. 8, pp. 1525–1542.

Seible, F., Dameron, R., and Hansen, B. (2003) Structural Evaluation of the 405-55 HOV Connector and the Curved Girder Cracking/ Spalling Problems, StD&A, San Diego, CA.

Sennah, K. M., and Kennedy, J. B. (2001) "State-of-the-Art in Curved Box-Girder Bridges," *Journal of Bridge Engineering*, ASCE, Vol. 6, No. 3, pp. 159–167.

Sennah, K. M., and Kennedy, J. B. (2002) "Literature Review in Analysis of Curved Box-Girder Bridges," *Journal of Bridge Engineering*, ASCE, Vol. 7, No. 2, pp. 134–143.

Song, S. T., Y. H. Chai, and S. E. Hida (2001) *Live Load Distribution in Multi-Cell Box-Girder Bridges and its Comparison with the AASHTO LRFD Bridge Design Specifications,* Final Report to Caltrans for Contract Number 59A0148.

Strasky, J. (2001) *Influence of Prestressing in Curved Members*, Betonve Mosty, Report TK21, Prague, Czech Republic.

Trikha, D. N., and Edwards, A. D. (1972) *Analysis of Concrete Box-girders Before and After Cracking*, Proceedings, Institution of Civil Engineers, Part 2, London, 59, pp. 743–761.

Tung, D. H. H. (1967) *Analysis of Curved Twin Box-girder Bridge*, presented at the May 8-12, 1967, ASCE National Meeting of Structural Engineering held at Seattle, WA.

Turkstra, C. J., and Fam, A. R. M. (1978) *Behavior Study of Curved Box Bridges*, *Journal of the Structural Division*, ASCE, Vol. 104, No. 3, pp. 453–462.

Van Landuyt, D. W. (1991) *The Effect of Duct Arrangement on Breakout of Internal Post-Tensioning Tendons in Horizontally Curved Concrete Box-girder Webs*, Theses, University of Texas at Austin.

Van Landuyt, D., and Breen, J. E. (1997) *Tendon Breakout Failures in Bridges,* Concrete International, American Concrete Institute, Farmington Hills, MI.

Vecchio, F. J., and Collins, F. P. (1986) "The Modified Compression Field Theory for Reinforced Concrete Elements Subjected to Shear," *ACI Journal*, Proceedings Vol. 83, No. 2, pp. 219–231.

Zhang, L., and Huang, J. (1989) *Three-Dimensional Analysis of Curved P. C. Box-Girder Bridges*, Proc., 6th Conf. on Computing in Civil Engineering, Atlanta, GA, pp. 867–874.

Zhang, L., Liu, M., and Huang, L. (1993) *Time-Dependent Analysis of Nonprismatic Curved PC Box-Girder Bridges*, Conference Proceeding Paper, Computing in Civil and Building Engineering, pp. 1703–1710.

Zokaie, T., Mish, K. D., and Imbsen, R. A. (1993) *Distribution of Wheel Loads on Highway Bridges, Phase 3,* Final Report to NCHRP Project 12-26 (2).

Zokaie, T., Osterkamp, T. A. and Imbsen, R. A. (1991) *Distribution of Wheel Loads on Highway Bridges,* Final Report to NCHRP Project 12-26 (1).

Appendixes

Appendixes A and C through F of the contractor's final report are available on the TRB website at http://trb.org/news/blurb_detail.asp?id=9596.

Abbreviations and acronyms used without definitions in TRB publications:

AAAE	American Association of Airport Executives
AASHO	American Association of State Highway Officials
AASHTO	American Association of State Highway and Transportation Officials
ACI–NA	Airports Council International–North America
ACRP	Airport Cooperative Research Program
ADA	Americans with Disabilities Act
APTA	American Public Transportation Association
ASCE	American Society of Civil Engineers
ASME	American Society of Mechanical Engineers
ASTM	American Society for Testing and Materials
ATA	Air Transport Association
ATA	American Trucking Associations
CTAA	Community Transportation Association of America
CTBSSP	Commercial Truck and Bus Safety Synthesis Program
DHS	Department of Homeland Security
DOE	Department of Energy
EPA	Environmental Protection Agency
FAA	Federal Aviation Administration
FHWA	Federal Highway Administration
FMCSA	Federal Motor Carrier Safety Administration
FRA	Federal Railroad Administration
FTA	Federal Transit Administration
IEEE	Institute of Electrical and Electronics Engineers
ISTEA	Intermodal Surface Transportation Efficiency Act of 1991
ITE	Institute of Transportation Engineers
NASA	National Aeronautics and Space Administration
NASAO	National Association of State Aviation Officials
NCFRP	National Cooperative Freight Research Program
NCHRP	National Cooperative Highway Research Program
NHTSA	National Highway Traffic Safety Administration
NTSB	National Transportation Safety Board
SAE	Society of Automotive Engineers
SAFETEA-LU	Safe, Accountable, Flexible, Efficient Transportation Equity Act: A Legacy for Users (2005)
TCRP	Transit Cooperative Research Program
TEA-21	Transportation Equity Act for the 21st Century (1998)
TRB	Transportation Research Board
TSA	Transportation Security Administration
U.S.DOT	United States Department of Transportation